MEDJ

Volume: 39 Issue: 3 September 2024

MEDENIYET MEDICAL JOURNAL

THE OFFICAL JOURNAL OF ISTANBUL MEDENIYET UNIVERSITY FACULTY OF MEDICINE

Formerly Göztepe Tıp Dergisi

ISSN 2149-2042
E-ISSN 2149-4606

www.medeniyetmedicaljournal.org

ISSN 2149-2042
E-ISSN 2149-4606

MEDENIYET MEDICAL JOURNAL

Formerly Göztepe Tıp Dergisi

Year 2024
Volume 39
Issue 3

www.medeniyetmedicaljournal.org

Owner
Dean, Sadrettin PENÇE
Istanbul Medeniyet University Faculty of Medicine

Administrative Office
Istanbul Medeniyet University Dumlupınar Mahallesi, D-100 Karayolu No:98, 34000 Kadıköy, İstanbul, Türkiye

Publication type: Periodical

Finance: Istanbul Medeniyet University Scientific Research Fund

Publisher
Galenos Publishing House
Address: Molla Gürani Mah. Kaçamak Sk. No: 21/1 34093 İstanbul, Türkiye
Phone: +90 (530) 177 30 97
E-mail: info@galenos.com.tr/yayin@galenos.com.tr
Web: www.galenos.com.tr

Printing at:
Son Sürat Daktilo Dijital Baskı San. Tic. Ltd. Şti.
Gayrettepe Mah. Yıldızposta Cad. Evren Sitesi A Blok No: 32 D: 1-3 34349 Beşiktaş/İstanbul
Phone: +90 212 288 45 75

Printing Date: September 2024

International scientific journal published quarterly.

Medeniyet Medical Journal is the official journal of Istanbul Medeniyet University

It is published four times a year (March, June, September, December).

MEDJ is an open Access, free and peer-reviewed journal

PubMed Abbreviation: Medeni Med J

"Please refer to the journal's webpage (**https://medeniyetmedicaljournal.org/jvis.aspx**) for "Publication Policy", "Instructions to Authors" and "Aims and Scope".

The Medeniyet Medical Journal and/or its editors are members of ICMJE, COPE, WAME, CSE and EASE, and follow their recommendations.

The Medeniyet Medical Journal is indexed in **Emerging Sources Citation Index (Web of Science), PubMed/MEDLINE, PubMed Central, Scopus, EBSCO Academic Search Complete, i-Journals, J-Gate, Türk Medline, Türkiye Atıf Dizini** and **TÜBİTAK ULAKBİM TR Index**.

The journal is printed on an acid-free paper and published electronically.

Owner: İSTANBUL MEDENİYET UNIVERSITY FACULTY OF MEDICINE

Responsible Manager: M. Tayyar KALCIOGLU

www.medeniyetmedicaljournal.org

International Advisory Board

MEDJ

International Advisory Board

Contents

Original Articles

MEDJ

Contents

Contents

DOI: 10.4274/MMJ.galenos.2024.20599
Medeni Med J 2024;39:152-160

Original Article

Association of Acute Kidney Injury with Bronchopulmonary Dysplasia in Preterm Infants

Prematüre Bebeklerde Akut Böbrek Hasarının Bronkopulmoner Displazi Gelişimindeki Etkisi

Saime Hacer OZDEMIR, Husnu Fahri OVALI

Medeniyet University Faculty of Medicine, Department of Pediatrics, Istanbul, Türkiye

ABSTRACT

Objective: Bronchopulmonary dysplasia (BPD) is among the most common complications of prematurity and is associated with high morbidity and mortality rates. Acute kidney injury (AKI) is also commonly observed in premature infants and significantly increases morbidity and mortality. Studies have shown that systemic changes in AKI may also trigger lung damage.

Methods: This study aimed to determine the effects of AKI on the development of BPD in preterm infants with a postconceptional age of ≤32 weeks and/or birth weight of ≤1500 grams. The relationship between demographic features and accompanying perinatal and postnatal morbidities among the patients was investigated.

Results: The incidence of BPD in infants with AKI was 52.6% (10 of 19 infants) and 38.3% (61 of 140 infants) in infants without AKI. In infants who developed BPD, the rate of AKI did not vary notably between babies born at ≤28 weeks and those born at >28 weeks [n=9, 17.3% (9 of 52 infants) and n= 1, 5.3%, (1 of 19 infants) respectively] of gestation (p>0.05).

Conclusions: AKI was associated with a greater need for resuscitation at birth, a greater need for invasive mechanical ventilation, fewer ventilator-free days, and a higher incidence of sepsis, patent ductus arteriosus, and necrotizing enterocolitis in premature infants. It was also more frequently associated with fluid-electrolyte imbalance, blood pressure, and hemodynamic disorders in the first postnatal week. The rate of BPD development was higher in infants with AKI, but this disparity was not statistically notable (p>0.05).

Keywords: Prematurity, acute kidney injury, bronchopulmonary dysplasia, organ crosstalk

ÖZ

Amaç: Bronkopulmoner displazi (BPD), prematüre doğan bebeklerde en sık görülen komplikasyonlarından biridir ve yüksek morbidite ve mortalite oranlarıyla ilişkilidir. Akut böbrek hasarı (ABH), prematüre bebeklerde oldukça yaygındır. ABH prematüre bebeklerde morbidite ve mortaliteyi önemli ölçüde artırır. Çalışmalar ABH'de görülen sistemik değişikliklerin akciğer hasarını tetikleyebileceğini göstermiştir.

Yöntemler: Bu çalışmada, gestasyon haftası ≤32 hafta ve/veya doğum tartısı ≤1500 gram olan prematüre bebeklerde ABH'nin BPD gelişimine etkisinin belirlenmesi amaçlanmıştır. Bu hastaların demografik özellikleri ile eşlik eden perinatal ve postnatal morbiditeler arasındaki ilişki araştırılmıştır.

Bulgular: ABH'li bebeklerde BPD görülme oranı %52,6 (19 bebekten 10'u), ABH olmayan bebeklerde ise %38,3 (140 bebekten 61'i) idi. BPD gelişen bebeklerde ABH görülme oranı, ≤28 hafta doğan bebekler ile >28 hafta doğan bebekler [sırasıyla n=9, %17,3 (52 bebekten 9'u) ve n=1, %5,3 (19 bebekten 1'i)] kıyaslandığında anlamlı farklılık göstermedi (p>0,05).

Sonuçlar: ABH, doğumda daha fazla resüsitasyon ihtiyacı, daha fazla invaziv mekanik ventilasyon ihtiyacı, daha az ventilatörsüz gün ve prematüre bebeklerde daha yüksek sepsis, patent duktus arteriozus ve nekrotize enterokolit insidansı ile ilişkiliydi. Bununla birlikte ABH; doğum sonrası ilk haftalarda sıvı-elektrolit dengesizliği, kan basıncı ve hemodinamik bozukluklarla daha sık ilişkili bulundu. ABH gelişen bebeklerde BPD gelişme oranı daha fazla olmakla birlikte bu fark istatistiksel olarak önemli değildi (p>0,05).

Anahtar kelimeler: Prematürite, akut böbrek hasarı, bronkopulmoner displazi, organ çapraz etkileşimi

Address for Correspondence: S.H. Ozdemir, Medeniyet University Faculty of Medicine, Department of Pediatrics, Istanbul, Türkiye
E-mail: ozdemirshacer@gmail.com **ORCID ID:** orcid.org/0009-0009-3168-4445

Received: 22 April 2024
Accepted: 12 June 2024
Online First: July 2024

Cite as: Ozdemir SH, Ovali HF. Association of Acute Kidney Injury with Bronchopulmonary Dysplasia in Preterm Infants. Medeni Med J. 2024;39:152-160

INTRODUCTION

Bronchopulmonary dysplasia (BPD) is among the most common diseases in prematurely born infants and is associated with high morbidity and mortality in the first years of life. BPD is also linked to lifelong impaired lung function and medical costs[1].

Many complex factors caused by the immaturity of organs and systems have been identified in the pathophysiology of BPD. Factors such as lung immaturity, infections, barotrauma caused by mechanical ventilation (MV), fluid overload, and inflammation have been shown to be effective in the pathogenesis of BPD[2].

Conversely, acute kidney injury (AKI)-induced systemic inflammation is observed in almost 40% premature infants[3]. AKI alone is associated with higher mortality in premature infants and chronic renal failure in both childhood and adult age groups[4]. Increased infection rates and the use of nephrotoxic drugs in preterm infants are among the factors associated with AKI[5].

Studies conducted in recent years have shown that systemic changes in AKI may also trigger lung damage. Although the mechanism underlying this phenomenon has not been fully understood, results in animal studies indicate that there is a mutual interaction between kidney and lung[6-9].

AKI may have deleterious effects on lung physiology due to fluid imbalance, changes in vascular tone and acid-base imbalance. Kidney damage also activates extrarenal inflammatory pathways and impairs lung function. Conversely, alveolar gas exchange disorders seen in lung diseases affect kidney function and cause homeostatic deterioration[10]. Hypoxia and hypercapnia can directly affect renal vascular tone and cause renal damage[10-12]. Prolonged MV in infants who develop BPD affects renal function as a result of neurohormonal changes, blood gas disorders and hemodynamic disorders[13].

This study aimed to determine the effects of AKI on the development of BPD in premature infants.

MATERIALS and METHODS

Premature infants with a postconceptional age of ≤32 weeks and/or a birth weight of ≤1500 grams, who developed AKI were included.

Infants with congenital heart disease, chromosomal disorders/diseases, those who died within the first 48 hours, those with severe kidney and/or urinary system anomalies or abdominal wall defects, patients whose families did not give consent, and patients whose data were missing at the end of the study were not included in the study.

Demographic information (gender, gestational age, birth weight, etc.) of the patients, antenatal steroid use, maternal morbidities (preeclampsia, gestational diabetes mellitus, chorioamnionitis, etc.), and other perinatal morbidities, cord blood gas values, 5th minute Apgar scores, presence of intrauterine growth restriction, multiple pregnancy, and need for oxygen, resuscitation, and intubation at birth were recorded.

Serum creatinine, urea, sodium, potassium, C-reactive protein, and blood gas values, which are routinely monitored in patients within the first 15 days of life, were recorded.

Daily weights, weight changes (+/- grams/day) of patients, and weight change rates at the end of the 15th day of life were investigated. If the weight on the 15th day had increased by more than 5% of the birth weight, it was considered weight gain; if there had been a loss of more than 5% of the birth weight, it was considered weight loss.

The total daily urine and fluid intake were recorded and evaluated as normal, oliguria (<1 mL/kg/hour) or anuria (no urine in the last 24 hours). Nephrotoxic drug use in infants within the first 15 postnatal days was also recorded.

Blood pressure (BP) was measured daily in the infants. Neonatal hypertension was defined as persistent systolic and/or diastolic BP above the 95th percentile for postmenstrual (also referred to as postconceptional) age. Hypotension was defined as BP below the 5th percentile for postconceptional and postnatal ages. Measurements between the 5th and 95th percentiles according to postconceptional age and postnatal age were considered within the normal range.

Morbidities that developed in the patients [respiratory distress syndrome, BPD, pneumonia, sepsis, patent ductus arteriosus (PDA), necrotizing enterocolitis (NEC), retinopathy of prematurity, etc.] were recorded.

AKI was diagnosed, and patients were categorized considering Kidney Disease: Improving Global Outcomes (KDIGO) criteria[14]. The patients' need for oxygen and/or assisted breathing on the 28th postnatal day and the 36th postconceptional week was recorded. The diagnosis of BPD was made according to the diagnostic criteria established by NIH (National Institute of Child Health and Human Development Workshop) and the patients were classified accordingly[15].

The rate of BPD development in premature babies born with a postconceptional age ≤32 weeks and/or a birth weight ≤1500 grams, in the patients who did and did not develop AKI according to the KDIGO classification, and the relationship between demographic features and accompanying perinatal and postnatal morbidities among these patient groups were investigated. Ethical approval was obtained from the Istanbul Medeniyet University Goztepe Training and Research Hospital Clinical Research Ethics Committee (decision no: 2021/0410, date: 25.08.2021). Written informed consent was obtained from the families of the patients who participated in the study.

Statistical Analysis

Descriptive statistics were analyzed by evaluating mean, standard deviation, median, lowest, highest, frequency, and ratio values. Kolmogorov-Smirnov test was used to determine the distribution of variables. Independent sample t-test and Mann-Whitney U test were used to analyze quantitative independent data. The chi-square test and Fisher's exact test were used to analyze qualitative independent data. SPSS 28.0 program was used in the analysis.

RESULTS

During the study period, 172 infants were born at or before 32 weeks of gestation and/or with a birth weight of 1500 g or less. Thirteen infants who did not meet the inclusion criteria were excluded, and the data of 159 infants were analyzed, including 79 girls (49.7%) and 80 boys (50.3%) (Figure 1). The mean gestational age of the infants was 29+2 weeks ±2 days, and the mean birth weight was 1200 g. The mean 5th minute Apgar score was 7.3±1.5. The mean duration of intubation during the first 15 days of life was 7.2 days ±5.5 days. 18 (11.3%) patients died during intensive care (Table 1).

The most common electrolyte abnormality in the first 15 days of life was hyponatremia (58.8%, 20 of 34 infants), and the most common blood gas disorders were metabolic acidosis (60.3%, 35 of 63 infants) and respiratory acidosis (41.4%, 24 of 63 infants). Daily urine output was normal in 86.2% (137 of 159 infants), whereas 2.5% (4 of 159 infants) were anuric and 11.3% (18 of 159 infants) were oliguric. The mean daily fluid intake of the infants was 125±18.5 mL/kg/day (minimum-maximum: 67-174 mL/kg/day, median: 125 mL/kg/day).

The rate of AKI was 11.9% (19 of 159 infants), 9 of them being stage 2 (47.3%, n=9). BPD developed in 44.7% (71 of 159 infants) of the patients. The rate of BPD among infants who developed AKI was 52.6% (10 of 19 infants) (Figure 2).

Gestational age, birth weights and 5th minute Apgar scores were notably lower in infants with AKI than in those without AKI ($p<0.05$). Although the rate of infants with AKI who exceeded their birth weight on the 15th day was higher (n=11, 84.6%), the rate was not notably higher than that of infants without AKI ($p>0.05$). The rate of intubation requirement and the total intubation time in the first 15 days were significantly higher in infants with AKI ($p<0.05$) (Table 2). Eleven of the infants with AKI died during neonatal intensive care unit follow-up, and this rate was significantly higher than the infants without AKI ($p<0.05$) (Table 2). The rate of antenatal steroid administration was comparable in both groups.

The mean daily fluid intake (130.5±17.7 mL/kg/g) was significantly higher in infants with BPD ($p<0.05$) compared to non-BPD infants (121.2±18.2 mL/kg/day).

The total daily fluid intake of infants with AKI (mean: 127.3±21.4 mL/kg/day, median: 127 mL/kg/day) and those without AKI (mean: 125.1±18.2 mL/kg/day, median:

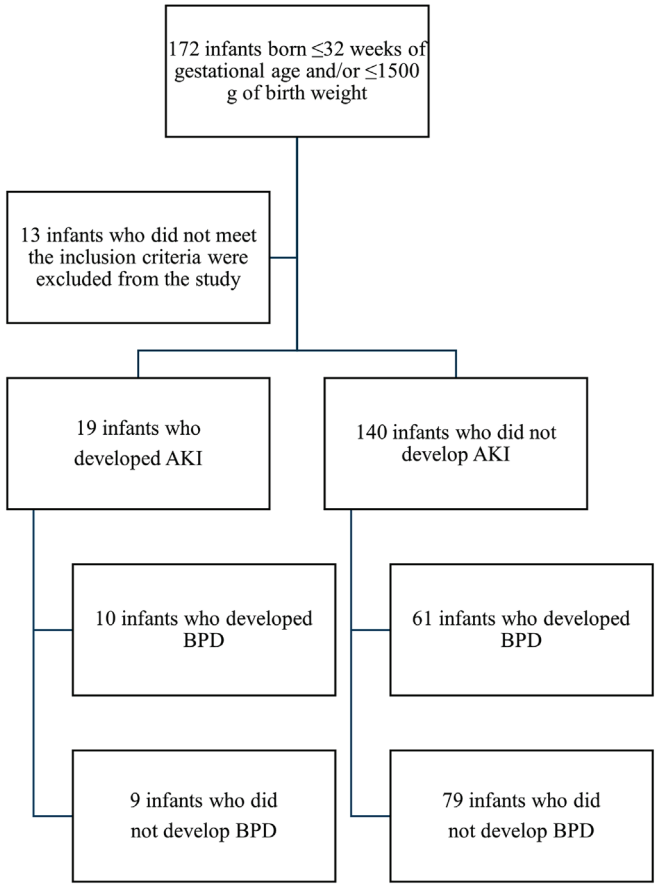

Figure 1. Flow chart of the study.

AKI: Acute kidney injury, BPD: Bronchopulmonary dysplasia

125 mL/kg/day) did not show any statistically notable variation (p>0.05).

There was no statistically notable variation with regard to oxygen need in the delivery room between patients with and without AKI (p>0.05). In patients with AKI, the rate of positive pressure ventilation (PPV) use at birth, the need for cardiopulmonary resuscitation in the delivery room, and the need for intubation in the delivery room were markedly higher than those in the non-AKI patients (p<0.05) (Table 3). The rate of electrolyte, blood gas, urine output abnormalities, and BP abnormalities were observed more frequently in patients with AKI (p<0.05) (Table 3).

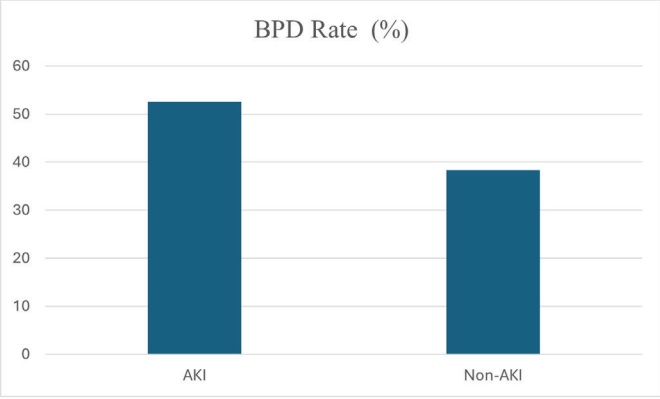

Figure 2. Bronchopulmonary dysplasia rate in infants with or without acute kidney injury (52.6 vs. 38.3%).

AKI: Acute kidney injury, BPD: Bronchopulmonary dysplasia

Table 1. Demographic data of the study group (n=159).	
Gestational age (weeks)	29.1±2.5 (23-26)
Male	80 (50.3%)
Female	79 (49.7%)
Birth weight (grams)	1184.1±416.1 (488-2313)
5th minute Apgar score	7.3±1.5 (1-10)
Intubation time within 15 days	7.2±5.5 (1-15) days
Death	18 (11.3%)

Clinical findings of respiratory distress syndrome were significantly longer in babies with AKI (p<0.05). The rate of surfactant treatment in infants with AKI was significantly higher than those in non-AKI babies (p<0.05). The rates of sepsis, pneumonia, hemodynamically significant PDA, and NEC were notably higher in babies with AKI were notably higher than the non- AKI infants (p<0.05) (Table 4).

The mean gestational age of non-AKI infants who developed BPD was significantly lower (27.5 vs. 30 weeks; p<0.05).

Among the non-AKI infants, the birth weight and 5th minute Apgar scores of the patients with BPD were markedly lower than those of the non-BPD infants (p<0.05). Additionally, the rate of maternal preeclampsia was significantly higher in patients with BPD (16 of 61 infants, 29.5%) (p<0.05). The rate of PPV application in the delivery room (47 of 61 infants, 77%) and the rate of need for intubation in the delivery room (33 of 61 infants, 54.1%) were higher in the group that developed BPD in non-AKI infants (p<0.05).

Among non-AKI infants who developed BPD, a higher incidence of electrolyte abnormalities (15 of 61 infants, 24.6%), blood gas abnormalities (n=32 of 61 infants, 54.2%), urine output abnormalities during the first 15 days of life (decrease in the amount of urine: 5 of 61 infants, 8.2%), rate of BP abnormalities (10 of 61 infants, 16.4%), and the use of nephrotoxic drugs (57 of 61 infants, 93.4%) (p<0.05) were observed. The surfactant treatment rate in non-AKI infants was significantly higher in patients with BPD (54 of 61 infants, 88.5%) (p<0.05). Among non-AKI

Table 2. Demographic features of infants who did and did not develop acute kidney injury.					
	AKI (-)		AKI (+)		p-value
	Mean ± SD/n, %	Median	Mean ± SD/n, %	Median	
Gestational age (weeks)	29.4±2.4	29.7	26.8±2.1	27.4	**0.000**
Birth weight (grams)	1241.7±404.2	1254.5	759.7±204.5	695.0	**0.000**
Apgar score 5th minute	7.4±1.4	8.0	6.1±1.7	6.0	**0.002**
Need for intubation within the first 15 days of life	58 (41.4%)		16 (84.2%)		**0.000**
Total intubation period during the first 15 days of life (days)	6.2±5.3	5.0	11.0±4.4	13.0	**0.001**
Death rate	7 (5.0%)		11 (57.9%)		**0.000**
AKI: Acute kidney injury, SD: Standard deviation					

Table 3. Prenatal, perinatal, and postnatal features in infants who did and did not develop acute kidney injury.				
n (%)		**AKI (-)**	**AKI (+)**	**p-value**
		n (%)		
PPV at birth	(+)	87 (62.1%)	18 (94.7%)	**0.005**[X²]
	(-)	53 (37.9 %)	1 (5.3%)	
Resuscitation at birth	(+)	3 (2.1%)	4 (21.1%)	**0.004**[X²]
	(-)	137 (97.9%)	15 (78.9%)	
Intubation at birth	(+)	56 (40.0%)	14 (73.7%)	**0.006**[X²]
	(-)	85 (60.0%)	5 (26.3%)	
Electrolyte abnormalities	(+)	23 (16.4%)	11 (57.9%)	**0.000**[X²]
	(-)	117 (83.6%)	8 (42.1%)	
Blood gas abnormalities	(+)	42 (33.9%)	16 (88.9%)	**0.000**[X²]
	Normal	82 (66.1%)	2 (11.1%)	
Urine output	Anuria	0 (0%)	4 (21.1%)	**0.000**[X²]
	Oliguria	6 (4.3%)	12 (63.2%)	
Blood pressure	Hypotensive	2 (1.4%)	9 (47.4%)	**0.000**[X²]
	Hypertensive	12 (8.6%)	4 (21.1%)	

[X²]Chi-square test (Fisher's exact). AKI: Acute kidney injury, PPV: Positive pressure ventilation

Table 4. Morbidities in infants with and without acute kidney injury.					
	AKI (-) (n=140)		**AKI (+) (n=19)**		**p-value**
	Mean ± SD/n-%	**Median**	**Mean ± SD/n-%**	**Median**	
Surfactant treatment	90 (64.3%)		17 (89.5%)		**0.028**[X²]
RDS recovery day	4.3±4.7	3.0	7.5±5.2	5.0	**0.001**[m]
Sepsis	106 (75.7%)		19 (100%)		**0.015**[X²]
Total number of days with sepsis	13.0±9.2	10.0	15.8±9.0	17.0	0.083[m]
Patent ductus arteriosus	32 (22.9%)		13 (68.4%)		**0.000**[X²]
Necrotizing enterocolitis	15 (10.7%)		9 (47.4%)		**0.000**[X²]

[m]Mann-Whitney U test, [X²]Chi-square test (Fisher test). AKI: Acute kidney injury, SD: Standard deviation

infants, the incidence of sepsis (56 of 61 infants, 91.8%) and total sepsis duration (16.1±10.1 days, median: 13.5) were markedly higher in patients with BPD (p<0.05).

Among non-AKI infants, the rate of hemodynamically significant PDA (25 of 61 infants, 41%) and NEC (13 of 61 infants, 21.3%) and daily fluid intake (130.4±18.9 mL/kg/g, median: 130 mL/kg/g) were significantly higher in infants with BPD (p<0.05). The duration of sepsis was found to be considerably (p<0.05) higher in the group that developed BPD (mean: 21.8±6.8 days) than in those who did not develop BPD (mean: 16.1±10.1 days).

DISCUSSION

AKI usually occurs as a complication of damage to organs, such as the lungs, heart, liver, intestine, and brain. However, the information obtained in recent studies supports that a damaged kidney can also be the reason for dysfunction in other organs[16]. AKI is a serious condition that may worsen prognosis, especially in critically ill patients. In our study, we found that AKI caused an important increase in the incidence of NEC and PDA in infants (p<0.05). Similar findings were reported by Starr et al.[17].

In Jetton et al.'s[3] multicenter, multinational observational cohort study, AKI was found to be common in newborns with congenital heart disease, sepsis, and hypoxic ischemic injury, in infants receiving extracorporeal membrane oxygenation, and in very low birth weight infants. In the same study, it was stated that newborns and children with AKI had a worse prognosis than those without AKI[3]. These findings also support the results of our study.

The same authors found that compared with non-AKI infants, infants with AKI belonged to a higher birth

weight category and had higher hospitalization rates for hypoxic ischemic encephalopathy, seizures, congenital heart disease, NEC, and surgical evaluation[3]. In our study, the incidence of NEC was greater in infants who had AKI than in those who did not ($p<0.05$). This suggests that pathophysiologic factors that predispose patients to AKI may also be instrumental in the development of NEC. The main pathway for these factors is inadequate intestinal circulation, leading to hypoxia.

The rate of AKI in preterm infants was reported to be 19% in a single-center study based on retrospective and prospective data[4]. In our single-center observational cohort study, the rate of AKI development in the first 15 days of life in infants born at or before 32 weeks of gestation and/or with a birth weight of 1500 g or less was 11.9%, which was comparable to other studies[1,2,4]. Hypotension due to impaired cardiac function or inadequate autoregulatory response of the peripheral vasculature in these tiny infants, as well as delicate fluid balance, which may be affected by various renal or extra-renal factors, leads to the cause of AKI.

In a prospective study, Koralkar et al.[4] examined the relationship between AKI and mortality in preterm infants born 1500 g in terms of incidence and outcomes and 41 of 229 (18%) patients were found to have AKI. In the same study, infants with AKI had a lower birth weight (mean 702 g vs. 1039 g) and gestational age (mean 25 weeks vs. 28 weeks). Infants with AKI had lower 1st and 5th minute Apgar scores and a higher need for umbilical arterial catheter, MV support, and inotropic support[4]. This finding also supports the notion that the more premature an infant is, the more are the complications of prematurity because the development of organ systems and balancing regulations are still immature.

In our study, gestational ages (mean: 26.8 weeks) and birth weights (mean: 759.7 g) of infants with AKI were found to be lower than those of non-AKI infants ($p<0.05$). Additionally, the 5th Apgar score of the AKI group was notably lower than that of the non-AKI group ($p<0.05$). In this case, hypoxia in the immediate postnatal period may have predisposed the infant to AKI.

We also observed that invasive MV requirement in the first 15 days (84.2%) and total invasive MV duration in the first 15 days (mean: 11 days) were significantly higher in patients with AKI than non-AKI patients ($p<0.05$). These results were compatible with those of Askenazi et al.[18] and Starr et al.[17]. Increased need for MV is associated with immaturity in infants, as well as possible complications such as hypoxia, sepsis, and NEC. Therefore, increased rates of AKI may be expected in infants who develop these complications.

In their study published in 2005, Abosaif et al.[19] emphasized that AKI in intensive care units was due to the combined effects of hypotension, sepsis, and toxic exposure. Sepsis is a well-known risk factor for the development of AKI and is known to cause 35-50% of AKI cases in intensive care units[20,21]. In our study, the rate of suspected or proven sepsis in preterm infants in the neonatal intensive care unit was found to be 78.6%. There are studies indicating that among patients with AKI, the mortality rate is higher in those with sepsis compared to those without[19]. Starr et al.[17] also found that the rate of sepsis was higher in preterm infants who developed AKI ($p<0.001$). As stated above, this finding is also an expected finding, since sepsis is associated with hypotension and/or toxic exposure, leading to deterioration of the infant, derangement of fluid status, and impairment of renal function.

Koralkar et al.[4] reported that infants with preeclampsia and maternal hypertension developed AKI at a lower rate. In that study, it was found that most infants with AKI had a birth weight of <750 g [29 of 41 (70%)] and a gestational age of less than 26 weeks of gestation [30 of 41 (73%)][4]. A similar result was reported by Askenazi et al.[18] in their study published in 2013. They suggested two possible explanations for this finding[18]. First, they stated that preeclampsia may indicate a response to a maternal problem rather than a primarily fetal/neonatal problem. Thus, the cause of prematurity or initial morbidities may be the mother, not the baby. Another possibility is that preeclampsia may have a protective effect against AKI. They hypothesized that small and repeated ischemic events may prevent AKI due to ischemic preconditioning. Some other studies have shown similar predictions[22-24]. In our study, there was no marked diversity in the rates of maternal preeclampsia, gestational diabetes mellitus, and chorioamnionitis between patients with and without AKI ($p>0.05$). The low rate of preeclampsia in our cohort was attributed to the small number of cases in our group.

The rate of BPD among babies born at 32 and/or earlier gestational weeks and with a birth weight of 1500 g or less was 44.7%. There was no significant difference in infants born before or after 28 weeks of gestation. These findings are consistent with other studies[17,25]. The association between BPD and renal function is another subject that should be addressed in depth in future studies.

For very-low-birth-weight newborns, the first week of life is a critical transition period. During this transition period, fluid and electrolyte imbalances can affect many

organs and systems[26]. Especially the lungs affected by MV, inflammation, and left-to-right shunt due to PDA; are highly prone to damage from these fluid and electrolyte imbalances and may be related to the development of BPD. However, in our study, no relationship was found between the electrolyte anomalies of infants and the rate of BPD development. This suggests that electrolyte abnormalities alone may not be a risk factor for BPD. However, they may be significant in patients with fluid imbalances.

Excessive fluid intake has been shown to cause the development of clinically significant PDA and congestive heart failure[27,28]. It has been suggested that this may also play a role in the pathogenesis of BPD. Arikan et al.[29] found that fluid overload was associated with an increase in the duration of MV. Santschi et al.[30] also highlighted similar findings and showed the relationship between fluid balance and pulmonary outcomes in critically ill patients. In a retrospective cohort study of 1382 extremely low birth weight newborns by Oh et al.[31], it was suggested that higher fluid intake and less weight loss in the first 10 days of life were associated with an increased risk of BPD.

Askenazi et al.[18], in their study on infants with a postconceptional age >34 weeks and birth weight >2000 g, found that fluid excess in the first 3 days of life was higher in babies with AKI in contrast to those who did not develop AKI. We did not detect any notable difference between the total amount of fluid taken in the first 15 days of life and the weight on the 15th day of life in our study group. Our unit's fluid protocol requires a more restricted approach, which might have prevented significant differences between the two groups. However, the mean total daily fluid intake of infants in the first 15 days of life was significantly higher (130 mL/kg/g, p=0.003) in our infants who developed BPD, which was comparable to that of other studies. Bell and Acarregui[32] found that limited water intake remarkably increased postnatal weight loss and reduced the risk of PDA and NEC.

In our study, the weights of infants who developed BPD were evaluated on the 15th postnatal day, and 67.6% were found to have exceeded their birth weight (> birth weight +5% of birth weight), and this rate was not found to be significantly higher than that of infants without BPD. This finding was also attributed to the restrictive fluid protocol in our unit.

AKI is known to negatively affect the lungs through many mechanisms, including impaired fluid homeostasis, dysregulation of angiogenesis, and disruptions in acid-base and electrolyte balance[17]. These effects lead to excessive extravascular fluid, secondary inflammatory reactions, more capillary-alveolar permeability, and disruption of the epithelial barrier, resulting in worsened lung dysfunction and disrupted gas exchange.

Complications such as pulmonary edema may develop in patients with AKI, and as a result, respiratory failure and the need for MV may occur[33]. This interaction is thought to be secondary to inflammatory reactions, oxidative stress, and increased vascular permeability in the lungs that occur with the increase in immune system mediators[33].

Damage caused by chemical mediators released into the bloodstream has been proposed as the mechanism of lung-induced kidney damage[33]. Additionally, the kidneys are extremely sensitive to changes in oxygen, and even a small amount of hypoxia can cause the kidneys to lose their autoregulation mechanisms. Similarly, hypercapnia secondary to acute lung injury causes vasoconstriction in the renal vascular network and activation of the renal angiotensin aldosterone system[33].

The functions of the lung as a respiratory organ include not only gas exchange but also immune modulation, hematopoietic, secretory, and metabolic function regulation, and under physiological conditions, this contributes to kidney and lung crosstalk[16]. The lungs and kidneys work together to maintain fluid acid-base balance by regulating BP via the renin-angiotensin-aldosterone system and bicarbonate and carbon dioxide concentrations via kallikrein-kinin[16].

Under pathological conditions, kidney-lung crosstalk mechanisms include inflammatory reactions (e.g., unbalanced immune reactions and increased inflammatory cytokine release, etc.) and the disruption of fluid balance caused by kidney or lung damage (e.g., fluid overload, uremic toxin retention, hypoxia, and hypercapnia etc.)[16].

AKI negatively affects the lungs mainly through increased respiratory failure, the need for invasive MV, and associated respiratory system complications[24,33-35]. Chertow et al.[36] concluded that patients with AKI were more than twice as likely to develop respiratory failure and nearly three times more likely to die than those without AKI. A similar result was obtained in our study, and this data was thought to be suggestive that improvement from lung dysfunction is also affected by kidney damage.

AKI is associated with increased permeability, inflammatory cell infiltration, and increased oxidative stress in the lungs[10]. Lung damage can also trigger kidney damage, and one of the most important reasons for this is that the kidneys are very sensitive to minimal oxygen changes[33].

van den Akker et al.[37] found that MV increased the incidence of AKI by 3 times. There is strong evidence of MV-induced hemodynamic changes and systemic mediator release[37]. In our study, the rate of invasive MV and total intubation time in the first 15 days were found to be markedly higher in the group that developed AKI among infants who developed BPD ($p<0.05$). This result indicates that invasive MV may be a risk factor for AKI, and this finding is consistent with the data presented in the literature. However, it may be related to not only the MV per se but also the conditions that necessitate MV, such as sepsis, pneumonia, and respiratory distress syndrome.

Grigoryev et al.[6] tested the hypothesis that AKI induces a strong inflammatory response and produces distinct genomic changes in the kidney and lung. Clinical studies have demonstrated a strong association between AKI and extrarenal organ dysfunction, and more recent animal studies have demonstrated a significant causal effect of AKI on remote organ dysfunction[6]. Recent studies have shown that there may be many negative crosstalk interactions between AKI and other organs because of imbalances in the metabolism of immune, inflammatory, and soluble mediators[8,9,38]. These mechanisms also explain why AKI may cause remote organ dysfunction in infants.

The major limitation of our study is the small sample size. Due to low numbers, logistic regression analysis could not be performed to delineate the effects of many factors that are instrumental in the development of BPD.

In our study, AKI was found to be associated with a greater need for resuscitation at birth, a greater need for invasive MV, fewer ventilator-free days, and a higher incidence of sepsis, PDA, and NEC in preterm infants. It was also associated with more frequent fluid-electrolyte imbalance, BP abnormalities, and hemodynamic disorders in the first postnatal week.

In infants with BPD, more resuscitation needs at birth, more invasive MV needs, fewer ventilator-free days, and a higher incidence of sepsis, pneumonia, PDA, and NEC were observed. The daily fluid intake was also higher in infants with BPD. This finding is consistent with other studies reporting that excess fluid poses a risk of BPD during this period of life.

CONCLUSION

In conclusion, the rate of BPD development was higher in babies who developed AKI. Although not statistically significant, we believe that the difference is important. We believe that a sound evaluation of the common risk factors for such morbidities, which are frequently encountered in preterm infants, is important in terms of long-term organ health and measures to be taken to ensure optimal growth and development in this sensitive patient group. More studies are needed to explain the exact relationship between AKI and BPD.

Ethics

Ethics Committee Approval: Ethical approval was obtained from the Istanbul Medeniyet University Goztepe Training and Research Hospital Clinical Research Ethics Committee (decision no: 2021/0410, date: 25.08.2021).

Informed Consent: Written informed consent was obtained from the families of the patients who participated in the study.

Author Contributions

Surgical and Medical Practices: S.H.O., H.F.O., Concept: S.H.O., H.F.O., Design: S.H.O., H.F.O., Data Collection and/or Processing: S.H.O., Analysis and/or Interpretation: S.H.O., H.F.O., Literature Search: S.H.O., Writing: S.H.O., H.F.O.

Conflict of Interest: The author of this article (H.F.O.) are member of the Editorial Board of this journal. He was completely blind to the paper's peer-review process. Other author have nothing to disclose.

Financial Disclosure: The authors declared that this study has received no financial support.

REFERENCES

1. Starr MC, Boohaker L, Eldredge LC, et al. Acute Kidney Injury and Bronchopulmonary Dysplasia in Premature Neonates Born Less than 32 Weeks' Gestation. Am J Perinatol. 2020;37:341-8.
2. Askenazi D, Patil NR, Ambalavanan N, et al. Acute kidney injury is associated with bronchopulmonary dysplasia/mortality in premature infants. Pediatr Nephrol. 2015;30:1511-8.
3. Jetton JG, Boohaker LJ, Sethi SK, et al. Incidence and outcomes of neonatal acute kidney injury (AWAKEN): a multicentre, multinational, observational cohort study. Lancet Child Adolesc Health. 2017;1:184-94.
4. Koralkar R, Ambalavanan N, Levitan EB, McGwin G, Goldstein S, Askenazi D. Acute kidney injury reduces survival in very low birth weight infants. Pediatr Res. 2011;69:354-8.
5. Askenazi DJ, Feig DI, Graham NM, Hui-Stickle S, Goldstein SL. 3-5 year longitudinal follow-up of pediatric patients after acute renal failure. Kidney Int. 2006;69:184-9.
6. Grigoryev DN, Liu M, Hassoun HT, Cheadle C, Barnes KC, Rabb H. The local and systemic inflammatory transcriptome after acute kidney injury. J Am Soc Nephrol. 2008;19:547-58.
7. Dodd-o JM, Hristopoulos M, Scharfstein D, et al. Interactive effects of mechanical ventilation and kidney health on lung function in an in vivo mouse model. Am J Physiol Lung Cell Mol Physiol. 2009;296:L3-11.

8. Hassoun HT, Lie ML, Grigoryev DN, Liu M, Tuder RM, Rabb H. Kidney ischemia-reperfusion injury induces caspase-dependent pulmonary apoptosis. Am J Physiol Renal Physiol. 2009;297:F125-37.
9. Hoke TS, Douglas IS, Klein CL, et al. Acute renal failure after bilateral nephrectomy is associated with cytokine-mediated pulmonary injury. J Am Soc Nephrol. 2007;18:155-64.
10. Basu RK, Wheeler DS. Kidney-lung cross-talk and acute kidney injury. Pediatr Nephrol. 2013;28:2239-48.
11. Doi K, Ishizu T, Fujita T, Noiri E. Lung injury following acute kidney injury: kidney-lung crosstalk. Clin Exp Nephrol. 2011;15:464-70.
12. Husain-Syed F, Slutsky AS, Ronco C. Lung-Kidney Cross-Talk in the Critically Ill Patient. Am J Respir Crit Care Med. 2016;194:402-14.
13. Chen D, Jiang L, Li J, et al. Interaction of Acute Respiratory Failure and Acute Kidney Injury on in-Hospital Mortality of Patients with Acute Exacerbation COPD. Int J Chron Obstruct Pulmon Dis. 2021;16:3309-16.
14. Khwaja A. KDIGO clinical practice guidelines for acute kidney injury. Nephron Clin Pract. 2012;120:c179-84.
15. Higgins RD, Jobe AH, Koso-Thomas M, et al. Bronchopulmonary Dysplasia: Executive Summary of a Workshop. J Pediatr. 2018;197:300-8.
16. Li X, Yuan F, Zhou L. Organ Crosstalk in Acute Kidney Injury: Evidence and Mechanisms. J Clin Med. 2022;11:6637.
17. Starr MC, Schmicker RH, Halloran BA, et al. Premature infants born <28 weeks with acute kidney injury have increased bronchopulmonary dysplasia rates. Pediatr Res. 2023;94:676-82.
18. Askenazi DJ, Koralkar R, Hundley HE, Montesanti A, Patil N, Ambalavanan N. Fluid overload and mortality are associated with acute kidney injury in sick near-term/term neonate. Pediatr Nephrol. 2013;28:661-6.
19. Abosaif NY, Tolba YA, Heap M, Russell J, El Nahas AM. The outcome of acute renal failure in the intensive care unit according to RIFLE: model application, sensitivity, and predictability. Am J Kidney Dis. 2005;46:1038-48.
20. Hoste EA, Lameire NH, Vanholder RC, Benoit DD, Decruyenaere JM, Colardyn FA. Acute renal failure in patients with sepsis in a surgical ICU: predictive factors, incidence, comorbidity, and outcome. J Am Soc Nephrol. 2003;14:1022-30.
21. Neveu H, Kleinknecht D, Brivet F, Loirat P, Landais P. Prognostic factors in acute renal failure due to sepsis. Results of a prospective multicentre study. The French Study Group on Acute Renal Failure. Nephrol Dial Transplant. 1996;11:293-9.
22. Endre ZH. Renal ischemic preconditioning: finally some good news for prevention of acute kidney injury. Kidney Int. 2011;80:796-8.
23. Zimmerman RF, Ezeanuna PU, Kane JC, et al. Ischemic preconditioning at a remote site prevents acute kidney injury in patients following cardiac surgery. Kidney Int. 2011;80:861–7.
24. Venugopal V, Laing CM, Ludman A, Yellon DM, Hausenloy D. Effect of remote ischemic preconditioning on acute kidney injury in nondiabetic patients undergoing coronary artery bypass graft surgery: a secondary analysis of 2 small randomized trials. Am J Kidney Dis. 2010;56:1043-9.
25. Neonatal outcomes of extremely preterm infants from the NICHD Neonatal Research Network. Pediatrics. 2010;126:443-56.
26. Rocha G, Ribeiro O, Guimarães H. Fluid and electrolyte balance during the first week of life and risk of bronchopulmonary dysplasia in the preterm neonate. Clinics (Sao Paulo). 2010;65:663-74.
27. Lorenz JM, Kleinman LI, Kotagal UR, Reller MD. Water balance in very low-birth-weight infants: relationship to water and sodium intake and effect on outcome. J Pediatr. 1982;101:423-32.
28. Bell EF, Warburton D, Stonestreet BS, Oh W. Effect of fluid administration on the development of symptomatic patent ductus arteriosus and congestive heart failure in premature infants. N Engl J Med. 1980;302:598-604.
29. Arikan AA, Zappitelli M, Goldstein SL, Naipaul A, Jefferson LS, Loftis LL. Fluid overload is associated with impaired oxygenation and morbidity in critically ill children. Pediatr Crit Care Med. 2012;13:253-8.
30. Santschi M, Jouvet P, Leclerc F, et al. Acute lung injury in children: therapeutic practice and feasibility of international clinical trials. Pediatr Crit Care Med. 2010;11:681-9.
31. Oh W, Poindexter BB, Perritt R, et al. Association between fluid intake and weight loss during the first ten days of life and risk of bronchopulmonary dysplasia in extremely low birth weight infants. J Pediatr. 2005;147:786-90.
32. Bell EF, Acarregui MJ. Restricted versus liberal water intake for preventing morbidity and mortality in preterm infants. Cochrane Database Syst Rev. 2014;2014:CD000503.
33. Domenech P, Perez T, Saldarini A, Uad P, Musso CG. Kidney-lung pathophysiological crosstalk: its characteristics and importance. Int Urol Nephrol. 2017;49:1211-5.
34. Joannidis M, Forni LG, Klein SJ, et al. Lung-kidney interactions in critically ill patients: consensus report of the Acute Disease Quality Initiative (ADQI) 21 Workgroup. Intensive Care Med. 2020;46:654-72.
35. Barakat MF, McDonald HI, Collier TJ, Smeeth L, Nitsch D, Quint JK. Acute kidney injury in stable COPD and at exacerbation. Int J Chron Obstruct Pulmon Dis. 2015;10:2067-77.
36. Chertow GM, Christiansen CL, Cleary PD, Munro C, Lazarus JM. Prognostic stratification in critically ill patients with acute renal failure requiring dialysis. Arch Intern Med. 1995;155:1505-11.
37. van den Akker JP, Egal M, Groeneveld AB. Invasive mechanical ventilation as a risk factor for acute kidney injury in the critically ill: a systematic review and meta-analysis. Crit Care. 2013;17:R98.
38. Li X, Hassoun HT, Santora R, Rabb H. Organ crosstalk: the role of the kidney. Curr Opin Crit Care. 2009;15:481-7.

DOI: 10.4274/MMJ.galenos.2024.59683
Medeni Med J 2024;39:161-168

Original Article

AMPK Activation in TET2 Downregulated Leukemia Cells Upon Glutamine Limitation

TET2 Baskılanmış Lösemi Hücrelerinde Glutamine Kısıtlamasında AMPK Aktivasyonu

Ahsen Merve BAYRAK[1,2], **Burcu YUCEL**[2,3,4]

[1]Istanbul Medeniyet University Institute of Graduate Studies, Department of Molecular Medicine, Istanbul, Türkiye
[2]Istanbul Medeniyet University Faculty of Medicine, Department of Medical Biology, Istanbul, Türkiye
[3]Istanbul Medeniyet University, Science and Advanced Technologies Research Center (BILTAM), Istanbul, Türkiye
[4]Health Institutes of Türkiye (TUSEB), Türkiye Cancer Institute, Istanbul, Türkiye

ABSTRACT

Objective: Metabolic rewiring is a characteristic of cancer cells. Cancer cells require more nutrients for survival and proliferation. Although glutamine can be produced in cells via a series of enzymatic reactions, a group of cancer cells are dependent on extracellular glutamine for survival. TET2 plays a role in DNA demethylation and is a tumor suppressor gene. The *TET2* gene is frequently mutated in various cancers, including acute myeloid leukemia (AML). Our study aimed to investigate the association between TET2-knockdown AML cell line HL-60 cells and glutamine metabolism.

Methods: To evaluate the association between TET2 expression and glutamine limitation, TET2 was downregulated in HL-60 cells using shRNA plasmids. The proliferation of TET2-knockdown HL-60 cells was calculated in normal and glutamine-deficient medium. GLUL mRNA expression was investigated using quantitative reverse transcription polymerase chain reaction and protein levels were evaluated using immunoblotting.

Results: The numbers and viability of TET2-knockdown HL-60 cells were decreased in low glutamine-containing medium, but the viability of TET2-knockdown HL-60 cells was higher than that of control cells. GLUL mRNA expressions were increased in TET2- knockdown cells in low glutamine. In addition, P-AMPKα protein expression was increased in TET2-knockdown HL-60 cells in low glutamine-containing medium.

Conclusions: Our findings indicate that TET2-knockdown HL-60 cells may be more resistant to glutamine deprivation. In glutamine-deficient medium, the mRNA expression of glutamine synthetase is increased, which could be related to glutamine addiction in cells. In addition, low-glutamyl medium increased the P-AMPKα protein level in TET2-knockdown HL-60 cells.

Keywords: Glutamine metabolism, TET2 expression, AML, AMPK, shRNA-mediated gene silencing

ÖZ

Amaç: Metabolik yeniden programlama, kanser hücrelerinin ayırt edici bir özelliğidir. Kanser hücreleri, hayatta kalmak ve çoğalmak için tümör mikroçevresinden glukoz ve glutamin alımını artırır. Glutamin *de novo* sentezlenebilmesine rağmen, birçok kanser hücresi hayatta kalabilmek için hücre dışı glutamine bağımlıdır. DNA demetilasyonunda görev alan *TET2* geni, aynı zamanda bir tümör baskılayıcı gen olarak bilinir. *TET2* geni, akut miyeloid lösemi (AML) dahil olmak üzere çeşitli kanserlerde sıklıkla mutasyona uğrar. Çalışmamız, *TET2* geni baskılanmış AML hücre hattı HL-60 hücreleri ile glutamin metabolizması arasındaki ilişkiyi araştırmayı amaçladı.

Yöntemler: TET2 ekspresyonu ile glutamin sınırlaması arasındaki ilişkiyi değerlendirmek için *TET2* geni, shRNA plazmitleri kullanılarak HL-60 hücrelerinde baskılandı. TET2-baskılanmış HL-60 hücrelerinin hücre proliferasyonu, normal ve düşük glutamin ortamındaki hücre sayıları ile hesaplandı. mRNA ekspresyonlarındaki değişiklikler, kantitatif ters transkriptaz kullanılarak araştırıldı. GLUL, AMPK-α ve P-AMPKα protein ekspresyonu immünoblotlama ile değerlendirildi.

Bulgular: Düşük glutamin ortamında TET2-baskılanmış HL-60 hücrelerinin hücre sayıları ve hücre canlılığı azaldı. TET2-baskılanmış HL-60 hücrelerinin hücre canlılığının kontrol hücrelerinden daha yüksek olduğu bulundu. Düşük glutaminde TET2-baskılanmış hücrelerde GLUL mRNA ekspresyonunun arttığı bulundu. Ayrıca, düşük glutamin ortamında TET2- baskılanmış HL-60 hücrelerinde P-AMPKα protein ekspresyonunun arttığı bulundu.

Sonuçlar: Bulgularımız, TET2-baskılanmış HL-60 hücrelerinin, glutamin yoksunluğuna karşı daha dirençli olabileceğini ve düşük glutamin ortamının, HL-60 hücrelerinin glutamin bağımlılığı ile bağlantılı olarak, glutamin metabolizmasında belirli genlerin ekspresyonunu artırdığını göstermektedir. Ek olarak, düşük glutamin ortamı, TET2-baskılanmış HL-60 hücrelerinde P-AMPKα protein seviyesini artırdı.

Anahtar kelimeler: Glutamin metabolizması, TET2 ekspresyonu, AML, AMPK, shRNA aracılı gen susturma

Address for Correspondence: B. Yucel, Istanbul Medeniyet University Faculty of Medicine, Department of Medical Biology; Istanbul Medeniyet University, Science and Advanced Technologies Research Center (BILTAM); Health Institutes of Türkiye (TUSEB), Turkish Cancer Institute, Istanbul, Türkiye
E-mail: burcu.yucel@medeniyet.edu.tr **ORCID ID:** orcid.org/0000-0002-6599-4558

Received: 15 April 2024
Accepted: 08 July 2024
Online First: 09 August 2024

Cite as: Bayrak AM, Yucel B. AMPK Activation in TET2 Downregulated Leukemia Cells Upon Glutamine Limitation. Medeni Med J. 2024;39:161-168

INTRODUCTION

Cancer cells constantly modify their metabolism due to the increased need for nutrients for survival, and hematologic malignancies are not the exception of this phenomenon[1]. Acute myeloid leukemia (AML), a common type of acute leukemia in adults, is caused by abnormal proliferation and differentiation of hematopoietic progenitor cells[2].

To maintain energy homeostasis, 5'-adenosine monophosphate (AMP)-activated protein kinase (AMPK) controls ATP production and consumption[3]. AMPK is a serine/threonine kinase family member and a heterotrimeric protein complex consisting of three subunits, α, β- and γ-subunits. At low cellular energy levels, AMPK is activated by the phosphorylation of threonine 172 (Thr172) in the kinase domain of the α-subunit[3-5]. AMPK functions by phosphorylating downstream targets to suppress ATP-consuming pathways and increase ATP-producing pathways[6]. In addition to maintaining energy homeostasis, AMPK plays significant roles in tumorigenesis by regulating cellular growth, autophagy, inflammation, stress responses, and cell polarity[5,7].

Glutamine is crucial for nitrogen (in nucleotides and amino acid biosynthesis) and carbon (in lipid and ATP biosynthesis) sources and is thus highly demanded by rapidly proliferating cells[8-10]. Glutamine synthetase (GS), encoded by GLUL, synthesizes *de novo* glutamine from purines and pyrimidines in a highly controlled process[11]. Despite this process, a group of cancer cells have been shown to be addicted to extracellular glutamine[1,8,12].

TET2 is a member of the ten-eleven translocation protein family (TET1-3) and is a well-known tumor suppressor[13]. TET2, an Fe (II)- and α-ketoglutarate (α-KG)-dependent dioxygenase, modulates active DNA demethylation by oxidizing 5-methylcytosine (5-mC), which is methylated by DNA methyltransferase, to 5-hydroxymethylcytosine (5-hmC)[14,15]. The loss of TET2 function due to mutations is associated with DNA hypermethylation and therefore transcriptional reprograming that promotes leukemogenesis[16-18].

This study aimed to investigate the association between TET2 expression and glutamine metabolism in HL-60 cells. For this aim, an shRNA-mediated gene silencing method was applied to downregulate TET2 in the HL-60 cell line, and then cell proliferation, expression levels of the GLUL gene involved in glutamine metabolism, and AMPK activity were determined in glutamine-deficient medium.

MATERIALS and METHODS

Cell Culture

HL-60 cells were cultured in RPMI 1640 (Gibco, Thermo Fisher, USA) supplemented with 10% fetal bovine serum, 1% l-glutamine, and a mixture of 1% penicillin-streptomycin in a 5% CO_2-humidified atmosphere at 37 °C.

Glutamine Limitation

HL-60 cells were cultured in RPMI 1640 medium without glucose/glutamine (Cat. No. P04-17550, PAN-Biotech, Germany) supplemented with 10% FBS, 10 mM glucose, and 1% pen/strep. The amount of glutamine in the FBS is 50 mM. Glutamine was added to its conventional glutamine counterpart at a final concentration of 2 mM. Cells with/without glutamine were cultivated for 3 days. For cell counting, manual counting was performed using a hemocytometer, and the percentage of cell proliferation in glutamine-limited compared with the normal medium was calculated.

Downregulation of TET2 Expression

Two puromycin-resistant shRNA plasmids targeting TET2 were purchased from Qiagen to knockdown TET2 (Sure-Silencing shRNA plasmids, Cat No KH17943P). TET2-targeting shRNAs cloned in puromycin-resistant plasmids were transformed into DH5a-competent bacteria. Subsequently, HL-60 cells were transfected according to the shRNA plasmid manufacturer's protocol. Wild-type HL-60 cells were used as the control group. 0.5 µg plasmid was used for transfection. Puromycin selection was applied for 3 days, and the medium was replaced. quantitative reverse transcription polymerase chain reaction (qRT-PCR) was performed to confirm downregulation of TET2 expression.

CellTiter Cell Viability Assay

CellTiter-Glo® Luminescent Cell Viability Assay (Promega, USA) was used for ATP measurement. HL-60 control and TET2-downregulated cells were seeded at a concentration of 2500 cells/well and incubated for 96 h. After incubation, 40 µL of reagent was added to each well, and the mixture was mixed for 5 min on an orbital shaker. The luminescence values were measured using a Cytation 5 Cell Imaging Multi-Mode Reader (BioTek, USA).

Quantitative Reverse Transcription Polymerase Chain Reaction

Single-stranded cDNA was synthesized from total RNA using a High-Capacity RNA-to-cDNA Synthesis Kit

Table 1. The primers sequences.	
Gene	**Primer sequence (5'-3')**
TET2	F: TGTTAGAAAGGAGACCCGACTG R: TTCCATTCTGGAGCTTTGTAGC
GLUL	F: TGGGAACTGGAATGGTGC R: CGTTGATGTTGGAGGTTTCATG
RPLP0	F: AGCATCTACAACCCTGAAGTG R: AGCAAGTGGGAAGGTGTAATC

(Applied Biosystems, USA). SYBR Green PCR Master Mix was used for the qRT-PCR reactions on the RotorGene (Qiagen) instrument. The primers listed in Table 1 were used to analyze TET2 and GLUL mRNA expression. The relative gene expression level was determined by comparing with RPLP0. Fold changes in mRNA levels were calculated using ΔΔCt method.

Western Blotting

After 72 h of culture with/without glutamine medium, TET2-downregulated HL-60 and control HL-60 cell lines were harvested, then washed with 1× PBS and lysed. BCA Protein Assay Kit (Pierce, Thermo Fisher, USA) was used to determine protein concentrations and 10 µg of proteins were electrophoresed in a 12% polyacrylamide gel. AMPKα, P-AMPKα and β-actin primary antibodies with HRP-conjugated secondary antibodies from Cell Signaling Technology (Beverly, MA) were used for blotting. The membranes visualized with an enhanced chemiluminescence substrate (SuperSignal, Thermo Fisher, USA) using the Azure C300 gel imaging system. Quantification of the bands in the blots was performed using the ImageJ software.

Statistical Analysis

The results are expressed as means ± standard deviation. Student's t-test with Welch's correction was used for the statistical analysis of the comparisons of data. Statistical analysis and graphing were performed using GraphPad V9 (GraphPad Software, San Diego, CA, USA). All experiments were performed in triplicate except for the viability experiment with quintuple technical replicates.

RESULTS

Glutamine Limitation Increases TET2 mRNA Expression in HL-60 Cells

We evaluated TET2 expression in response to glutamine limitation. It was found that in 50 µM glutamine-containing medium, TET2 mRNA expression was nearly doubled compared with that in 2 mM glutamine-containing normal medium (*p<0.05) (Figure 1).

Downregulation of TET2

As TET2 mRNA expression was found to increase in glutamine-deficient medium (50 µM glutamine), we downregulated its expression. TET2 mRNA expression was downregulated by approximately 50% compared with the control plasmid using two different shRNAs (**p<0.01, ***p<0.001) (Figure 2).

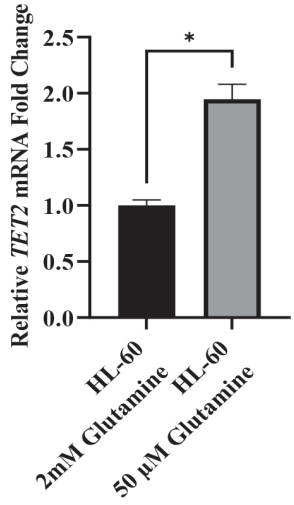

Figure 1. Effect of glutamine limitation on TET2 mRNA expression. TET2 mRNA expression was increased by nearly 2-fold in low glutamine-containing medium in HL-60 cells. Data are presented as mean ± SD, *p<0.05.

SD: Standard deviation

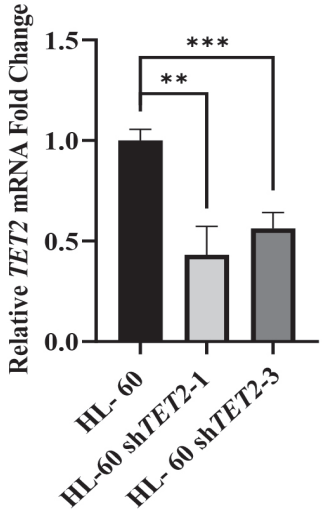

Figure 2. shRNA-mediated downregulation of TET2 mRNA expression. Two different shRNA decreased mRNA expression to half that of control HL-60 cells. Data presented as mean ± SD, **p<0.01, ***p<0.001.

SD: Standard deviation

Cell Proliferation in Glutamine-deficient Medium

In comparison with the control group, total cell number declined in HL-60 shTET2-1 cells in 50 μM glutamine (*p<0.05), whereas it was slightly increased in HL-60 sh*TET2*-3 cells, which was not statistically significant (^{ns}p≥0.05) (Figure 3).

Cell Viability in Low-glutamine Medium

In glutamine-deficient medium, the survival percentage decreased from 100% to 52.79% in the control group, to 69.81% in HL-60 shTET2-1 cells, and to 70.53% in HL-60 shTET2-3 cells (shTET2-1; *p<0.05, and shTET2-3; **p<0.01). Additionally, we found that cell viability decreased in the glutamine-deficient condition compared with the normal concentration (Figure 4).

GLUL mRNA and Protein Expression in TET2-knockdown HL-60 Cells Under Low Glutamine

GLUL mRNA expression was increased in all cells in glutamine-deficient medium (Figure 5A). Although the increase in low glutamine levels in HL-60 shTET2-1 cells was statistically significant (*p<0.05), the increase in HL-60 and HL-60 shTET2-3 cells was not statistically significant (^{ns}p≥0.05). Moreover, GS protein expression was increased in all cell lines under glutamine-deficient conditions (Figure 5B). Additionally, GS protein expression in TET2-knockdown HL-60 cells was remotely increased in cells incubated with low glutamine compared with control cells, which was not statistically significant (^{ns}p≥0.05) (Figure 5C).

AMPK-α and Phospho-AMPK-α Protein Expressions in TET2-knockdown HL-60 Cells Under Low Glutamine Condition

Immunoblotting was used to assess the regulation of AMPK-α and P-AMPK-α protein expressions in the low glutamine medium. To confirm increased activation of AMPK-α, oligomycin complex (Cayman Chemical, USA) was added to HL-60 cells at a ratio of 1:1000 for 3 days in normal and low glutamine medium. AMPK-α protein expression was examined to control AMPK activity in the HL-60 cell line (Figures 6A, B).

P-AMPK-α protein expression was increased at low glutamine levels in all three cell lines, although statistically significant only in HL-60 shTET2-3 cells (Figures 6A, C). P-AMPK-α protein expression in TET2-knockdown HL-60 cells was increased compared with

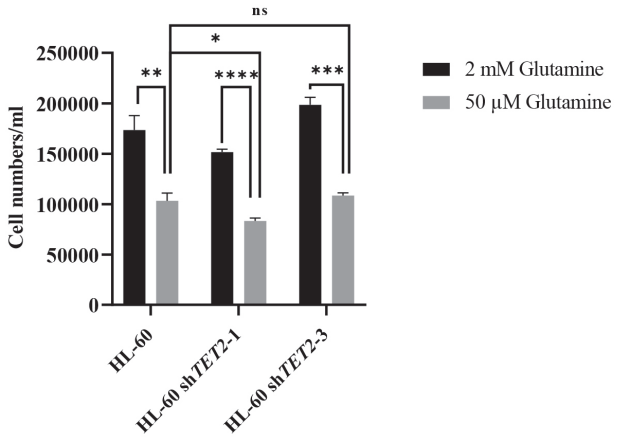

Figure 3. Cell proliferation in normal (2 mM) and low-glutamine (50 μM) medium. Cell proliferation was calculated using cell numbers. Cells were plated at a concentration of 20,000 cells/mL and cultured for 72 h. Then, cells were washed and counted using a hemacytometer. Cell numbers decreased at low glutamine concentrations in all cell lines. In the presence of low glutamine, HL-60 shTET2-1 cell counts and HL-60 shTET2-3 cell counts increased. Data are presented as mean ± SD. nsp≥0.05, *p<0.05, **p<0.01, ***p<0.001, ****p<0.0001.

SD: Standard deviation

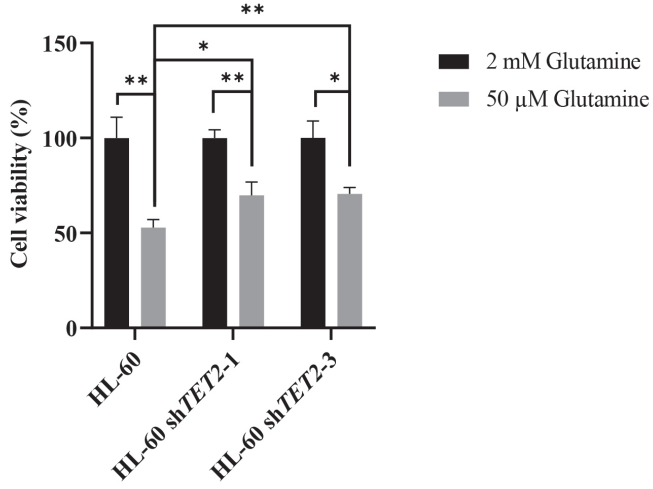

Figure 4. Effect of low glutamine medium on cell viability in TET2-downregulated HL-60 cells. Cells were plated at a concentration of 20,000 cells/mL and cultured for 4 days. Cell viability was assessed using the CellTiter-Glo® Luminescent Cell Viability Assay. shRNA1 and shRNA2 OD values compared with control cells in percentage. Cell viability was found to be higher in TET2-downregulated HL-60 cells in low glutamine-containing medium compared to control cells. Data are presented as mean ± SD, *p<0.05, **p<0.01.

SD: Standard deviation

the control cell line in both normal and low glutamine media. In addition, we found that P-AMPK-α expression increased in TET2-knockdown cells under low glutamine compared to normal glutamine.

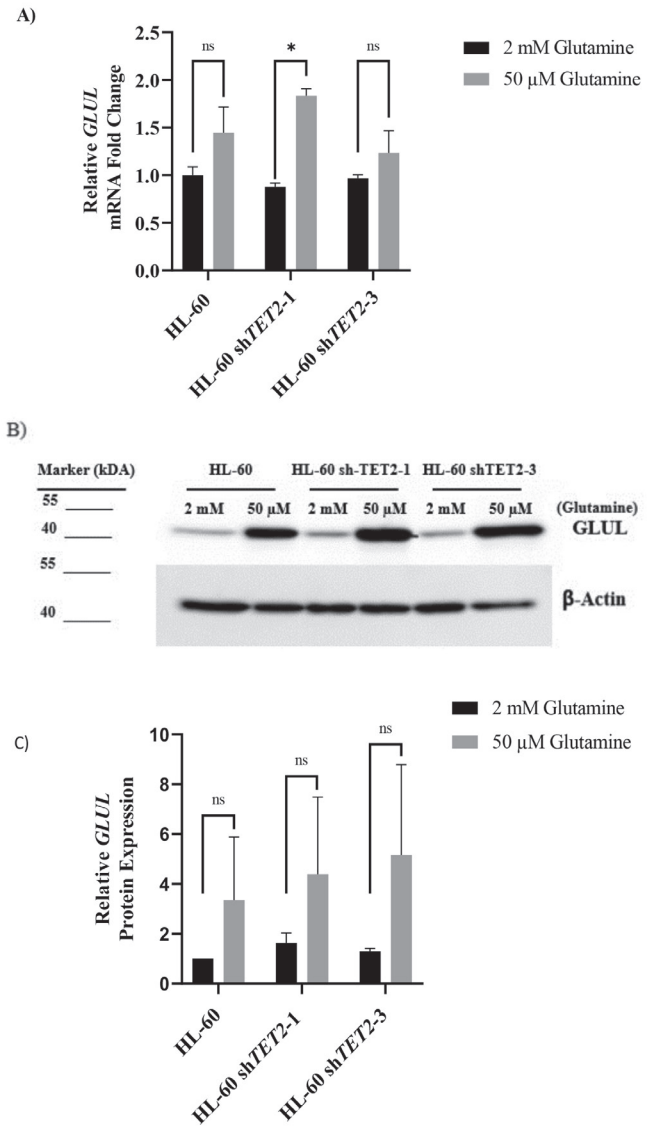

Figure 5. Glutamine synthetase (GLUL) mRNA expression and protein levels of TET2-knockdown HL-60 cells in low glutamine medium. **A)** GS-encoding relative GLUL mRNA expression levels in 2 mM and 50 µM glutamine-containing medium. **B)** Western blot analysis and **C)** Quantification of GLUL protein expression were performed in TET2-knockdown and control HL-60 cells cultured in medium containing 2 mM and 50 µM glutamine. β-actin was used as a housekeeping protein. Data are presented as mean ± SD, $^{ns}p \geq 0.05$, $p < 0.05$, $^{**}p < 0.01$.

SD: Standard deviation

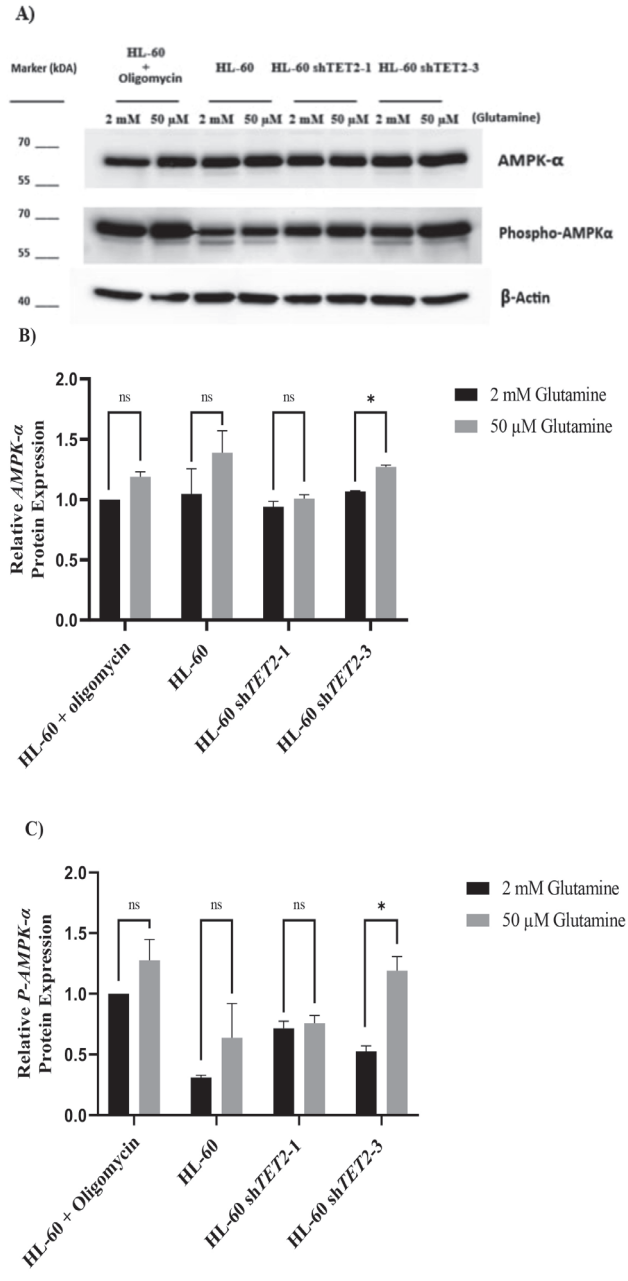

Figure 6. A) Immunoblotting and quantification of **B)** AMPK-α and **C)** Phospho-AMPK-α proteins were performed in TET2-knockdown and control HL-60 cells cultured in medium containing 2 mM and 50 µM glutamine. Control cells were treated with oligomycin to confirm the increased activation of AMPK-α and P-AMPK-α. P-AMPK-α protein expression was increased in TET2-knockdown cells in low glutamine compared with normal glutamine levels, as well as in control cells. α-actin was used as a housekeeping protein. Data are presented as mean ± SD, $^{ns}p \geq 0.05$.

SD: Standard deviation

DISCUSSION

Glutamine plays an important role in ATP synthesis as well as most carbon and nitrogen metabolism for cancer cell proliferation[9]. Low glutamine levels have been observed in tumor microenvironments *in vivo* and *in vitro* in various types of cancer. Therefore, cancer cells adapt their metabolism to their environment for survival and proliferation[12,19]. Glutamine deprivation in many cancer cell types, including AML, has been shown to cause cell death through glutamine addiction[20].

A study with 4 different AML cell lines showed that the cell line most addicted to glutamine was HL-60 cells, and the proliferation of HL-60 cells was reduced by glutamine restriction and rescued by the addition of the tricarboxylic acid cycle intermediate oxaloacetic acid[21]. It was shown that a group of AML cell lines become addicted to glutamine for cell proliferation, and the level of glucose in the tumor microenvironment does not affect this addiction[12]. In addition to glutamine deprivation, inhibition of glutamine metabolism by the glutaminase inhibitor CB-839 reduced antioxidant glutathione production, leading to mitochondrial ROS accumulation and apoptotic cell death in several AML cell lines[22].

The *TET2* gene encodes a member of the TET family of enzymes that alter the epigenetic state of DNA by converting 5-mC to 5-hmC. Somatic loss-of-function mutations in TET2 are associated with poor prognosis and advanced disease progression in myelodysplastic syndromes, AML, and chronic myelomonocytic leukemia[17,23]. Loss of TET2 function models have shown that TET2 plays a role in the regulation of myeloid progenitor cell proliferation and differentiation[24].

This study found an almost 2-fold increase in TET2 mRNA expression in HL-60 cells in low glutamine medium (Figure 1). TET2 expression was reduced in HL-60 cells using two different shRNA-mediated plasmids (Figure 2), and cell proliferation and viability were assessed under normal and low glutamine conditions. Cell counts were decreased in both control and TET2-downregulated cells in glutamine-deficient medium (Figure 3). In both normal and low glutamine media, HL-60 shTET2-1 cells showed less proliferation than control cells. In contrast, the opposite result was observed in HL-60 shTET2-3 cells. Furthermore, the viability of TET2-downregulated HL-60 cells in low glutamine-containing medium was higher than that of control HL-60 cells. Our results suggest that downregulation of TET2 expression in HL-60 cells is resistant to glutamine deficiency.

In a recent study, TET2 expression in the K562 cell line was downregulated by the shRNA-mediated system, and it was found that downregulation of TET2 did not change cell proliferation, but TET2-downregulated K562 cells were more resistant to CAPE treatment[25]. In a study of SUM149 triple-negative breast cancer cells, it was shown that metabolically adaptable SUM149-MA cells obtained by culturing SUM149 cells in a medium lacking glutamine had a 90% lower TET2 protein level and selected an undifferentiated therapy-resistant phenotype similar to that of TET2-mutant cancer[26].

Under normoxic conditions (20% O_2), the HepG2 human hepatoma cell line was found to increase TET2 and TET3 mRNA levels when cultured with low glucose (5 mM) or glutamine (0.5 mM). In hypoxic conditions (1% O_2), the mRNA levels of *TET* genes decreased more in the presence of low glucose than in the presence of low glutamine[27].

The GS enzyme synthesizes glutamate from glutamate and ammonia in an ATP-dependent manner[28]. High GLUL expression is linked to poor prognosis in liver cancer, ovarian cancer, glioblastoma, and hepatocellular carcinoma[12,29,30]. In addition, when the *GLUL* gene was knocked out in the HL-60 cell line, it was found that GLUL-knockout cells were shown to have decreased cell viability in both glucose- and glutamine-deficient media[12].

Our results showed that in low glutamine-containing media, GLUL mRNA expression was elevated in both TET2-knockdown HL-60 cells and control cells. However, the change was significant only in HL60 shTET2-1 cells (Figure 5A). The differences in GLUL mRNA expression levels between HL-60 shTET2-1 and HL-60 shTET2-3 cells were attributed to variations in the rate of TET2 expression knockdown. Furthermore, our immunoblotting results confirmed the qPCR results, showing that the GLUL protein level was increased in all cells in low glutamine-containing medium, and the increase in GLUL expression was higher in TET2-knockdown cells (Figure 5B).

It has been shown that AMPK alters DNA methylation by phosphorylating TET2 and plays an important role in cell differentiation[31,32]. Recently, AMPK was shown to phosphorylate TET2 at serine 99. However, hyperglycemia-mediated AMPK inactivation was found to result in the inhibition of AMPK-mediated TET2 phosphorylation and increased calpain-mediated degradation. Treatment with metformin increased 5-hmC levels and suppressed tumor growth by maintaining AMPK-mediated TET2 phosphorylation, indicating the tumor suppressor role

of TET2[31]. Furthermore, a study of monocytic U937 cells showed that it activates AMPK and adaptive mechanisms to overcome glutamine deficiency in response to glutamine starvation[33].

In endometrial carcinoma, silencing of *AMPK* gene expression using siRNA has been found to significantly decrease TET2 expression and 5-hmC levels, and metformin treatment regulates TET2 expression by activating AMPK. In addition, siRNA-mediated TET2 knockdown increased the proliferation of cancer cells[34]. In human AML U937 cells, exposure to malignant progression-inducing hydroquinone (HQ) increased AMPK activity, resulting in increased TET2 and FOXP3 expression in both U937 and U937/HQ cells[35].

We determined higher P-AMPK-α protein levels in TET2-downregulated HL-60 cells than in control cells in low glutamine-containing medium (Figure 6). Therefore, we speculate that the knockdown of *TET2* gene expression in HL-60 cells may increase the energy demand of cells in low glutamine-containing media. In the literature, it has been shown that TET2 expression is regulated by glucose-dependent AMPK activity[31]. Our results suggest that, in addition to the literature, a low-glutamine medium may regulate TET2 expression by activating AMPK.

CONCLUSION

Our findings indicate that the knockdown of *TET2* gene expression in HL-60 cells treated with shRNA reduced cell viability and proliferation in low glutamine-containing media. Furthermore, cell viability in TET2-downregulated cells was higher in low glutamine concentrations than in control HL-60 cells. We also found that GLUL expression and P-AMPK-α protein levels were increased in TET2-downregulated HL-60 cells in low glutamine concentrations. In further studies, TET2 expression can be completely silenced by the *CRISPR/Cas9* gene editing method, and the mRNA expression and protein levels of genes related to glutamine metabolism, such as GLUL, GLS1, GLS2, and GLUD1, can also be examined. To further investigate the association between TET2 and AMPK, it is necessary to determine which TET2 residue is phosphorylated by AMPK in low-glucose media. In TET2-downregulated HL-60 cells, 5-hmC levels should be assessed in normal and low-glucose media.

Ethics

Ethics Committee Approval: Our research is conducted only with cell lines *in vitro* conditions. Thus, no ethical approval is required.

Informed Consent: No informed consent is required.

Author Contributions

Design: B.Y., Data Collection and/or Processing: A.M.B., Analysis and/or Interpretation: A.M.B., B.Y., Literature Search: A.M.B., B.Y., Writing: A.M.B., B.Y.

Conflict of Interest: The authors have no conflict of interest to declare.

Financial Disclosure: The authors are grateful to the Scientific and Technological Research Council of Türkiye (TÜBİTAK) 3001-Initial R&D Projects Support Program (Grant #217S792) for financial support.

REFERENCES

1. Nguyen TL, Durán RV. Glutamine metabolism in cancer therapy. Cancer Drug Resistance. 2018;1:126-38.
2. Cheng Y, Su Y, Wang S, et al. Identification of circRNA-lncRNA-miRNA-mRNA Competitive Endogenous RNA Network as Novel Prognostic Markers for Acute Myeloid Leukemia. Genes (Basel). 2020;11:868.
3. Carling D. AMPK signalling in health and disease. Curr Opin Cell Biol. 2017;45:31-37.
4. Mihaylova MM, Shaw RJ. The AMPK signalling pathway coordinates cell growth, autophagy and metabolism. Nat Cell Biol. 2011;13:1016-23.
5. Rehman G, Shehzad A, Khan AL, Hamayun M. Role of AMP-activated protein kinase in cancer therapy. Arch Pharm (Weinheim). 2014;347:457-68.
6. Russell FM, Hardie DG. AMP-Activated Protein Kinase: Do We Need Activators or Inhibitors to Treat or Prevent Cancer? Int J Mol Sci. 2020;22:186.
7. Jacquel A, Luciano F, Robert G, Auberger P. Implication and Regulation of AMPK during Physiological and Pathological Myeloid Differentiation. Int J Mol Sci. 2018;19:2991.
8. Cluntun AA, Lukey MJ, Cerione RA, Locasale JW. Glutamine Metabolism in Cancer: Understanding the Heterogeneity. Trends Cancer. 2017;3:169-80.
9. Li T, Copeland C, Le A. Glutamine Metabolism in Cancer. Adv Exp Med Biol. 2021;1311:17-38.
10. Jin J, Byun JK, Choi YK, Park KG. Targeting glutamine metabolism as a therapeutic strategy for cancer. Exp Mol Med. 2023;55:706-15.
11. Cruzat V, Macedo Rogero M, Noel Keane K, Curi R, Newsholme P. Glutamine: Metabolism and Immune Function, Supplementation and Clinical Translation. Nutrients. 2018;10:1564.
12. Yücel B, Ada S. Leukemia Cells Resistant to Glutamine Deprivation Express Glutamine Synthetase Protein. Turk J Haematol. 2022;39:22-8.
13. Lee M, Li J, Li J, et al. Tet2 Inactivation Enhances the Antitumor Activity of Tumor-Infiltrating Lymphocytes. Cancer Res. 2021;81:1965-76.
14. Liu X, Wang X, Liu N, et al. TET2 is involved in DNA hydroxymethylation, cell proliferation and inflammatory response in keratinocytes. Mol Med Rep. 2020;21:1941-9.

15. Feng Y, Li X, Cassady K, Zou Z, Zhang X. TET2 Function in Hematopoietic Malignancies, Immune Regulation, and DNA Repair. Front Oncol. 2019;9:210.
16. Jiang S. Tet2 at the interface between cancer and immunity. Commun Biol. 2020;3:667.
17. Cimmino L, Dolgalev I, Wang Y, et al. Restoration of TET2 Function Blocks Aberrant Self-Renewal and Leukemia Progression. Cell. 2017;170:1079-95.
18. Stölzel F, Fordham SE, Nandana D, et al. Biallelic TET2 mutations confer sensitivity to 5'-azacitidine in acute myeloid leukemia. JCI Insight. 2023;8:e150368.
19. Cairns RA, Harris IS, Mak TW. Regulation of cancer cell metabolism. Nat Rev Cancer. 2011;11:85-95.
20. Kim GW, Lee DH, Jeon YH, et al. Glutamine Synthetase as a Therapeutic Target for Cancer Treatment. Int J Mol Sci. 2021;22:1701.
21. Goto M, Miwa H, Shikami M, et al. Importance of glutamine metabolism in leukemia cells by energy production through TCA cycle and by redox homeostasis. Cancer Invest. 2014;32:241-7.
22. Gregory MA, Nemkov T, Park HJ, et al. Targeting Glutamine Metabolism and Redox State for Leukemia Therapy. Clin Cancer Res. 2019;25:4079-90.
23. Wang Z, Liu F, Fan N, et al. Targeting Glutaminolysis: New Perspectives to Understand Cancer Development and Novel Strategies for Potential Target Therapies. Front Oncol. 2020 Oct 26;10:589508.
24. Ganguly BB, Kadam NN. Mutations of myelodysplastic syndromes (MDS): An update. Mutation Research/Reviews in Mutation Research. 2016;769:47-62.
25. Yucel B, Fural MA, Sonmez B, Bektas O, Sonmez M. Investigation of the association between tet2 expression and response to cape. International Journal of Hematology and Oncology. 2021;31:146-52.
26. Singh B, Sarli VN, Kinne HE, Shamsnia A, Lucci A. Evaluation of 6-mercaptopurine in a cell culture model of adaptable triple-negative breast cancer with metastatic potential. Oncotarget. 2019;10:3681-93.
27. Lai AG, Forde D, Chang WH, et al. Glucose and glutamine availability regulate HepG2 transcriptional responses to low oxygen. Wellcome Open Res. 2018;3:126.
28. Zhang J, Pavlova NN, Thompson CB. Cancer cell metabolism: the essential role of the nonessential amino acid, glutamine. EMBO J. 2017;36:1302-15.
29. Cha YJ, Kim ES, Koo JS. Amino Acid Transporters and Glutamine Metabolism in Breast Cancer. Int J Mol Sci. 2018;19:907.
30. Fan S, Wang Y, Zhang Z, et al. High expression of glutamate-ammonia ligase is associated with unfavorable prognosis in patients with ovarian cancer. J Cell Biochem. 2018;119:6008-15.
31. Wu D, Hu D, Chen H, et al. Glucose-regulated phosphorylation of TET2 by AMPK reveals a pathway linking diabetes to cancer. Nature. 2018;559:637-41.
32. Zhang T, Guan X, Choi UL, et al. Phosphorylation of TET2 by AMPK is indispensable in myogenic differentiation. Epigenetics Chromatin. 2019;12:32.
33. Eliasen MM, Winkler W, Jordan V, et al. Adaptive cellular mechanisms in response to glutamine-starvation. Front Biosci. 2006;11:3199-211.
34. Zhang J, Kuang L, Li Y, et al. Metformin Regulates TET2 Expression to Inhibit Endometrial Carcinoma Proliferation: A New Mechanism. Front Oncol. 2022;12:856707.
35. Chiou JT, Huang CH, Lee YC, et al. Compound C induces autophagy and apoptosis in parental and hydroquinone-selected malignant leukemia cells through the ROS/p38 MAPK/AMPK/TET2/FOXP3 axis. Cell Biol Toxicol. 2020;36:315-31.

DOI: 10.4274/MMJ.galenos.2024.87094
Medeni Med J 2024;39:169-174

Original Article

The Anti-proliferative Effect of a Novel Glutaminase Inhibitor IN-3 on Prostate Cancer Cells

Yeni Bir Glutaminaz Baskılayıcı Olan IN-3'ün Prostat Kanseri Hücrelerinde Büyüme Karşıtı Etkisi

Ummuhan DEMIR[1,2], Ayse Busranur CELIK[2,3]

[1]Istanbul Medeniyet University Faculty of Engineering and Natural Sciences, Department of Molecular Biology and Genetics, Istanbul, Türkiye
[2]Istanbul Medeniyet University, Science and Advanced Technologies Research Center (BILTAM), Istanbul, Türkiye
[3]Health Sciences University Faculty of Medicine, Department of Molecular Biology and Genetics, Istanbul, Türkiye

ABSTRACT

Objective: This study aimed to evaluate anti-cancer potential of a novel glutaminase (GLS) inhibitor IN-3 in prostate cancer cells.

Methods: The cell viability upon IN-3 treatment was examined using crystal violet staining and IC_{50} values were calculated for cancer cell lines PC-3 and LNCaP and normal fibroblasts CCD1072sk. The expression levels of GLS isoforms were determined by real-time polymerase chain reaction after IN-3 treatment. The metastatic prostate cancer dataset was downloaded from C-Bioportal and the expressions of GLS isoforms were analyzed.

Results: The IC_{50} values of IN-3 for LNCaP, PC-3 and CCD1072sk were 2.13, 6.14 and 15.39 μM respectively. The dose dependent effect of IN-3 was evident even in low concentration with 1 μM in LNCaP and 2 μM in PC-3 and these anti-proliferative effects of IN-3 were highly significant with p-values lower than 0.0001. The treatment of PC-3 cells with 10 μM IN-3 elevated the expression of kidney type GLS isoform of GLS1 but not GLS2. Comparison of metastatic and localized prostate cancer tissues showed that GLS1 was highly expressed not only in primary but also in metastatic prostate cancer tissues. GLS1 expression was significantly higher than GLS2 expression with p-values lower than 0.001.

Conclusions: The GLS inhibitor IN-3 may be a potent anti-cancer agent in prostate cancer by demonstrating its differential effect between cancer and normal cells. Further studies are warranted to elucidate its drug potential in prostate cancer.

Keywords: Prostate cancer, GLS1, IN-3

ÖZ

Amaç: Bu çalışma yeni bir glutaminaz (GLS) baskılayıcı olan IN-3'ün prostat kanseri hücrelerinde kanser karşıtı etkisini değerlendirmeyi amaçlamaktadır.

Yöntemler: IN-3'ün hücre canlılığına etkisi kristal viyole boyaması ile incelenerek PC-3 ve LNCaP prostat kanseri hücrelerinde ve normal fibroblastik CCD1072sk hücrelerinde IC_{50} değerleri hesaplanmıştır. GLS izoformlarının ekspresyon düzeyleri gerçek zamanlı polimeraz zincir reaksiyonu ile belirlenmiştir. C-Bioportal veri bankasından metastatik prostat kanseri verileri indirilerek GLS izoformlarının ekspresyonları analiz edilmiştir.

Bulgular: LNCaP, PC-3 ve CCD1072sk için IC_{50} değerleri sırasıyla 2,13, 6,14 ve 15,39 μM'dır. LNCaP hücrelerinde 1 ve PC3 hücrelerinde 2 μM gibi düşük dozlarda bile IN-3'ün doz bağımlı etkisi belirgindir ve IN-3'ün büyüme karşıtı etkisi 0,0001'in altında p-değeri ile yüksek derecede anlamlıdır. PC-3 hücrelerinin 10 μM IN-3 ile muamelesi sonrası GLS1'in böbrek tipi GLS izoformunun ekspresyonu artarken GLS2 ekspresyonu değişmemiştir. Metastatik ve lokalize prostat kanseri örneklerinin karşılaştırılması göstermiştir ki; GLS1 sadece primer prostat kanseri örneklerinde değil metastatik prostat kanseri örneklerinde de yüksek düzeyde eksprese edilmektedir. GLS1 ekspresyonu 0,001'in altında p-değeri ile GLS2 ekspresyonundan anlamlı şekilde yüksektir.

Sonuçlar: GLS baskılayıcı IN-3 normal ve kanser hücrelerinde farklı etki göstermesi sebebiyle önemli bir kanser karşıtı ajan olabilir. Prostat kanserinde ilaç olma potansiyelinin ortaya çıkarılması için daha ileri çalışmalar yapılması gerekmektedir.

Anahtar kelimeler: Prostat kanseri, GLS1, IN-3

Address for Correspondence: U. Demir, Istanbul Medeniyet University Faculty of Engineering and Natural Sciences, Department of Molecular Biology and Genetics; Istanbul Medeniyet University, Science and Advanced Technologies Research Center (BILTAM), Istanbul, Türkiye
E-mail: ummuhan.demir@medeniyet.edu.tr **ORCID ID:** orcid.org/0000-0002-4155-2325

Received: 09 March 2024
Accepted: 10 July 2024
Online First: 23 July 2024

Cite as: Demir U, Celik AB. The Anti-proliferative Effect of a Novel Glutaminase Inhibitor IN-3 on Prostate Cancer Cells. Medeni Med J. 2024;39:169-174

INTRODUCTION

The metabolic vulnerabilities of cancer cells have been gaining much more attention recently because of the promising new treatment options. The dependence of cancer cells on glutamine has long been known. Although glutamine is a non-essential amino-acid meaning that there is cell-intrinsic biosynthesis of glutamine, the cancer cells highly depend on external glutamine supply. Indeed, from the very early stages of *in vitro* cancer research, glutamine-supplemented growth media have been shown to promote better growth of cancer cells. Glutamine is utilized by the cancer cells for several purposes such as energy production, nucleotide and amino acid biosynthesis. Glutaminase (GLS) converts glutamine to glutamate to further fuel Krebs cycle with α-ketoglutarate[1]. GLS has two isoforms as GLS1 and GLS2. GLS1 has been commonly studied in several cancer types with an oncogenic role. However, GLS2 is known for tumor suppressor function and its expression is low in cancer cells. GLS1 is represented with two isoforms produced from the same gene with an alternative splicing event. Kidney type glutaminase (KGA) isoform has lower catalytic activity than glutaminase C (GAC) isoform[2].

First inhibitor reported in the literature to target GLS was bis-2-(5-phenylacetamido-1, 3, 4-thiadiazol-2-yl) ethyl sulphide (BPTES). Because of its promising anti-cancer effect both in *in vitro* and *in vivo*, more potent derivatives of BPTES have been developed. Telaglenastat (CB839) is a BPTES derivative already progressing to the clinical trials[3]. There are several cancers, including breast, kidney, colon and leukemia, where promising results of combination therapies with CB839 have been shown[4,5].

Several therapy options are available when prostate cancer (PCa) is in early, localized stage. However, in advanced stage, castration resistant prostate cancer (CRPC) and metastatic CRPC (mCRPC) emerge and the therapy options for them are limited. Therefore, many current studies have been prospecting single or combination therapy alternatives in mCRPC.

In our study, anti-proliferative effect of glutaminase inhibitor 3 (IN-3) was explored in cells for the first time in the literature. To understand the differential effect of IN-3 inhibition on expression of GLS isoforms, real-time polymerase chain reaction (PCR) analysis was performed. The expression levels of GLS isoforms were also investigated in PCa tissue samples using publicly available datasets.

MATERIALS and METHODS

Chemicals

GLS-IN-3 was supplied by Medchem. The primary stock solution was prepared by diluting the compound in dimethyl sulfoxide (DMSO) to a concentration of 20 mM and stored at -20 °C. The final concentrations of 1 µM, 2 µM, 5 µM, and 10 µM were used to treat the cells.

Cell Culture

PC-3 cell line is a bone metastatic and LNCaP cell line is a lymph node metastatic PCa cell lines. PC-3 and LNCaP cells were cultured in Roswell Park Memorial Institute 1640 medium supplemented with 10% fetal bovine serum (FBS) and 1% penicillin-streptomycin. Normal human fibroblast cells CCD-1072Sk was cultured in Dulbecco's modified Eagle's medium with 10% FBS and 1% penicillin-streptomycin. The cells were incubated at 37 °C and 5% CO_2 conditions.

Cell Viability

The cell viability was determined using the crystal violet staining. Firstly, 6×10^3 cells for PC-3 and 12×10^3 cell for LNCaP and CCD-1072sk were seeded per well in 96-well plate and incubated at 37 °C with 5% CO_2 for 24 hours. Afterwards, GLS-IN-3 was applied to the cells at three different concentrations with three technical replicates. 2 µM, 5 µM, and 10 µM for PC-3 cells and 1 µM, 5 µM, and 10 µM for LNCaP and CCD-1072Sk cells were used as final concentrations. An equal volume of DMSO was added as a control, and the cells were incubated for 48 hours. Then, the medium was removed, and the cells were washed with 200 µL of phosphate buffer saline (PBS). 50 µL of 0.05% crystal violet solution was added to the wells and incubated for 20 minutes. The dye was discarded, and the cells were washed first with 200 µL of PBS and then with 400 µL of distilled water. Finally, 200 µL methanol was added to the wells and incubated for another 20 minutes to release the dye, followed by measuring the absorbance at 590 nm in a plate-based spectrophotometer.

RNA Extraction, cDNA Synthesis and qRT-PCR

For RNA isolation, 2×10^5 PC-3 cells were seeded per well in a 6-well plate and incubated at 37 ˚C with 5% CO_2 for 24 hours. After 24 hours, 10 µM of GLS-IN-3 was applied to the cells and an equal amount of DMSO was used as a control. After 24-hour incubation, the cell pellets were collected and stored at -80 ˚C. After three biological replicates, RNA was isolated by Innu PREP RNA Mini Kit 2.0 (Analytik Jena, Cat #845-KS-2040050) and stored at -80 ˚C. The cDNA was synthesized according

to the Gscript First-Strand Synthesis Kit (Gene DireX, Cat #MB305-0050) and stored at -20 ˚C. PCR reaction was set up for each sample with two technical replicates, following the instructions provided in the GoTaq® qPCR Master Mix manual (Promega, Cat #A6001). The cDNA was diluted at a 1:5 ratio. The sequences for the primers GAC, KGA, and GLS2 were selected from the literature (Table 1), and were synthesized by Bioligo. As a housekeeping gene, B-Actin was used. The expression levels of GAC, KGA, and GLS2 were calculated with the ΔΔCt method.

Statistical Analysis

The statistical analyses were conducted using GraphPad Prism. Student's t-test was performed to assess the differences between groups. The statistical significance was considered at p-values less than 0.05 (*: p<0.05, **: p<0.01, ***: p<0.001, and ****: p<0.0001).

Analysis of GLS Expression

The mRNA data of GLS were downloaded from C-Bioportal database[6]. Fred Hutchinson 2016 data were analyzed to compare the expressions of GLS1 and GLS2 in primary and metastatic samples using SPSS. Wilcoxon signed rank test was applied to determine statistical significance between expression of GLS1 and GLS2.

RESULTS

Cytotoxic Effect of GLS-IN-3

The cytotoxic effect of GLS-IN-3 on PCa cells (PC-3 and LNCaP) and normal cell (CCD 1072sk) has been examined. IC_{50} graphs and dose-dependent cell viability graphs were presented in Figure 1. All applied doses diminished the cell viability of PC-3 and LNCaP cancer cells in a highly significant manner with p-values lower than 0.001 according to Student t-test. The IC_{50} values for PC-3, LNCaP, and CCD1072sk cells were determined as 6.14 μM, 2.13 μM, and 15.39 μM, respectively (Table 2). IN-3 decreased the viability of highly aggressive bone metastatic PC-3 cells and lymph node metastatic LNCaP cells in a lower concentration than the normal CCD1072sk cells.

Effect of GLS-IN-3 on the Expression of GLS Isoforms

After the application of 10 μM GLS-IN-3 to PC-3 cells, the expression levels of *KGA*, *GAC*, and *GLS-2* genes were examined (Figure 2). In PC-3 cells, GLS2 isoform was expressed lower than both KGA and GAC isoforms. GAC isoform is the highly expressed form in PC-3 cells. Upon IN-3 treatment, while GLS2 expression stayed stable, the fold changes in the expression of KGA and GAC were 2.64 and 1.5 respectively.

mRNA Expression Data of GLS1 and GLS2 in mCRPC Tissue

mRNA expression levels of GLS1 and GLS2 in primary and metastatic PCa tissue samples were analyzed (Figure 3). Primary PCa tissue and matched metastatic samples from 16 patients were included. GLS1 expression was significantly higher than GLS2 expression both in primary and metastatic PCa tissue samples according to Wilcoxon signed rank test with p-value lower than 0.001. GLS1 expression kept its high level also in metastatic samples.

DISCUSSION

In this study, the anti-cancer activity of GLS inhibitor IN-3 on PCa cells was evaluated. The PCa cell lines PC-3 and LNCaP presented the differential sensitivity to IN-3 compared to normal fibroblasts CCD1072Sk cells. Inhibition of GLS1 isoform of GLS by IN-3 in PC-3 cells did not cause increase in the expression of GLS2 isoform.

Table 1. Sequences of GAC, KGA, and GLS2 in qPCR.

	Forward sequence (5'to 3')	Reverse sequence (5'to 3')
GAC	GAAGGTGGTGATCAAAGGCATTC	CCTCATTTGACTCAGGTGACACT
KGA	TGGAGATGTGTCTGCACTTCG	AACTTCAACATGACCCTCTGC
GLS2	ACACCCTCAGCCTCATGCAT	ATGGCTCCTGATACAGCTGACTT

KGA: Kidney (K-type) glutaminase, GAC: Glutaminase C, GLS2: Glutaminase 2

Table 2. IC_{50} values of glutaminase-IN-3.

Cell line	IC50 value (μM)
PC-3	6.14 μM ±4.35
LNCaP	2.13 μM ±0.62
CCD1072sk	15.39 μM ±2.97

IC_{50}: Half inhibitory concentration

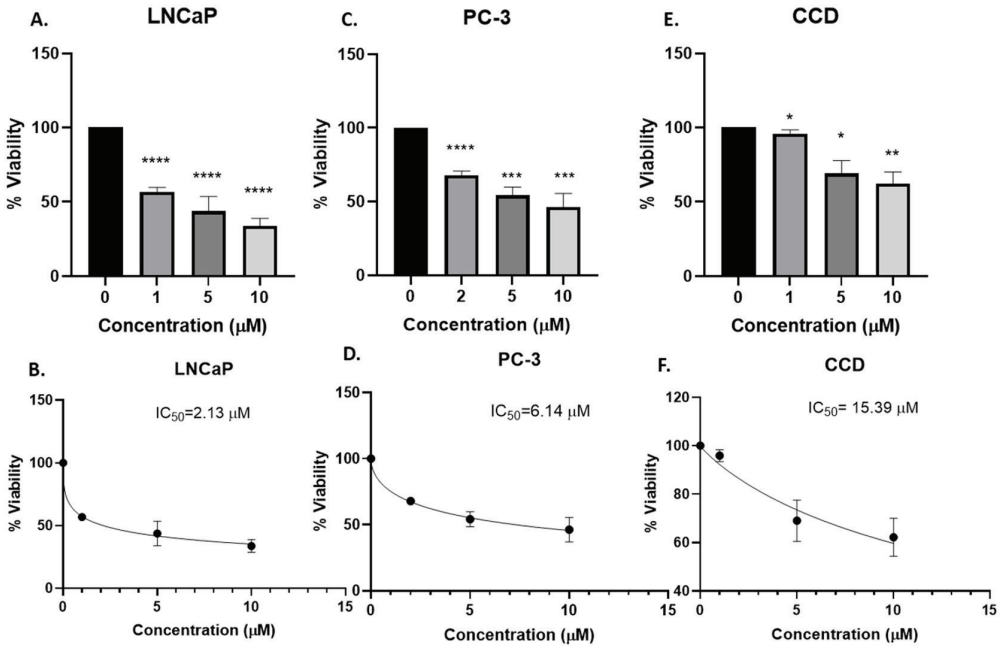

Figure 1. IC_{50} graphs of glutaminase-IN-3 on prostate cancer cells LNCaP **A)**, PC-3 **C)**, and normal cell CCD1072sk **E)** and the dose dependent effect of glutaminase-IN-3 on prostate cancer cells LNCaP **B)**, PC-3 **D)**, and normal cell CCD1072sk **F)** (Student t-test was applied to determine statistical significance. *: p<0.05, **: p<0.01, ***: p<0.001, and ****: p<0.0001).

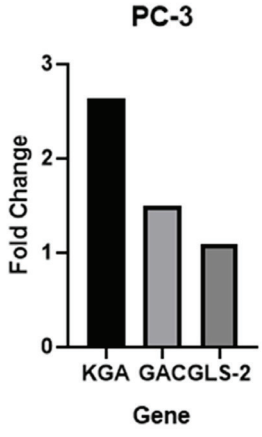

Figure 2. Changes in the expression levels of KGA, GAC, and GLS2 in response to glutaminase IN-3 in PC-3 cells.

KGA: Kidney (K-type) glutaminase, GAC: Glutaminase C, GLS2: Glutaminase 2

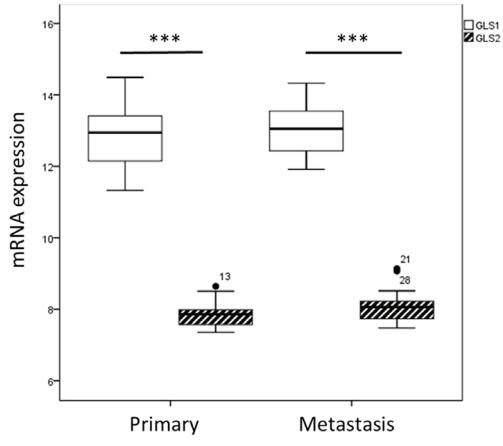

Figure 3. mRNA expression of GLS1 and GLS2 in primary and metastatic prostate cancer tissue. (Wilcoxon signed-rank test was applied to determine statistical significance. *: p<0.05, **: p<0.01, ***: p<0.001).

Our analysis in publicly available dataset in metastatic PCa tissue confirmed that GLS1 was the highly expressed isoform in PCa patients and this high expression level was maintained in the metastatic PCa tissue samples.

The idea of glutamine metabolism as a drug target is based on the information about high levels of GLS1 enzyme in cancer tissues. Several studies analyzed the expression level of GLS enzymes in primary PCa. Pan et al.[7] compared PCa with bening prostatic hyperplasia

(BPH) in terms of GLS1 protein expression and reported that GLS1 protein levels were elevated in PCa tissue compared to BPH. In addition, they showed a correlation with the increased GLS1 expression and the advanced Gleason scores and TNM stage. In another study, high GLS1 expression was correlated with shorter overall survival in 87 PCa patients[8]. Zhang et al.[9] compared mRNA levels of GLS1 in PCa tissue in respect to adjacent normal tissue. They reported that GLS1 mRNA expressions were high in mCRPC compared to normal tissue and there was a correlation between GLS1 mRNA expression and Gleason score and TNM stage. In contrast to these studies, Myint et al.[10] unable to show any correlation between GLS1 expression and the survival in both publicly available mRNA data from TCGA and protein data from their tissue microarray. However, this study still confirmed high GLS1 expressions in PCa compared to benign tissues. They concluded that their patient population have less advanced disease compared to the other studies[10]. In our study we compared GLS1 and GLS2 mRNA levels in primary and metastatic PCa tissue samples using publicly available data. GLS1 mRNA level was higher than GLS2 both in primary and metastatic PCa. The maintenance of high GLS1 level in metastatic samples ensures that glutamine metabolism is still active and viable target of therapy both in primary and metastatic PCa. Our *in vitro* results also confirmed this finding by demonstrating the high anti-proliferative potential of IN-3 in metastatic PCa cell lines.

The anti-proliferative activity of GLS inhibitor IN-3 has not been tested in any other study before. It is a patent derived compound. In our study, we found out that the IC_{50} values of IN-3 against PC-3 and LNCaP cell lines were 6.14 and 2 μM respectively. Xu et al.[11] reported that androgen receptor (AR) negative PC-3 cells displayed much higher sensitivity to CB839 compared to AR positive LNCaP cells. They explained this discrepancy with isoform switch of GLS1 from KGA isoform to GAC isoform in AR negative or castrate resistant conditions and claimed that the sensitivity to CB839 was correlated with GAC expression level. Because of the higher sensitivity of AR positive LNCaP cells to IN-3 compared to AR negative PC-3 cells in our study, it was suggested that sensitivity to IN-3 was not correlated with AR status. The prominent anti-proliferative activity of IN-3 both in AR positive and negative cells is an indicator of superior potential of IN-3 over CB839 as a GLS1 inhibitor.

Another concern about CB839 activity in PCa was upregulation of GLS2 level upon CB839 treatment. GLS2 compensates inactivity of GLS1 and maintain GLS activity in PCa cells[12]. In our study, we showed that inhibition of GLS1 with IN-3 had no effect on the expression of GLS2. However, the increase in the expression of KGA isoform of GLS1 was a main concern. It is a common phenomenon that when the activity of an enzyme is inhibited, the mRNA expression for this protein is increased to compensate the inhibitory effect. In parallel to that, Timofeeva et al.[13] also showed that upon CB839 treatment in lymphocytes from chronic lymphoblastic leukemia patients, GAC expression was increased. However, after a prolonged inhibition of the activity, mRNA levels would be decreased also. In our study, we evaluated the expression levels of GLS isoforms in 24 hours. Further experiments for time-dependent changes in the expression levels of GLS isoforms were warranted.

Although our study presented preliminary results about potential of IN-3 as an anti-cancer therapy, only two mCRPC cell lines were included in IC_{50} calculations. It is foremost important to expand the study to confirm this finding in other cell lines in PCa or in any other cancer type. Several studies about mRNA or protein levels of GLS isoforms in PCa tissue samples have been highlighted in the literature. However, our study analyzed the mRNA expression of GLS isoforms in metastatic PCa for the first time. The downsides for that part is the limited number of metastatic samples and unavailability of KGA and GAC isoforms data separately. It is crucial to explore KGA and GAC isoform levels in a larger metastatic PCa cohort.

CONCLUSION

This was the first study in the literature showing anti-cancer potential of GLS inhibitor IN-3. The differential effect of IN-3 in cancer cells compared to normal cells was noteworthy. This warrants further study about IN-3 as a potential drug in cancer. This study analyzed the expression level of GLS1 in metastatic PCa tissues for the first time. The high expression levels of GLS1 in metastatic PCa tissue samples also further prove GLS1 as an important drug target in PCa.

Ethics

Ethics Committee Approval: The authors declare that this study did not include any human or animal subjects.

Informed Consent: The authors declare that this study did not include any human or animal subjects.

Author Contributions

Concept: U.D., A.B.C., Design: U.D., A.B.C., Data Collection and/or Processing: U.D., A.B.C., Analysis and/or Interpretation: U.D., A.B.C., Literature Search: U.D., A.B.C., Writing: U.D., A.B.C.

Conflict of Interest: The authors have no conflict of interest to declare.

Financial Disclosure: This study was supported by TUBITAK 2209 program (project number: 1919B012214650).

REFERENCES

1. Fidelito G, Watt MJ, Taylor RA. Personalized Medicine for Prostate Cancer: Is Targeting Metabolism a Reality? Front Oncol. 2022;11:778761.
2. Altman BJ, Stine ZE, Dang CV. From Krebs to clinic: glutamine metabolism to cancer therapy. Nat Rev Cancer. 2016;16:619-34.
3. Gross MI, Demo SD, Dennison JB, et al. Antitumor activity of the glutaminase inhibitor CB-839 in triple-negative breast cancer. Mol Cancer Ther. 2014;13:890-901.
4. Yang WH, Qiu Y, Stamatatos O, Janowitz T, Lukey MJ. Enhancing the Efficacy of Glutamine Metabolism Inhibitors in Cancer Therapy. Trends Cancer. 2021;7:790-804.
5. Meric-Bernsta F, Tannir NM, Iliopoulos O, et al. Telaglenastat Plus Cabozantinib or Everolimus for Advanced or Metastatic Renal Cell Carcinoma: An Open-Label Phase I Trial. Clin Cancer Res. 2022;28:1540-8.
6. Gao J, Aksoy BA, Dogrusoz U, et al. Integrative analysis of complex cancer genomics and clinical profiles using the cBioPortal. Sci Signal. 2013;6:pl1.
7. Pan T, Gao L, Wu G, et al. Elevated expression of glutaminase confers glucose utilization via glutaminolysis in prostate cancer. Biochem Biophys Res Commun. 2015;456:452-8.
8. Li Y, Li X, Li X, et al. PDHA1 gene knockout in prostate cancer cells results in metabolic reprogramming towards greater glutamine dependence. Oncotarget. 2016;7:53837-52.
9. Zhang J, Mao S, Guo Y, Wu Y, Yao X, Huang Y. Inhibition of GLS suppresses proliferation and promotes apoptosis in prostate cancer. Biosci Rep. 2019;39:BSR20181826.
10. Myint ZW, Sun RC, Hensley PJ, et al. Evaluation of Glutaminase Expression in Prostate Adenocarcinoma and Correlation with Clinicopathologic Parameters. Cancers (Basel). 2021;13:2157.
11. Xu L, Yin Y, Li Y, et al. A glutaminase isoform switch drives therapeutic resistance and disease progression of prostate cancer. Proc Natl Acad Sci U S A. 2021;118:e2012748118.
12. Zacharias NM, McCullough C, Shanmugavelandy S, et al. Metabolic Differences in Glutamine Utilization Lead to Metabolic Vulnerabilities in Prostate Cancer. Sci Rep. 2017;7:16159.
13. Timofeeva N, Ayres ML, Baran N, et al. Preclinical investigations of the efficacy of the glutaminase inhibitor CB-839 alone and in combinations in chronic lymphocytic leukemia. Front Oncol. 2023;13:1161254.

DOI: 10.4274/MMJ.galenos.2024.32585
Medeni Med J 2024;39:175-182

Original Article

The Relationship Between the Modified Glasgow Prognostic and SYNTAX Scores in Patients with Non-ST Elevation Myocardial Infarction

ST Yükselmesi Olmayan Miyokard Enfarktüslü Hastalarda Modifiye Glasgow Prognostik ve SYNTAX Skorları Arasındaki İlişki

Ahmet KARADUMAN[1], Cemalettin YILMAZ[2], Mustafa Ferhat KETEN[3], Ismail BALABAN[3], Zeynep Esra GUNER[3], Mehmet CELIK[3]

[1]Tatvan State Hospital, Clinic of Cardiology, Bitlis, Türkiye
[2]Malazgirt State Hospital, Clinic of Cardiology, Mus, Türkiye
[3]University of Health Sciences Türkiye, Kartal Kosuyolu Yuksek Ihtisas Training and Research Hospital, Clinic of Cardiology, Istanbul, Türkiye

ABSTRACT

Objective: This study investigated the modified Glasgow prognostic score (mGPS) to determine its predictive value and how it could be compared with various inflammatory markers, including C-reactive protein (CRP) to albumin ratio and neutrophil-to-lymphocyte ratio, for determining the extent and severity of coronary artery disease (CAD) in patients with non-ST-elevated myocardial infarction (NSTEMI).

Methods: This study analyzed the cases of 295 patients with NSTEMI who had undergone coronary angiography. In an effort to determine the seriousness and scope of CAD in each patient, the Synergy between Percutaneous Coronary Intervention with Taxus and Cardiac Surgery (SYNTAX) score was calculated and then assessed. The study sample was divided into two separate groups based on the SYNTAX score: moderate to high SYNTAX (>22) and low SYNTAX (≤22).

Results: There were 295 patients (23.1% female, 76.9% male) included in the research, with an average age being 61.2±10.9 years, and the mean SYNTAX score being 7.3±10.4 (range: 0-40). Those with a SYNTAX score >22 were observed to possess significantly higher levels of CRP, CRP/albumin ratio, and mean mGPS 1-2 ratios compared with those with a SYNTAX score ≤22 (all p<0.001). Smoking [odds ratio (OR): 3.341, 95% confidence interval (CI): 1.531-7.294; p=0.002], CRP/albumin ratio (OR: 4.958, 95% CI: 1.335-18.418; p=0.017), and mGPS score of 1-2 (OR: 3.121, 95% CI: 1.430-6.814; p=0.004) were independent factors used to help predict a high SYNTAX score.

Conclusions: It seems possible to make use of the mGPS when estimating the degree and intricacies of CAD in patients with NSTEMI, as there appears to be a connection with higher SYNTAX scores.

Keywords: Modified Glasgow prognostic score (mGPS), SYNTAX score, coronary artery disease, non-ST-elevated myocardial infarction

ÖZ

Amaç: Bu çalışmada, non-ST yükselmeli miyokard enfarktüsü (NSTEMI) geçiren hastalarda koroner arter hastalığının (KAH) yaygınlığını ve şiddetini belirlemede, nötrofil-lenfosit oranı (NLO) ve C-reaktif protein (CRP)-albümin oranı gibi diğer enflamatuvar belirteçlerle karşılaştırıldığında, modifiye Glasgow prognostik skorunun (mGPS) öngörü değerini araştırmayı amaçladık.

Yöntemler: Çalışma, koroner anjiyografi yapılan 295 ardışık NSTEMI hastasını içermekteydi. Her hasta için, KAH şiddeti ve yaygınlığını belirlemek amacıyla Taxus ile Perkütan Koroner Girişim ve Kardiyak Cerrahi Arasındaki Sinerji Skoru (SYNTAX) skoru hesaplandı. Çalışma örneği, SYNTAX skoruna göre orta-yüksek SYNTAX (>22) ve düşük SYNTAX (≤22) olarak iki gruba ayrıldı.

Bulgular: İki yüz doksan beş hastanın (%23,1 kadın, %76,9 erkek) yaş ortalaması 61,2±10,9 yıl olup, ortalama SYNTAX skoru 7,3±10,4 (aralık: 0-40) idi. SYNTAX skoru >22 olan hastaların CRP düzeyleri, CRP/albümin oranı ve ortalama mGPS 1-2 oranları, SYNTAX skoru ≤22 olanlara göre anlamlı derecede yüksekti (hepsi p<0,001). Sigara içme [olasılık oranı (OO): 3,341, %95 güven aralığı (GA): 1,531-7,294; p=0,002], CRP/albümin oranı (OR: 4,958, %95 GA: 1,335-18,418; p=0,017) ve mGPS skoru 1-2 (OR: 3,121, %95 GA: 1,430-6,814; p=0,004), yüksek SYNTAX skorunun bağımsız öngördürücüleriydi.

Sonuçlar: Yüksek bir SYNTAX skoru ile ilişkili olduğu görülen mGPS, NSTEMI hastalarında KAH yaygınlığını ve karmaşıklığını tahmin etmek için kullanılabilir.

Anahtar kelimeler: Değiştirilmiş Glasgow prognostik skoru (mGPS), SYNTAX skoru, koroner arter hastalığı, ST yükselmesi olmayan miyokard enfarktüsü

Address for Correspondence: A. Karaduman, Tatvan State Hospital, Clinic of Cardiology, Bitlis, Türkiye
E-mail: ahmetkaradumanmd@gmail.com **ORCID ID:** orcid.org/0000-0002-4039-1259

Received: 24 March 2024
Accepted: 28 July 2024
Online First: 02 September 2024

Cite as: Karaduman A, Yilmaz C, Keten MF, Balaban I, Guner ZE, Celik M. The Relationship Between the Modified Glasgow Prognostic and SYNTAX Scores in Patients with Non-ST Elevation Myocardial Infarction. Medeni Med J. 2024;39:175-182

INTRODUCTION

Among the most dangerous health crises across the globe, cardiovascular diseases (CVD) are near the top of the list. Acute coronary syndrome (ACS) manifests clinically as unstable angina, non-ST segment elevation myocardial infarction (NSTEMI), and ST segment elevation myocardial infarction (STEMI). The Synergy between Percutaneous Coronary Intervention with Taxus and Cardiac Surgery (SYNTAX) score was formulated to evaluate the amount and level of intricacy of coronary artery disease (CAD), as well as late and early results[1-3]. Based on the angiographic results, the SYNTAX scoring method separates patients into numerous risk groups and provides insight into revascularization success and prognosis according to risk group. Controlled studies evaluating percutaneous coronary intervention (PCI) and coronary artery bypass graft surgery were similar in patients with SYNTAX scores that were considered low (<22)[4].

Inflammation certainly contributes to the progression and instability of atherosclerosis, as well as the onset of ACS, by causing vascular inflammation, plaque rupture, and subsequent thrombosis. Serum albumin (SA) is considered the most common and fundamental protein in human serum because it participates in several physiological functions. Reduced SA synthesis and enhanced catabolism are correlated with increased inflammatory response[5,6]. Decreased SA can result in high blood viscosity and endothelial dysfunction. Moreover, SA inhibits platelet activation and aggregation[7]. The C-reactive protein (CRP)-to-albumin ratio (CAR) was seen to predict the inflammatory state and prognosis on several occasions[8-10]. There has been research that exposes a connection between the severity of CAD and the CAR[11-13]. This study aimed to implement the modified Glasgow prognostic score (mGPS) to determine how well it predicted the severity and complexity of CAD in patients with NSTEMI by implementing the SYNTAX score, as the innovative mGPS considers CRP and reduced albumin levels while also having the capacity to help predict heart disease[14,15].

MATERIALS and METHODS

Study Population

The goal of this study was to evaluate relevant clinical information about patients admitted due to a health emergency between January and June 2019. NSTEMI patients who underwent coronary angiography with or without PCI were among those able to be included in the study. The University of Health Sciences Türkiye, Kartal Kosuyolu Yuksek Ihtisas Training and Research Hospital Clinical Research Ethics Committee approved our research plan (decision no: 2024/06/797) on March 19, 2024. The initial medical and socioeconomic parameters, including hyperlipidemia (HL), hypertension, smoking history, diabetes mellitus (DM), and history of cerebrovascular disease, were collected from the hospital records.

In total, 396 patient medical records were examined and evaluated retrospectively using our database. Patients who had a history of coronary artery bypass grafting or PCI (n=73), as well as those with end-stage kidney disease (n=15), cancer (n=6), and active infection (n=7) were excluded.

The ACS diagnostic standard and American Heart Association recommendations were used to diagnose ACS based on symptoms, electrocardiogram results, and other supplementary procedures. In the absence of sustained ST elevation, the presence of sudden chest pain or significant breathing difficulty suggested non-ST-elevated ACS. NSTEMI may additionally be classified based on myocardial necrosis indicators, such as cardiac troponin. NSTEMI is diagnosed when cardiac markers are increased and physical symptoms are consistent[16].

Laboratory Analysis

Upon admission to the hospital and before any reperfusion or heparin medication, a blood sample was extracted from each patient via the antecubital vein. A Sysmex XT2000i analyzer was used to perform complete blood counts (Sysmex Corporation, Kobe, Japan). An autoanalyzer was applied for the testing of total cholesterol, fasting blood glucose, potassium, sodium, creatinine, liver enzymes (aspartate aminotransferase, alanine aminotransferase), high-density lipoprotein, low-density lipoprotein, and triglyceride levels (Siemens Advia 2400 Chemistry System, Siemens Diagnostic, Tarrytown, USA). A Roche Diagnostics Cobas 8000 c502 analyzer (Roche Holding AG, Basel, Switzerland) was used to gage albumin and CRP levels.

Modified Glasgow Prognostic Score

Inflammation-based mGPS is linked to survival in cancer, heart failure, STEMI[14,17]. Previous research has demonstrated that the mGPS (0, 1, and 2) can be discriminated according to the degree of malnutrition. Patients were separated into three categories: Patients with raised hypoalbuminemia (<35 g/L) and CRP (>10 mg/L) were scored with a 2; those with just elevated CRP (>10 mg/L) were scored as 1; and patients possessing neither abnormality were scored as 0.

Coronary Angiography and SYNTAX Score

Coronary angiograms were acquired digitally for quantification (DICOM viewer; MedCom GmbH, Darmstadt, Germany). They were then assessed by two experienced interventional cardiologists who were restricted from comparing the data with the clinical data of the patients. Upon retrieval of a version from http://www.syntaxscore.com, the anatomical SYNTAX score was implemented to numerically evaluate the intricacy of coronary lesions. Using this score, the population sample was separated into two groups based on the severity of CAD: low (22), and moderate-high (>22).

Statistical Analysis

SPSS 19.0. (IBM Corp. Armonk, NY) for Windows was used to statistically analyze the data. Descriptive statistics; standard deviation, mean, minimum, maximum, and median for numerical variables; numbers and percentages for categorical variables. The chi-square test was used as a basis for comparison with the rates collected from the groups. By using the Mann-Whitney U test, comparisons could be made between the groups because the numerical variables failed to meet the condition of normal distribution. Logistic regression analysis was then performed to ascertain any independent predictors of a moderate to high SYNTAX score existed. The significance level was set as $p<0.05$ in all statistical analyses.

RESULTS

All in all, 295 patients, 68 women (23.1%) and 227 men (76.9%), with 31 being the youngest and 85 being the oldest, and a mean age of 61.2±10.9 years, were included in the study. The average patient SYNTAX score was 7.3±10.4 (minimum: 0-maximum: 40). The SYNTAX score of the patients were 22 or less in 238 (80.7%) and above 22 in 57 (19.3%). A flowchart of the study population is presented in Figure 1.

The mean body mass index (BMI), DM, HL, CVD, smoking rates, left ventricular hypertrophy, and heart valve disorder rates of patients with SYNTAX score >22 were statistically significantly higher than those scoring score 22 and below (p=0.015, p=0.008, p=0.003, p=0.039, p<0.001, p<0.001, p<0.001) (Table 1).

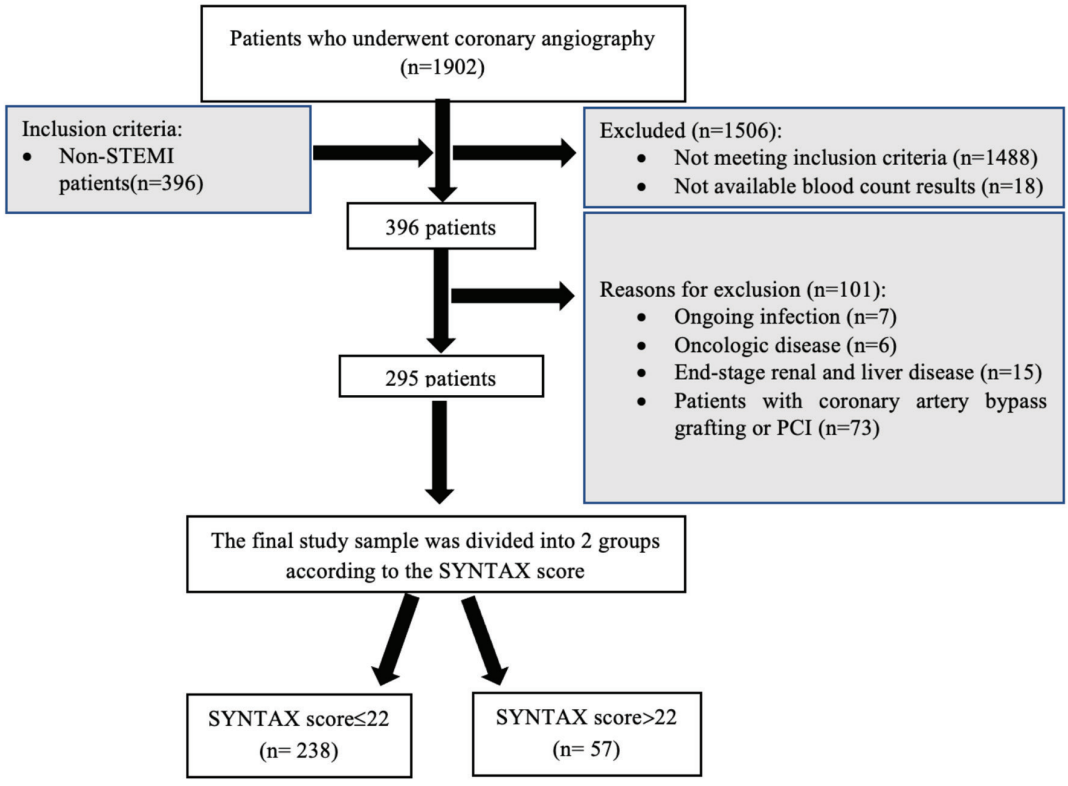

Figure 1. Flowchart of study population.

STEMI: ST segment elevation myocardial infarction, SYNTAX: Synergy between Percutaneous Coronary Intervention with Taxus and Cardiac Surgery, PCI: Percutaneous coronary intervention

Table 1. Baseline characteristics and laboratory and echocardiographic findings of the groups.					
Variables		**All**	**SYNTAX score ≤22 (n=238)**	**SYNTAX score >22 (n=57)**	**p-value**
Baseline characteristics					
Age (years), median (IQR)		62 (54-70.5)	61 (53-70)	64 (58-72)	0.133
Gender (female), n (%)		68 (23.1)	55 (23.1)	13 (22.8)	0.961
Body mass index (kg/m^2), mean ± SD		25.1±2.5	25.0±2.5	26.0±2.3	0.015
Atrial fibrillation, n (%)		8 (2.7)	6 (2.5)	2 (3.5)	0.654
Hypertension, n (%)		198 (67.1)	154 (64.7)	44 (77.2)	0.071
Diabetes mellitus, n (%)		87 (29.5)	62 (26.1)	25 (43.9)	0.008
Hyperlipidemia, n (%)		74 (25.3)	51 (21.6)	23 (40.4)	0.003
Cerebrovascular disease, n (%)		2 (0.7)	0 (0.0)	2 (3.5)	0.039
Current smoker, n (%)		150 (50.8)	109 (45.8)	41 (71.9)	<0.001
Laboratory findings					
Glucose (mg/dL), mean ± SD		132.38±67.4	132.24±72.74	134.65±55.50	0.505
BUN (mg/dL), mean ± SD		35.21±14.16	35.41±15.56	34.48±9.74	0.639
Creatinine (mg/dL), median (IQR)		0.85 (0.71-1.07)	0.83 (0.7-1.06)	0.95 (0.73-1.1)	0.061
Aspartate aminotransferase (U/L), median (IQR)		19.2 (16.6-24)	19.5 (16.9-24.5)	18.8 (16.3-23.8)	0.312
Alanine aminotransferase (U/L), median (IQR)		17.8 (12.6-23)	17.7 (12.7-22.8)	17.9 (12.3-28.0)	0.619
Sodium (mmol/dL), median (IQR)		138 (135-140)	138 (135-139.2)	137.5 (135.75-140)	0.419
Potassium (mmol/dL), mean ± SD		4.34±0.44	4.36±0.42	4.25±0.48	0.083
Calcium (mg/dL), mean ± SD		8.9±0.6	8.9±0.6	8.8±0.5	0.401
Magnesium (mg/dL), mean ± SD		1.9±0.3	1.9±0.3	2.0±0.3	0.761
LDL (mg/dL), median (IQR)		119 (89-149)	117 (88-146)	127 (100-157)	0.141
HDL (mg/dL), median (IQR)		40 (32-47)	40 (32-47)	37.5 (31-48)	0.332
Total cholesterol level (mg/dL), median (IQR)		192 (151-230)	190 (150-230)	206 (159.7-236)	0.167
Triglyceride (mg/dL), median (IQR)		141 (95.7-195.7)	140.5 (90.7-192)	152.5 (105-209)	0.440
Hemoglobin (g/dL), mean ± SD		13.6±1.7	13.6±1.8	13.6±1.5	0.976
WBC (x10^3/µL), median (IQR)		9 (7.4-10.6)	9 (7.4-10.8)	8.7 (7.3-9.8)	0.235
Neutrophil (x10^3/µL), median (IQR)		6.2 (4.8-7.7)	6.2 (4.7-7.9)	6 (5-7.2)	0.461
Lymphocyte (x10^3/µL), median (IQR)		2.04 (1.5-2.5)	2.1 (1.5-2.7)	2.0 (1.5-2.4)	0.202
Neutrophil/lymphocyte, median (IQR)		3.16 (1.99-4.84)	3.09 (1.98-4.90)	3.36 (2.26-4.55)	0.782
CRP (mg/dL), median (IQR)		4.4 (3.1-8.9)	3.68 (2.46-7.09)	10.6 (5.03-13.9)	<0.001
Albumin (g/dL), median (IQR)		3.9 (3.6-4.3)	3.9 (3.6-4.3)	3.9 (3.5-4.4)	0.991
CRP/albumin, median (IQR)		0.107 (0.077-0.216)	0.095 (0.072-0.188)	0.25 (0.14-0.35)	<0.001
Echocardiography					
Left ventricular ejection fraction, (%), median (IQR)		60 (60-65)	60 (60-65)	60 (50-65)	0.065
SPAP (mmHg), median (IQR)		20 (0-25)	0 (0-25)	25 (0-30)	<0.001
Left ventricular hypertrophy, n (%)		103 (35.5)	65 (27.9)	38 (66.7)	<0.001
Heart valve disorder, n (%)		9 (3.1)	3 (1.3)	6 (10.5)	<0.001
Angiographic characteristics					
LMCA, n (%)		8 (2.7)	6 (2.5)	2 (3.5)	0.680
LAD, n (%)		73 (24.7)	29 (12.2)	44 (77.2)	<0.001
CX, n (%)		74 (25.1)	43 (18.1)	31 (54.4)	<0.001
RCA, n (%)		81 (27.5)	44 (18.5)	37 (64.9)	<0.001
Risk scores					
mGPS, n (%)	0	198 (68.0)	179 (76.5)	19 (33.3)	<0.001
	1	75 (25.8)	48 (20.5)	27 (47.4)	
	2	18 (6.2)	7 (3.0)	11 (19.3)	

SYNTAX: Synergy between Percutaneous Coronary Intervention with Taxus and Cardiac Surgery, BUN: Blood urea nitrogen, HDL: High density lipoprotein, IQR: Interquartile range, LDL: Low density lipoprotein, LVEDD: Left ventricular end diastolic diameter, mGPS: Modified Glasgow prognostic score, SD: Standard deviation, SPAP: Systolic pulmonary artery pressure, CRP: C-reactive protein, WBC: White blood cell

The CRP and CRP/albumin mean mGPS 1-2 ratios of patients with SYNTAX scores >22 were statistically significantly higher than those with SYNTAX scores >22 (p<0.001 for all) (Table 1).

When the univariate effects of the factors thought to be risk factors for moderate to high SYNTAX scores were examined, it was determined that BMI increase, DM, HL, smoking, decreased ejection fraction, increased CRP/albumin ratio, and mGPS 1 or 2 (p=0.007, p=0.009, p=0.004, p=0.001, p=0.003, p<0.001, p<0.001, p<0.001) (Table 2). Smoking [odds ratio (OR): 3.341, 95% confidence interval (CI): 1.531-7.294; p=0.002], CRP/albumin ratio (OR: 4.958, 95% CI: 1.335-18.418; p=0.017) and mGPS score of 1-2 (OR: 3.121, 95% CI: 1.430-6.814; p=0.004) were found to be independent associates of moderate to high SYNTAX scores (Table 2). Furthermore, analysis of the respective receiver operating characteristic curves yielded the optimal cut-off values of CAR and mGPS for predicting high SYNTAX scores. A cut-off value of 0.109 for CAR [area under the curve (AUC): 0.811] had 89.47% sensitivity and 60.5% specificity, whereas a cutoff value of 2 for mGPS scores (AUC: 0.729) had 66.67% sensitivity and 76.5% specificity (Figure 2).

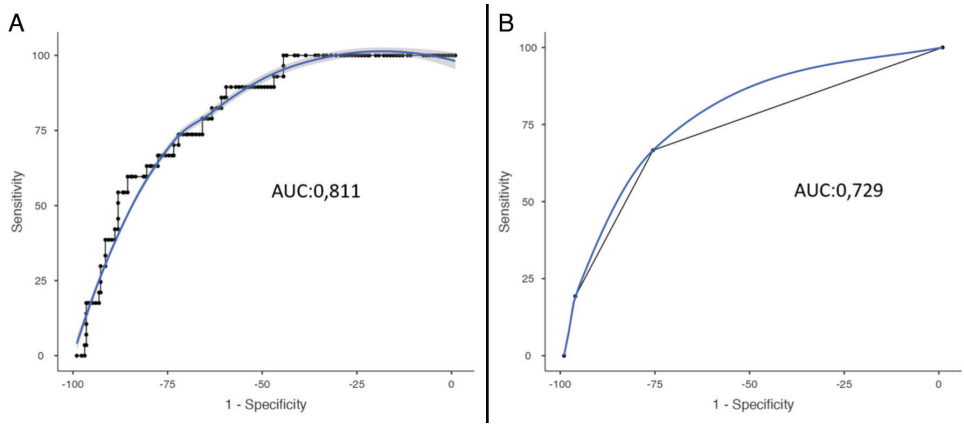

Figure 2. Receiver operating characteristic curves for the CRP/albumin ratio (A) and mGPS (B) scores for predicting high SYNTAX scores.

AUC: Area under the curve, SYNTAX: Synergy between Percutaneous Coronary Intervention with Taxus and Cardiac Surgery, CRP: C-reactive protein, mGPS: Modified Glasgow prognostic score

Table 2. Regression analysis of potential predictor factors for the high SYNTAX score.

	Univariate analysis				Multivariable analysis			
	p	OR	95%-CI		p	OR	95%-CI	
Age	0.136	1.021	0.994	1.049	0.345	1.017	0.982	1.054
Body mass index	0.007	1.178	1.046	1.328	0.258	1.098	0.934	1.290
Hypertension	0.074	1.846	0.941	3.620	0.959	0.978	0.421	2.270
Diabetes mellitus	0.009	2.218	1.220	4.033	0.588	1.278	0.526	3.105
Hyperlipidemia	0.004	2.454	1.329	4.531	0.704	1.183	0.496	2.821
Smoking	0.001	3.033	1.613	5.703	0.002	3.341	1.531	7.294
Left ventricular ejection fraction	0.003	0.932	0.889	0.977	0.237	0.965	0.911	1.023
CRP/albumin	<0.001	14.892	4.867	45.567	0.017	4.958	1.335	18.418
Neu/lym	0.621	0.984	0.924	1.048	0.364	0.941	0.826	1.073
mGPS (reference: 0) 1-2	<0.001	5.299	2.718	10.333	0.004	3.121	1.430	6.814

Multivariable analysis Cox & Snell R square: 0.193

SYNTAX: Synergy between Percutaneous Coronary Intervention with Taxus and Cardiac Surgery, CRP: C-reactive protein, Neu/lym: Neutrophil/lymphocyte, mGPS: Modified Glasgow prognostic score, OR: Odds ratio, CI: Confidence interval

DISCUSSION

Potential connections between the mGPS and SYNTAX scores of individuals with NSTEMI were thoroughly examined in this study. The study's essential conclusion was that in these patients, there appeared to be a strong link between the mGPS and SYNTAX scores. High mGPS and CRP-to-albumin ratio independently help predict SYNTAX score. Thus, in patients with NSTEMI, the mGPS may be associated with the degree and level of complexity of CAD and can be implemented to assess these factors in affected individuals.

Several scoring systems are used to evaluate the severity of angiographic CAD. The SYNTAX score was the most often used of these. The SYNTAX score was calculated by assessing the number, complexity, location, and effect of the lesions. The SYNTAX score should be consulted when describing the seriousness of CAD and to guide the operator in deciding on the best treatment approach. A number of clinical studies have looked into the association between the SYNTAX score and other factors. Minamisawa et al.[18] Found higher MACE rates in patients with high SYNTAX scores who experienced heart failure. Similarly, Bayam et al.[19] Found high MACE rates within the first 30 days in patients with NSTEMI and high SYNTAX scores. Therefore, the SYNTAX score is a useful tool for effective risk stratification in these patients.

Inflammation is a key factor in each stage of coronary atherosclerosis. There is a discernable association between CAD severity and adverse cardiovascular outcomes[20,21]. According to several studies, inflammatory markers, such as CAR and NLR, are linked to CAD severity and poor cardiovascular outcomes[12,22]. Although total white blood cell count appears to have a connection to the presence and severity of coronary atherosclerosis, as well as increased mortality and poor outcomes following acute myocardial infarction, NLR has been demonstrated to provide more accurate findings. A meta-analysis study involving 7,017 patients with CAD found that NLR was an effective tool for predicting severe stenosis in CAD[23]. A high NLR indicates a high level of inflammation, which can help explain why NLR has been linked to the severity and severity of CAD in previous studies. NLR was not found to be an independent predictor of moderate to high SYNTAX scores in our study.

CRP is not only a systemic inflammatory marker, but it is also one of the main acute-phase reactants, and it may be an active and direct component associated with the disruption of atherogenesis and atheromatous plaque. It was noted that independent links existed between CRP levels and the prevalence of CAD and recurrent cardiovascular events in individuals with stable CAD and ACS[24,25]. Additional evidence suggests that lower plasma albumin levels could be linked to the growth and progression of atherosclerosis[26]. Compared with the predictive values of these two markers independently, CAR is better suited to intricately perceive and specifically predict the systemic inflammatory state and prognosis in a variety of non-cardiac clinical disorders[8,9]. Recent studies have evaluated the predictive values of CAR and other inflammatory indicators, such as NLR, CRP, and albumin, in patients with ACS. These studies showed that CAR performs better than NLR, CRP, and albumin in predicting moderate-to-high SYNTAX score[12,13,27]. Our study also showed that CAR predicts a moderate-to-high SYNTAX score with a better probability than NLR.

The nutritional and inflammatory conditions of patients affect the severity and prognosis of many diseases. mGPS, calculated by high serum CRP level and low albumin levelIt has been studied mostly to demonstrate the prognostic status of patients with cancer. This scoring system has been used to determine the prognosis of the disease in patients with STE myocardial infarction, pulmonary embolism, inflammatory bowel disease, and heart failure, as well as in cancer patients[14-16,28,29]. However, an association between mGPS and CAD severity in patients with NSTEMI has not been established. Previous studies have shown that increased inflammatory response and worsening nutritional status in patients with ACS increase the prevalence of the disease. We found that the mGPS score was associated with a moderate to high SYNTAX score in patients with NSTEMI. The present study revealed that the mGPS score is an independent predictor of the severity of CAD.

There are a few limitations to this research. First, the retrospective design was based on a relatively small sample size at a single center. Second, coronary artery severity was assessed using visual coronary angiograms. Applying different methods, such as intravascular ultrasound, to analyze the degree of coronary atherosclerosis would have provided additional valuable information but were not used in this study. Third, we only examined albumin levels and baseline CRP at the time of administration. Changes observed with the following tests may have additional prognostic value. Fourth, given that we only obtained limited volume and event rate data, we were unable to assess the predictive utility of the mGPS for adverse cardiovascular events.

CONCLUSION

According to this study, the mGPS appears to have a significant relationship with the SYNTAX score and

is likely to be an available, easily quantifiable, and affordable parameter when determining the severity of coronary atherosclerosis. Therefore, identifying individuals with NSTEMI who are at high risk of CAD and in need of a more direct and aggressive approach to therapy and follow-up may be part of the cardiovascular examination. However, more expansive and prospective studies are necessary to assess the predictive and, especially, prognostic value of the mGPS in patients with NSTEMI.

Ethics

Ethics Committee Approval: The University of Health Sciences Türkiye, Kartal Kosuyolu Yuksek Ihtisas Training and Research Hospital Clinical Research Ethics Committee approved our research plan (decision no: 2024/06/797) on March 19, 2024.

Informed Consent: An informed consent for publication was obtained from all patients.

Author Contributions

Concept: A.K., C.Y., M.F.K., I.B., M.C., Design: A.K., C.Y., M.F.K., Z.E.G., M.C., Data Collection and/or Processing: A.K., I.B., Analysis and/or Interpretation: A.K., C.Y., I.B., Z.E.G., Literature Search: A.K., M.F.K., Z.E.G., M.C., Writing: A.K., C.Y., M.F.K., Z.E.G.

Conflict of Interest: The authors have no conflict of interest to declare.

Financial Disclosure: The authors declared that this study has received no financial support.

REFERENCES

1. Sianos G, Morel MA, Kappetein AP, et al. The SYNTAX Score: an angiographic tool grading the complexity of coronary artery disease. EuroIntervention. 2005;1:219-27.
2. Garg S, Sarno G, Serruys PW, et al. Prediction of 1-year clinical outcomes using the SYNTAX score in patients with acute ST-segment elevation myocardial infarction undergoing primary percutaneous coronary intervention: a substudy of the STRATEGY (Single High-Dose Bolus Tirofiban and Sirolimus-Eluting Stent Versus Abciximab and Bare-Metal Stent in Acute Myocardial Infarction) and MULTISTRATEGY (Multicenter Evaluation of Single High-Dose Bolus Tirofiban Versus Abciximab With Sirolimus-Eluting Stent or Bare-Metal Stent in Acute Myocardial Infarction Study) trials. JACC Cardiovasc Interv. JACC Cardiovasc Interv. 2011;4:66-75.
3. Libby P. Mechanisms of acute coronary syndromes and their implications for therapy. N Engl J Med. 2013;368:2004-13.
4. Doucet S, Jolicœur EM, Serruys PW, et al. Outcomes of left main revascularization in patients with acute coronary syndromes and stable ischemic heart disease: Analysis from the EXCEL trial. Am Heart J. 2019;214:9-17.
5. Don BR, Kaysen G. Serum albumin: relationship to inflammation and nutrition. Semin Dial. 2004;17:432-7.
6. Joles JA, Willekes-Koolschijn N, Koomans HA. Hypoalbuminemia causes high blood viscosity by increasing red cell lysophosphatidylcholine. Kidney Int. 1997;52:761-70.
7. Zhang WJ, Frei B. Albumin selectively inhibits TNF alpha-induced expression of vascular cell adhesion molecule-1 in human aortic endothelial cells. Cardiovasc Res. 2002;55:820-9.
8. Fairclough E, Cairns E, Hamilton J, Kelly C. Evaluation of a modified early warning system for acute medical admissions and comparison with C-reactive protein/albumin ratio as a predictor of patient outcome. Clin Med (Lond). 2009;9:30-3.
9. Ranzani OT, Zampieri FG, Forte DN, Azevedo LC, Park M. C-reactive protein/albumin ratio predicts 90-day mortality of septic patients. PLoS One. 2013;8:e59321.
10. Kinoshita A, Onoda H, Imai N, et al. The C-reactive protein/albumin ratio, a novel inflammation-based prognostic score, predicts outcomes in patients with hepatocellular carcinoma. Ann Surg Oncol. 2015;22:803-10.
11. Karabağ Y, Cağdaş M, Rencuzogullari I, et al. Relationship between C-reactive protein/albumin ratio and coronary artery disease severity in patients with stable angina pectoris. J Clin Lab Anal. 2018;32:e2245.
12. Çağdaş M, Rencüzoğullari I, Karakoyun S, et al. Assessment of relationship between C-reactive protein to albumin ratio and coronary artery disease severity in patients with acute coronary syndrome. Angiology. 2017;70:361-8.
13. Kalyoncuoglu M, Durmus G. Relationship between C-reactive protein-to-albumin ratio and the extent of coronary artery disease in patients with non-ST-elevated myocardial infarction. Coron Artery Dis. 2020;31:130-6.
14. Cho A, Arfsten H, Goliasch G, et al. The inflammation-based modified Glasgow prognostic score is associated with survival in stable heart failure patients. ESC Heart Fail. 2020;7:654-62.
15. Zehir R, Yılmaz AS, Çırakoğlu ÖF, Kahraman F, Duman H. Modified Glasgow Prognostic Score Predicted High-Grade Intracoronary Thrombus in Acute Anterior Myocardial Infarction. Angiology. 2023;75:454-61.
16. Amstardam EA, Wenger NK, Brindis RG, et al. 2014 AHA/ACC Guideline for the Management of Patients With Non-ST-Elevation Acute Coronary Syndromes: A Report of the American College of Cardiology/American Heart Association Task Force on Practice Guidelines. J Am Coll Cardiol. 2014;64:139-228.
17. He L, Li H, Cai J, et al. Prognostic value of the Glasgow prognostic score or modified Glasgow prognostic score for patients with colorectal cancer receiving various treatments: a systematic review and meta-analysis. Cell Physiol Biochem. 2018;51:1237-49.
18. Minamisawa M, Miura T, Motoki H, et al. Prediction of 1-year clinical outcomes using the SYNTAX score in patients with prior heart failure undergoing percutaneous coronary intervention: sub-analysis of the SHINANO registry. Heart Vessels. 2017;32:399-407.
19. Bayam E, Kalçık M, Öztürkeri B, et al. The relationship between H2FPEF and SYNTAX scores in patients with non-ST elevation myocardial infarction. Acta Cardiol. 2021;76:870-7.
20. Nikolsky E, Grines CL, Cox DA, et al. Impact of baseline platelet count in patients undergoing primary percutaneous coronary intervention in acute myocardial infarction (from the CADILLAC trial). Am J Cardiol. 2007;99:1055-61.
21. Gaul DS, Stein S, Matter CM. Neutrophils in cardiovascular disease. Eur Heart J. 2017;38:1702-4.

22. Sari I, Sunbul M, Mammadov C, et al. Relation of neutrophil-to-lymphocyte and platelet-to-lymphocyte ratio with coronary artery disease severity in patients undergoing coronary angiography. Kardiol Pol. 2015;73:1310-6.
23. Li X, Ji Y, Kang J, Fang N. Association between blood neutrophil-to-lymphocyte ratio and severity of coronary artery disease: Evidence from 17 observational studies involving 7017 cases. Medicine (Baltimore). 2018;97:e12432.
24. Van Wijk DF, Boekholdt SM, Wareham NJ, et al. C-reactive protein, fatal and nonfatal coronary artery disease, stroke, and peripheral artery disease in the Prospective EPIC-Norfolk Cohort Study. Arterioscler Thromb Vasc Biol. 2013;33:2888-94.
25. Karadeniz M, Duran M, Akyel A, et al. High sensitive CRP level is associated with intermediate and high SYNTAX score in patients with acute coronary syndrome. Int Heart J. 2015;56:377-80.
26. Schillinger M, Exner M, Mlekusch W, et al. Serum albumin predicts cardiac adverse events in patients with advanced atherosclerosis – interrelation with traditional cardiovascular risk factors. Thromb Haemost. 2004;91:610-8.
27. Çakmak EÖ, Bayam E, Çelik M, et al. Uric Acid-to-Albumin Ratio: A Novel Marker for the Extent of Coronary Artery Disease in Patients with Non-ST-Elevated Myocardial Infarction. Pulse (Basel). 2021;8:99-107.
28. Celik AI, Bezgin T, Biteker M. Predictive role of the modified Glasgow prognostic score for in-hospital mortality in stable acute pulmonary embolism. Med Clin (Barc). 2022;158:99-104.
29. Zhao C, Ding C, Xie T, et al. Validation and optimization of the Systemic Inflammation-Based modified Glasgow Prognostic Score in predicting postoperative outcome of inflammatory bowel disease: preliminary data. Sci Rep. 2018;8:747.

DOI: 10.4274/MMJ.galenos.2024.60533
Medeni Med J 2024;39:183-191

Original Article

Systemic Immune-inflammation Index in Evaluation of Inflammation in Rheumatoid Arthritis Patients

Romatoid Artrit Hastalarında Enflamasyonun Değerlendirilmesinde Sistemik İmmün Enflamasyon

Amela DERVISEVIC[1], Almir FAJKIC[2], Elmedina JAHIC[3], Lejla DERVISEVIC[4], Zurifa AJANOVIC[4], Enisa ADEMOVIC[5], Asija ZACIRAGIC[1]

[1]University of Sarajevo Faculty of Medicine, Department of Human Physiology, Sarajevo, Bosnia and Herzegovina
[2]University of Sarajevo Faculty of Medicine, Department of Pathophysiology, Sarajevo, Bosnia and Herzegovina
[3]Clinical Center University of Sarajevo, Clinic for Heart, Blood Vessel and Rheumatic Diseases, Sarajevo, Bosnia and Herzegovina
[4]University of Sarajevo Faculty of Medicine, Department of Anatomy, Sarajevo, Bosnia and Herzegovina
[5]University of Sarajevo Faculty of Medicine, Department of Epidemiology and Biostatistics, Sarajevo, Bosnia and Herzegovina

ABSTRACT

Objective: To evaluate the systemic immune-inflammation (SII) index in patients with rheumatoid arthritis (RA) stratified by systemic inflammatory status.

Methods: Seropositive patients with RA (n=58) were divided into two groups based on serum hs-C-reactive protein (hs-CRP) levels: RA patients with hs-CRP levels of at or 3 mg/L or above (high systemic inflammatory status; n=38) and RA patients with hs-CRP levels of less than 3 mg/L (low systemic inflammatory status; n=20). The control group comprised 31 healthy individuals. Blood samples were tested for the next parameters: leukocytes, neutrophilic granulocytes, lymphocytes, thrombocytes [platelet (PLT)], high-sensitivity hs-CRP, sed rate [erythrocyte sedimentation rate (ESR)], neutrophil-to-lymphocyte ratio (NLR), platelet-to-lymphocyte ratio (PLR), and monocyte-to-lymphocyte ratio (MLR). The SII index was derived as Neu x PLT/Lym.

Results: In patients with RA, the SII index was elevated compared with that of healthy individuals and positively correlated with hs-CRP, erythrocyte sedimentation rate, NLR, MLR, PLR, tender joint count, and swollen-to-tender joint count ratio. Patients with RA who had hs-CRP levels of 3 mg/L above exhibited a statistically significant increase in the SII compared with those with hs-CRP levels below 3 mg/L. Additionally, within the cohort of RA patients with hs-CRP levels at or above 3 mg/L, a positive correlation was found between the SII index and both NLR and PLR. The SII index was positively correlated with NLR, MLR, and PLR in RA patients with hs-CRP levels below 3 mg/L. The cut-off point of the SII index for distinguishing between RA cases with hs-CRP levels 3 mg/L and those with hs-CRP levels 3 mg/L or higher was ≥323.4, with a sensitivity of 77.6% and a specificity of 54.8%.

Conclusions: The serum SII index can be a potentially useful marker for evaluating the inflammatory process and clinical progression of RA.

Keywords: Systemic immune-inflammation index, inflammation, hs-CRP, rheumatoid arthritis

ÖZ

Amaç: Romatoid artritli (RA) hastalarda sistemik enflamatuvar duruma göre düzenlenmiş sistemik immün-enflamasyon (SII) indeksini değerlendirmektir.

Yöntemler: Seropozitif RA hastaları (n=58) serum hs-C-reaktif protein (hs-CRP) düzeylerine göre iki gruba ayrıldılar: hs-CRP düzeyleri 3 mg/L veya üzerinde olan RA hastaları (yüksek sistemik enflamatuvar durum; n=38) ve hs-CRP düzeyleri 3 mg/L'nin altında olan RA hastaları (düşük sistemik enflamatuvar durum; n=20). Kontrol grubu 31 sağlıklı bireyden oluştu. Kan örnekleri şu parametreler açısından test edildi: lökositler (beyaz kan hücresi), nötrofilik granülositler, lenfositler, trombositler [platelet (PLT)], yüksek hassasiyetli hs-CRP, sedimantasyon hızı [eritrosit sedimantasyon hızı (ESR)], nötrofil-lenfosit oranı (NLR), platelet-lenfosit oranı (PLR) ve monosit-lenfosit oranı (MLR). SII endeksi Neu x PLT/Lym olarak elde edildi.

Bulgular: RA'lı hastalarda, SII endeksi sağlıklı bireylere kıyasla yüksekti ve hs-CRP, eritrosit sedimantasyon hızı, NLR, MLR, PLR, hassas eklem sayısı ve şişmiş eklem sayısının hassas eklem sayısına oranı ile pozitif korelasyon gösterdi. Hs-CRP düzeyleri 3 mg/L'nin üzerinde olan RA'lı hastalar, hs-CRP düzeyleri 3 mg/L'nin altında olanlara kıyasla SII'de istatistiksel olarak anlamlı bir artış sergilediler. Ayrıca, hs-CRP düzeyleri 3 mg/L veya üzerinde olan RA hastaları kohortunda, SII endeksi ile hem NLR hem de PLR arasında pozitif bir korelasyon bulundu. SII indeksi, hs-CRP düzeyleri 3 mg/L'nin altında olan RA hastalarında NLR, MLR ve PLR ile pozitif korelasyon gösterdi. SII endeksinin hs-CRP düzeyi 3 mg/L olan RA olguları ile hs-CRP düzeyi 3 mg/L veya daha yüksek olan olguları ayırt etmek için kesme noktası ≥323,4 olup, duyarlılığı %77,6 ve özgüllüğü %54,8 idi.

Sonuçlar: Serum SII indeksi, RA'nın enflamatuvar sürecini ve klinik ilerlemesini değerlendirmek için potansiyel olarak yararlı bir belirteç olabilir.

Anahtar kelimeler: Sistemik immün-enflamasyon indeksi, enflamasyon, hs-CRP, romatoid artrit

Address for Correspondence: A. Dervisevic, University of Sarajevo Faculty of Medicine, Department of Human Physiology, Sarajevo, Bosnia and Herzegovina
E-mail: amela.dervisevic@mf.unsa.ba **ORCID ID:** orcid.org/0000-0002-4251-1437

Received: 22 March 2024
Accepted: 31 July 2024
Online First: 05 September 2024

Cite as: Dervisevic A, Fajkic A, Jahic E, Dervisevic L, Ajanovic Z, Ademovic E, Zaciragic A. Systemic Immune-inflammation Index in Evaluation of Inflammation in Rheumatoid Arthritis Patients. Medeni Med J. 2024;39:183-191

INTRODUCTION

Rheumatoid arthritis (RA) is a complex disorder of the immune system accompanied by inflammation and destruction of joint structures, with a global prevalence of 0.24%[1]. Patients diagnosed with RA can experience increasing pain, swelling, stiffness, and functional loss in any synovial joint, ultimately resulting in a reduced standard of living. Approximately 50% of patients with RA may exhibit extra-articular manifestations, primarily affecting the skin, eyes, heart, respiratory, urinary, nervous, and gastrointestinal systems[2]. Although the exact mechanisms underlying the pathophysiological process of RA remain unknown, a growing body of scientific evidence suggests that immune-mediated inflammation plays a crucial role in the onset and progression of RA. The interaction between immune and inflammatory responses, which leads to increased production of pro-inflammatory cytokines and chemokines, activates endothelial cells and promotes alterations in the production and activation of both innate and adaptive immune cells within the joint synovium[3]. Accurately monitoring the intensity of inflammation and disease status RA patients is crucial. Developing a straightforward and quantifiable biomarker would enable more efficient, rapid, and comprehensive assessment of pathological processes in RA. The ideal hematologic diagnostic marker of systemic inflammatory response should be simple, non-invasive, readily available, inexpensive, and exact. C-reactive protein (CRP) is frequently utilized to evaluate systemic inflammation in RA. Additionally, it functions as an immune regulator and contributes to the inflammatory processes linked to RA and its atherogenic effects. Elevated CRP levels in patients with RA indicate a higher degree of disease activity, which can also be assessed and confirmed through the components of the 28 joints Disease Activity score 28 (DAS28)[4].

New indirect hematological parameters, such as the neutrophil-to-lymphocyte ratio (NLR), monocyte-to-lymphocyte ratio (MLR), and platelet-to-lymphocyte ratio (PLR), have been recognized as valuable hematological indicators for numerous diseases[5].

The SII index is based on three peripheral immune and inflammatory cell types: thrombocytes, neutrophils, and lymphocytes (Lym) and is easily obtained from routine blood count data[6,7]. As a complex inflammatory biomarker, the SII index may better reflect systemic inflammatory status than other standard inflammatory markers, such as NLR or PLR alone[8]. To date, this inflammatory biomarker has been used to assess prognosis in various malignancies, including glioma, nasopharyngeal carcinoma, breast cancer, and hepatocellular carcinoma. In addition, research has shown its efficacy in various clinical conditions wherein inflammation is a key factor, including cardiovascular disease, ophthalmological disease, and autoimmune disorders[9].

Given the significance of inflammation in the pathogenesis of RA, this study aimed to determine the SII index levels in patients with RA categorized by systemic inflammatory status and to examine the association of the SII index with the DAS28-erythrocyte sedimentation rate (ESR) score, as well as with clinical and functional disease parameters.

MATERIALS and METHODS

Patients and Control Subjects

This single-institution, cross-sectional study included 58 patients of both sexes with a diagnosis of seropositive RA, all of whom were admitted to the Clinic for heart, blood vessels, and rheumatism at the Clinical Center University of Sarajevo. RA diagnosis was validated by an independent rheumatologist based on the 1987 American College of Rheumatology (ACR) revised classification criteria[10].

The experienced physician assessed disease activity in RA patients using DAS28, a formula with four components: DAS28 = 0.56 × √(TEN28) + 0.28 × √(SW28) + 0.70 × Ln(ESR) + 0.014x (GH). [TEN28: tender joint count; SW28: swollen joint count; Ln(ESR): the natural logarithm of Westergren's ESR; GH: general health, i.e., the patient's subjective assessment of disease activity based on a visual analog scale (VAS) of 100 mm][11].

Based on serum hs-CRP levels, which reflect the degree of systemic inflammation, RA patients were categorized into two groups: those with high systemic inflammation (n=38; hs-CRP ≥3 mg/L) and those with low systemic inflammation (n=20; hs-CRP <3 mg/L)[12].

The control group (n=31) consisted of healthy participants drawn from the general population, matched for age and gender, and exhibited neither subjective nor objective indicators of acute or chronic illness.

The inclusion criteria for the study were laboratory-confirmed seropositive RA patients aged 18 years or older, of both sexes, and who met the ACR diagnostic criteria for RA.

Participants were excluded from the study if they had any coexisting pathological conditions, including other forms of rheumatic diseases, malignant diseases, active inflammation of a local or systemic nature, thyroid gland dysfunction, liver or kidney diseases, coronary artery

diseases, hematological disorders, or other autoimmune disorders.

Patients who were taking enzyme-inducing or enzyme-inhibiting medications, as well as statins, were also excluded from the study.

We excluded current smokers, pregnant or lactating women, as well as individuals unable to provide informed consent from both the patient and control groups in this study.

After a detailed explanation of the research protocol, all participants voluntarily agreed to sign an informed consent form to complete the survey questionnaire and donate blood for biochemical analyses.

During blood collection, all patients were treated with disease-modifying anti-rheumatic drugs (DMARDs). In this cohort, methotrexate (MTX) was the most frequently used DMARD, administered in 51 cases. MTX was used as monotherapy in 36 cases, combined with sulfasalazine in 5 cases, with cyclosporine in 3 cases, and in 7 cases, it was combined with TNF-α inhibitors.

Of the remaining 7 cases treated with sulfasalazine, 5 received sulfasalazine alone, while 2 patients used cyclosporine in addition to sulfasalazine.

The most prevalent extra-articular complications observed among the 58 included patients were muscular weakness (14 patients, 24.1%), muscular hypotrophy (10 patients, 17.2%), rheumatoid scleritis (8 patients, 13.8%), conjunctivitis (6 patients, 10.3%), osteoporosis (12 patients, 20.7%), and Sy. Caplan (8 patients, 13.8%). Patients with other extra-articular manifestations, such as anemia, vasculitis purpura, pleuritis, and central nervous system injuries, were excluded from the study to preserve cohort homogeneity.

The study was approved by the Clinical Center of the University of Sarajevo Ethics Committee (approval no.: 0305-33957, date: 30.11.2010) and was conducted following a protocol that adhered strictly to the ethical guidelines established by the Declaration of Helsinki, as revised in 2000.

Laboratory Analysis

Samples of blood from both patients and healthy subjects were obtained in the early morning using the vacutainer technique, through venipuncture in the antecubital area, following a 12 h overnight fasting period and after a 30-min rest.

In the blood samples collected from all subjects, biochemical laboratory analyses were performed to determine the leukocyte count (WBC), neutrophilic granulocyte count, lymphocytes count (Lym), thrombocyte count (PLT), hs-CRP concentration, and sed rate (ESR).

All laboratory tests were conducted utilizing standardized and automated procedures at the Department of clinical chemistry and biochemistry.

Serum levels of hs-CRP were assessed using the particle-enhanced immunonephelometry technique with a BN II analyzer (Siemens Healthineers Global, Erlangen, Germany) and the Roche, Hitachi Cobas C system (Mannheim, Germany).

The SII index for each research participant was calculated by dividing the product of the number of neutrophil granulocytes and platelets by the number of Lyms.

The NLR represents the quotient of the total number of neutrophils and lymphocytes in peripheral blood. Similarly, the PLR was calculated by dividing the total number of platelets by the total number of lymphocytes. MLR was calculated by dividing the total number of monocytes by the total number of lymphocytes.

Statistical Analysis

The distribution of the analyzed data was assessed using the Shapiro-Wilk test. Normally distributed data are reported as mean and standard deviation, whereas non-normally distributed data are presented as median and interquartile range (25th to 75th percentile). Categorical data are expressed as a whole numbers (n) or percentages (%).

The independent t-test was used to compare normally distributed data, whereas the Mann-Whitney U test was employed for non-normally distributed data.

Spearman's correlation coefficient was used to examine the relationships between quantitative variables. Receiver operating characteristic (ROC) curves and the corresponding area under the curve (AUC) were used to determine the optimal cut-off values of the SII index for distinguishing patients with RA based on the level of systemic inflammation. Diagnostic accuracy was calculated with 95% confidence intervals (CI). A p-value of less than 0.05 was considered statistically significant. Statistical analysis was conducted using Statistical Package for the Social Sciences (SPSS) software for Windows (version 13.0; SPSS, Chicago, IL, USA).

RESULTS

The baseline parameters, including sex and age, along with the laboratory findings for patients with RA and healthy individuals are presented in Table 1.

The subjects in the observed groups did not differ significantly in terms of age or gender. RA patients had

significantly higher hs-CRP (p<0.001), ESR (p<0.001), PLT count (p=0.031), WBC count (p=0.002), neutrophil count (p=0.001), NLR (p=0.002) and SII index (p=0.001) compared to control individuals.

The observed differences in the numbers of monocytes (p=0.392), Lyms (p=0.743), MLR (p=0.524), and PLR (p=0.188) between RA patients and healthy individuals did not reach statistical significance.

We then analyzed the differences in laboratory parameters between RA patients exhibiting hs-CRP levels below 3.0 mg/L and those with hs-CRP levels at or above 3.0 mg/L. RA patients with hs-CRP levels of 3.0 mg/L demonstrated significantly elevated values for hs-CRP (p<0.001), ESR (p<0.001), PLT (p<0.001), neutrophil count (p=0.003), NLR (p=0.018), PLR (p=0.015), and SII index (p<0.001) in comparison to RA patients with hs-CRP levels below 3.0 mg/L.

The observed differences in the numbers of monocytes (p=0.382), WBCs (p=0.051), Lyms (p=0.765), and MLR (p=0.839) between the groups did not reach statistical significance (Table 2).

Table 1. Baseline characteristics and laboratory results observed in RA cases and healthy individuals.

Variables	RA group (n=58)	Control group (n=31)	p-value
Female (n/%)	56 (96.6)	27 (87.1)	0.09
Male (n/%)	2 (3.4)	4 (12.9)	
Age (years)	55.2±12.3	50.6±7.6	0.06
hs-CRP (mg/L)	6.4 (1.5-24.3)	0.8 (0.4-1.6)	**<0.001**
ESR (mm/h)	31.0 (19.8-55.0)	11.0 (7.0-20.0)	**<0.001**
Platelet count (10^9/L)	278.5±82.7	243.3±46.0	**0.031**
Monocyte count (10^9/L)	0.41±0.17	0.38±0.15	0.392
White blood cell count (10^9/L)	6.7±2.0	5.4±1.1	**0.002**
Neutrophil counts (10^9/L)	3.5 (2.7-4.8)	2.8 (2.1-3.7)	**0.001**
Lymphocyte count (10^9/L)	2.2±0.8	2.1±0.5	0.743
NLR	1.8 (1.3-2.5)	1.3 (1.0-1.7)	**0.002**
MLR	0.19 (0.13-0.28)	0.17 (0.14-0.23)	0.524
PLR	139.2 (91.6-184.4)	120.4 (102.4-150.0)	0.188
SII index	472.7 (342.3-712.9)	319.5 (252.0-342.0)	**0.001**

The findings are presented as mean values with standard deviations, median values with interquartile ranges (25th to 75th percentile), and percentages (%). RA: Rheumatoid arthritis, hs-CRP: hs-C-reactive protein, ESR: Erythrocyte sedimentation rate, NLR: Neutrophil-to-lymphocyte ratio, MLR: Monocyte-to-lymphocyte ratio, PLR: Platelet-to-lymphocyte ratio, SII: Systemic immune-inflammation

Table 2. Laboratory findings in patients with RA according to hs-CRP levels.

Variables	RA group hs-CRP <3 mg/L (n=20)	RA group hs-CRP ≥3 mg/L (n=38)	p-value
hs-CRP (mg/L)	1.5 (1.3-1.8)	17.2 (6.5-32.0)	**<0.001**
ESR (mm/h)	20.0 (12.0-22.0)	38.5 (24.3-61.5)	**<0.001**
Platelet count (10^9/L)	213.0 (184.0-268.0)	291.5 (233.5-258.8)	**0.001**
Monocyte count (10^9/L)	0.45±0.15	0.40±0.18	0.382
White blood cells count (10^9/L)	6.06±1.4	6.87±2.1	0.051
Neutrophil counts (10^9/L)	3.3±0.8	4.2±1.5	**0.003**
Lymphocytes count (10^9/L)	2.18±0.8	2.07±0.8	0.765
NLR	1.51 (1.26-1.9)	2.0 (1.4-2.7)	**0.018**
MLR	0.23±0.1	0.20±0.1	0.839
PLR	111.94 (86.5-142.5)	158.01 (102.2-226.8)	**0.015**
SII index	357.7 (236.4-434.9)	570.4 (391.7-918.8)	**<0.001**

The findings are presented as mean values with standard deviations, median values with interquartile ranges (25th to 75th percentile), and percentages (%). RA: Rheumatoid arthritis, hs-CRP: hs-C-reactive protein, ESR: Erythrocyte sedimentation rate, NLR: Neutrophil-to-lymphocyte ratio, MLR: Monocyte-to-lymphocyte ratio, PLR: Platelet-to-lymphocyte ratio, SII: Systemic immune-inflammation

Significantly higher tender joint count (p=0.008), VAS pain score (p=0.028), and DAS28-ESR (p=0.001) were observed in RA patients with hs-CRP levels of 3 mg/L or above compared with RA patients with hs-CRP levels below 3 mg/L.

The differences in disease duration (p=0.600), number of swollen joints (p=0.238), and swollen-to-tender joint count ratio (p=0.279) between the observed groups did not reach statistical significance (Table 3).

Among the RA patients, a statistically significant positive correlation was identified between the SII index and hs-CRP (rho=0.468; p<0.001), ESR (rho=0.302; p=0.021), NLR (rho=0.846; p<0.001), MLR (rho=0.287; p=0.029) and PLR (rho=0.715; p<0.001).

The SII index exhibited a linear positive correlation with NLR (rho=0.698; p=0.001), MLR (rho=0.538; p=0.017), and PLR (rho=0.765; p<0.001) among patients with RA and hs-CRP level of 3 mg/L or above. Likewise, in patients with RA and hs-CRP levels of 3 mg/L or above, the SII index showed a significant positive correlation with NLR (rho=0.895; p<0.001) and PLR (rho=0.664; p<0.001) (Table 4).

The SII index demonstrated a significant positive correlation only with tender joint count (rho=0.303; p=0.021) and swollen-to-tender joint count ratio (rho=0.293; p=0.026) in the sum of all RA patients. However, correlations did not occur between the SII index and clinical parameters of disease in the RA group with hs-CRP <3 mg/L and the RA group with hs-CRP ≥3 mg/L, as shown in Table 5.

Additionally, we performed ROC curve analysis to evaluate the ability of the SII index to distinguish RA cases with hs-CRP values lower than 3 mg/L and those with hs-CRP levels of 3 mg/L or above.

The ROC curve illustrated in Figure 1 identified an optimal cut-off value of the SII index that effectively distinguished between RA patients with hs-CRP levels below 3 mg/L and those with hs-CRP levels of 3 mg/L or higher, set at ≥323.4.

Table 3. Clinical characteristics of all RA patients and subgroups of RA patients stratified according to hs-CRP levels.

Variables	RA group (n=58)	RA group hs-CRP <3 mg/L (n=20)	RA group hs-CRP ≥3 mg/L (n=38)	p-value
Disease duration (months)	72.0 (24.0-180.0)	78.0 (45.0-183.0)	72.0 (24.0-180.0)	0.600
Swollen joint count	5.1±3.9	4.0 (0.0-8.0)	5.0 (2.0-8.75)	0.238
Tender joint count	5.0 (3.0-10.0)	4.0 (2.0-4.0)	6.0 (3.25-12.0)	**0.008**
STR	0.67 (0.31-1.0)	1.0 (0.0-1.0)	0.6 (0.35-0.96)	0.279
VAS of pain score (mm)	25.0 (15.0-50.0)	20.0 (10.0-30.0)	30.0 (16.25-70.0)	**0.028**
DAS28-ESR	4.7 (3.2-5.9)	3.75 (3.0-4.36)	5.32 (3.53-6.43)	**0.001**

The findings are presented as mean values with standard deviations, median values with interquartile ranges (25th to 75th percentile), and percentages (%). RA: Rheumatoid arthritis, hs-CRP: hs-C-reactive protein, DAS28-ESR: Diseases Activity score 28-erythrocyte sedimentation rate, STR: Swollen-to-tender joint count ratio, VAS: Visual analog scale

Table 4. Correlation between SII index and inflammatory markers in RA patients according to hs-CRP levels.

Variables	RA group (n=58)		RA group hs-CRP <3 mg/L (n=20)		RA group hs-CRP ≥3 mg/L (n=38)	
	SII index					
	rho	p-value	rho	p-value	rho	p-value
hs-CRP (mg/L)	0.468	**<0.001**	0.132	0.589	0.136	0.429
ESR (mm/h)	0.302	**0.021**	0.150	p=0.539	0.115	0.502
White blood cell count (10^9/L)	0.256	0.052	-0.154	p=0.528	0.287	0.090
NLR	0.846	**<0.001**	0.696	**p=0.001**	0.895	**<0.001**
MLR	0.287	**0.029**	0.538	**p=0.017**	0.323	0.055
PLR	0.715	**<0.001**	0.765	**p<0.001**	0.664	**<0.001**

RA: Rheumatoid arthritis, hs-CRP: hs-C-reactive protein, SII: Systemic immune-inflammation, ESR: Erythrocyte sedimentation rate, NLR: Neutrophil-to-lymphocyte ratio, MLR: Monocyte-to-lymphocyte ratio, PLR: Platelet-to-lymphocyte ratio

The AUC for the established cutoff point was 0.721, accompanied by a 95% CI ranging from 0.613 to 0.829 (p=0.001). At the identified optimal SII cut-off of ≥323.4, the maximal sensitivity achieved was 77.6%, whereas the maximal specificity recorded was 54.8%.

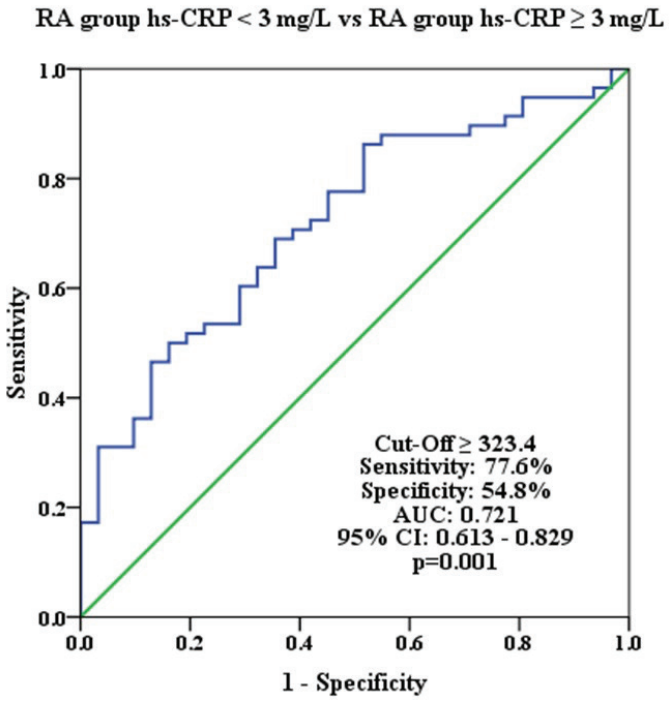

Figure 1. Receiver operating characteristic curve analysis of the SII index for distinguishing between RA patients with hs-CRP levels below 3 mg/L and those with hs-CRP levels at or exceeding 3 mg/L.

SII: Systemic immune-inflammation, RA: Rheumatoid arthritis, AUC: Area under the curve, CI: Confidence intervals, hs-CRP: hs-C-reactive protein

DISCUSSION

It has been documented that inflammatory processes, along with dysregulated immune responses, are crucial in the onset, development, and progression of RA[13,14].

However, no consensus has been established regarding the definite specific biomarkers that can be used to evaluate systemic inflammatory response in RA. The SII index is a circulating blood cell-derived index based on platelets and the two WBC subtypes neutrophils and Lyms. The importance of the SII index in identifying local immune responses and systemic inflammation is specified by the different roles that Lyms, neutrophils, and platelets play in the immune response.

This study represents the first study in which the SII index was examined in patients with RA categorized according to their systemic inflammation status. This finding underscores the significance of early inflammation assessment as a proactive measure to prevent the onset of cardiovascular comorbidities in this population.

The findings of our research indicated that patients with RA demonstrated significantly elevated SII index levels compared with healthy controls.

Elevated SII index levels suggest an intensified immune response, which may influence the mechanisms underlying the development and progression of RA. Previous research by Choe et al.[15] highlights the significance of the SII index as a marker for assessing clinical severity in RA and demonstrates significant associations with DAS28-ESR, DAS28 CRP, Clinical Disease Activity index, and Simplified Disease Activity index, indicating its potential diagnostic utility. However, its sensitivity in detecting disease remission was limited.

Table 5. Correlation between SII index and clinical indicators associated with RA according to hs-CRP levels.

Variables	RA group (n=58)		RA group hs-CRP <3 mg/L (n=20)		RA group hs-CRP ≥3 mg/L (n=38)	
	SII index					
	rho	p-value	rho	p-value	rho	p-value
Disease duration (months)	-0.211	0.115	-0.268	0.282	-0.256	0.132
Swollen joint count	0.134	0.315	0.005	0.983	0.136	0.428
Tender joint count	0.303	**0.021**	-0.003	0.991	0.174	0.309
STR	0.293	**0.026**	-0.035	0.888	0.026	0.881
VAS pain (mm)	0.257	0.051	-0.178	0.466	0.239	0.160
DAS28-ESR	-0.122	0.363	0.004	0.989	0.144	0.402

RA: Rheumatoid arthritis, hs-CRP: hs-C-reactive protein, SII: Systemic immune-inflammation, DAS28-ESR: Diseases Activity score 28-Erythrocyte sedimentation rate, NLR: Neutrophil-to-lymphocyte ratio, MLR: Monocyte-to-lymphocyte ratio, PLR: Platelet-to-lymphocyte ratio, STR: Swollen-to-tender joint count ratio, VAS: Visual analog scale

Based on a study by Aletaha et al.[16], Lyms, neutrophils, and platelets are recognized for their crucial roles in regulating inflammatory processes in RA patients, and their serum levels are considered valuable markers for assessing disease activity. Various T-cell-mediated immune processes are linked to inflammation and matrix degradation in RA. These processes encompass the migration of T-cells, their recruitment, and subsequent activation within synovial tissue, leading to the swift release of cytokines[17]. Neutrophils exhibit the highest cytotoxic capacity among the various cell types involved in the pathology of RA. In individuals with RA, neutrophils exhibit functional differences compared with those found in healthy individuals because the neutrophils present in the bloodstream of patients with RA are pre-activated to generate reactive oxygen species (ROS)[18]. Additionally, platelets enhance the recruitment of leukocytes into the vascular compartment of the RA synovium[19,20]. Our study suggests that systemic inflammatory status significantly influences not only parameters such as ESR, PLT count, neutrophil count, NLR, PLR, tender joint count, VAS of pain score, and DAS28-ESR but also SII index values in RA patients. The established correlation of the SII with hs-CRP, ESR, NLR, MLR, and PLR, as well as with the clinical and functional characteristics of disease activity, revealed significant changes in the immune system, including changes in both the quantity and role of immune cells, such as neutrophils and Lyms, in RA. In general, systemic inflammation is associated with variations in the number and composition of circulating inflammatory blood cells. The SII index combines the predictive value of three circulating inflammatory blood cell parameters from the complete blood count and is considered more powerful for predicting inflammation than single-component or two-component inflammatory markers[21].

The findings of our study align with those of the existing literature on juvenile arthritis patients, which has shown a significant positive correlation between the SII and various indicators of disease activity, encompassing both clinical assessments Juvenile Arthritis Disease Activity score-10 and laboratory evaluations (CRP and ESR)[22].

Similarly, the statistically significant positive linear associations between the SII index and both CRP and ESR in patients with ankylosing spondylitis (AS) highlight the importance of the SII index in assessing systemic inflammation in AS. However, this study also indicated that the SII is not effective in assessing disease activity, functional status, and general health status in AS[23].

Timely recognition of inflammatory processes in patients with RA is crucial for the outcome of the disease, with regard to CRP. CRP production shows a late response after infections, reaching a peak approximately 48 h after the onset of inflammation or initiation of infection[24].

Elevated SII index, platelet and neutrophil counts, NLR, and PLR in patients with high systemic inflammatory status indicate that inflammatory cytokines, along with ROS, contribute to increased disease severity in RA by promoting inflammation.

The findings of our study are consistent with those reported in prior research in which the SII index values of patients with RA were investigated. Satis[25] found that the SII index was higher in active RA patients than in remission RA patients.

In addition to disease activity, the author concluded that the SII index has the potential to be utilized as a novel index that efficiently reflects disease activity. By analyzing the ROC curve, the authors determined that a cut-off value of 574.20 was the optimal value for differentiating between patients with active RA and those in remission. Based on these findings, the SII index could be a valuable tool for monitoring inflammation and disease progression in patients with RA.

Liu et al.[26] Conducted their research on a large number of subjects using the National Health and Nutrition Examination Survey database.

In their study, all rheumatic cases had significantly higher SII index levels than control subjects. Additionally, the ROC analysis revealed that a cut-off value higher than 578.25 significantly increased RA risk. The authors concluded that the SII index, as a novel, valuable, and convenient inflammatory marker that can predict the risk of RA in adults.

The reasons for the different SII index cut-off values between studies is unclear. This explanation may be attributed to the sample size, study design, disease duration, or characteristics of the study population.

The interpretation of the results is limited by several factors. Conducted as a case-control study, this research has inherent limitations associated with its design.

The single-center observational study design made eliminating potential remnants of residual confounding. Only a single blood sample from each patient was utilized for the analysis, which may not accurately represent fluctuations in blood-derived parameters. Our subgroups were relatively small; therefore, the results we obtained need to be validated in controlled studies with more patients.

CONCLUSION

Our research results indicate a relationship between the SII index and the systemic inflammatory response in patients with RA, suggesting that the serum SII index could be a significant parameter for evaluating the inflammatory process and clinical progression of RA.

Ethics

Ethics Committee Approval: The study was approved by the Ethical Committee of the University Clinical Center Sarajevo (UCCS) (approval no.: 0305-33957, date: 30.11.2010).

Informed Consent: After a detailed explanation of the research protocol, all participants voluntarily agreed to sign an informed consent form to complete the survey questionnaire and donate blood for biochemical analyses.

Author Contributions

Surgical and Medical Practices: E.J., Concept: A.D., E.J., E.A., A.Z., Design: A.D., E.J., E.A., A.Z., Data Collection and/or Processing: A.D., A.F., L.D., Analysis and/or Interpretation: A.D., L.D., Z.A., E.A., Literature Search: A.D., A.F., L.D., Z.A., A.Z., Writing: A.D., A.F., Z.A., A.Z.

Conflict of Interest: The authors have no conflict of interest to declare.

Financial Disclosure: The authors declared that this study has received no financial support.

REFERENCES

1. Cross M, Smith E, Hoy D, et al. The global burden of rheumatoid arthritis: estimates from the global burden of disease 2010 study. Ann Rheum Dis. 2014;73:1316-22.
2. Das S, Padhan P. An Overview of the Extraarticular Involvement in Rheumatoid Arthritis and its Management. J Pharmacol Pharmacother. 2017;8:81-6.
3. Smolen JS, Aletaha D, McInnes IB. Rheumatoid arthritis. Lancet. 2016;388:2023-38.
4. Pope JE, Choy EH. C-reactive protein and implications in rheumatoid arthritis and associated comorbidities. Semin Arthritis Rheum. 2021;51:219-29.
5. Djordjevic D, Rondovic G, Surbatovic M, et al. Neutrophil-to-Lymphocyte Ratio, Monocyte-to-Lymphocyte Ratio, Platelet-to-Lymphocyte Ratio, and Mean Platelet Volume-to-Platelet Count Ratio as Biomarkers in Critically Ill and Injured Patients: Which Ratio to Choose to Predict Outcome and Nature of Bacteremia? Mediators Inflamm. 2018;2018:3758068.
6. Hu B, Yang XR, Xu Y, et al. Systemic immune-inflammation index predicts prognosis of patients after curative resection for hepatocellular carcinoma. Clin Cancer Res. 2014;20:6212-22.
7. Zhang Y, Chen Z, Jin F, et al. The Value of the Systemic Immune-Inflammation Index in Predicting Survival Outcomes in Patients with Brain Metastases of Non-Small-Cell Lung Cancer Treated with Stereotactic Radiotherapy. Mediators Inflamm. 2021;2021:2910892.
8. Aziz MH, Sideras K, Aziz NA, et al. The Systemic-immune-inflammation Index Independently Predicts Survival and Recurrence in Resectable Pancreatic Cancer and its Prognostic Value Depends on Bilirubin Levels: A Retrospective Multicenter Cohort Study. Ann Surg. 2019;270:139-46.
9. Xie Y, Zhuang T, Ping Y, et al. Elevated systemic immune inflammation index level is associated with disease activity in ulcerative colitis patients. Clin Chim Acta. 2021;517:122-6.
10. Arnett FC, Edworthy SM, Bloch DA, et al. The American Rheumatism Association 1987 revised criteria for the classification of rheumatoid arthritis. Arthritis Rheum. 1988;31:315-24.
11. Hensor EM, Emery P, Bingham SJ, Conaghan PG; YEAR Consortium. Discrepancies in categorizing rheumatoid arthritis patients by DAS-28(ESR) and DAS-28(CRP): can they be reduced? Rheumatology (Oxford). 2010;49:1521-9.
12. Vlachopoulos C, Xaplanteris P, Aboyans V, et al. The role of vascular biomarkers for primary and secondary prevention. A position paper from the European Society of Cardiology Working Group on peripheral circulation: Endorsed by the Association for Research into Arterial Structure and Physiology (ARTERY) Society. Atherosclerosis. 2015;241:507-32.
13. Shrivastava AK, Singh HV, Raizada A, et al. Inflammatory markers in patients with rheumatoid arthritis. Allergol Immunopathol (Madr). 2015;43:81-7.
14. Edilova MI, Akram A, Abdul-Sater AA. Innate immunity drives pathogenesis of rheumatoid arthritis. Biomed J. 2021;44:172-82.
15. Choe JY, Lee CU, Kim SK. Association between Novel Hematological Indices and Measures of Disease Activity in Patients with Rheumatoid Arthritis. Medicina (Kaunas). 2023;59:117.
16. Aletaha D, Neogi T, Silman AJ, et al. 2010 Rheumatoid arthritis classification criteria: an American College of Rheumatology/European League Against Rheumatism collaborative initiative. Arthritis Rheum. 2010;62:2569-81.
17. Giacomelli R, Passacantando A, Perricone R, et al. T lymphocytes in the synovial fluid of patients with active rheumatoid arthritis display CD134-OX40 surface antigen. Clin Exp Rheumatol. 2001;19:317-20.
18. Zhang L, Yuan Y, Xu Q, Jiang Z, Chu CQ. Contribution of neutrophils in the pathogenesis of rheumatoid arthritis. J Biomed Res. 2019;34:86-93.
19. Mikhak Z, Agace WW, Luster AD. Luster, Mucosal Immunology. 4th ed. Cambridge, MA, USA: Academic Press; 2015. p: 805-30.
20. Boilard E, Nigrovic PA, Larabee K, et al. Platelets amplify inflammation in arthritis via collagen-dependent microparticle production. Science. 2010;327:580-3.
21. Sazak Kundi FC. Association of Systemic Immune-Inflammation Index with the Presence and Severity of Obstructive Sleep Apnea Syndrome. ACH Med J. 2023;3:152-7.
22. Nicoară DM, Munteanu AI, Scutca AC, et al. Examining the Relationship between Systemic Immune-Inflammation Index and Disease Severity in Juvenile Idiopathic Arthritis. Cells. 2024;13:442.
23. Sariyildiz A, Benlidayi IC, Turk I, Acemoglu SSZ, Unal I. Evaluation of the relationship between blood cell markers and inflammation, disease activity, and general health status in ankylosing spondylitis. Rev Assoc Med Bras (1992). 2023;69:e20230722.

24. Hupp JR, Ferneini EM. Head, Neck, and Orofacial Infections: An Interdisciplinary Approach. 1st ed. St. Louis, MO, USA: Mos-by-Elsevier; 2016. p. 203-20.

25. Satis S. New Inflammatory Marker Associated with Disease Activity in Rheumatoid Arthritis: The Systemic Immune-Inflammation Index. Curr Health Sci J. 2021;47:553

26. Liu B, Wang J, Li YY, Li KP, Zhang Q. The association between systemic immune-inflammation index and rheumatoid arthritis: evidence from NHANES 1999-2018. Arthritis Res Ther. 2023;25:34.

DOI: 10.4274/MMJ.galenos.2024.91668
Medeni Med J 2024;39:192-203

Original Article

Head and Neck Paragangliomas: 16-year Single-center Experience and Mini Review on Diagnosis, Treatment, and Follow-up

Baş-boyun Paragangliomu: 16 Yıllık Tek Merkez Deneyimi ve Tanı, Tedavi, Takip için Kısa Derleme

Gokce AYDEMIR[1], Fazil Necdet ARDIC[1], Cuneyt Orhan KARA[1], Ferda BIR[2]

[1]Pamukkale University Faculty of Medicine, Department of Otorhinolaryngology and Head and Neck Surgery, Denizli, Türkiye
[2]Pamukkale University Faculty of Medicine, Department of Medical Pathology, Denizli, Türkiye

ABSTRACT

Objective: To investigate head and neck paraganglioma cases treated at a tertiary center from 2007 to 2023. The research includes a thorough examination of published studies that have focused on long-term outcomes. The additional goal is to contribute to the existing knowledge on head and neck paraganglioma, with a particular emphasis on refining diagnostic algorithms, treatment selection, and follow-up procedures.

Methods: A total of 44 patients were retrospectively analyzed, and 39 were included. Demographic information, symptoms, radiological examination results, types, stages, and postoperative complications were recorded. A review was conducted to select articles that reported single-center experiences with large cohorts, long follow-ups, and different treatment modalities since 2010.

Results: The mean age of the patients was 54 years, and the female/male ratio was 3.55:1. Among the 39 cases examined, 18 and 19 were identified as cervical paraganglioma and 19 as temporal bone paraganglioma. All patients initially underwent surgical resection. The mean follow-up duration was 5.42 years. Four residual cases and two recurrences were identified postoperatively, and a Gamma Knife was used as additional treatment. Subsequently, 17 articles were selected and summarized, and then a flowchart was prepared showing the possible options for diagnosis, treatment, and follow-up.

Conclusions: Preoperative staging is essential for surgical planning and predicting potential intraoperative complications. Based on our findings and review of the articles, we have prepared a flowchart that includes all possibilities depending on the tumor stage to help in the diagnosis, treatment, and follow-up of head and neck paragangliomas.

Keywords: Head and neck paraganglioma, surgery, radiation therapy, glomus tumors, staging paraganglioma

ÖZ

Amaç: Ana amacımız 2007 ile 2023 arasında bir üçüncü basamak merkezde tedavi edilen baş ve boyun paragangliomu olgularını araştırmaktır. Daha önce yayınlanmış tek merkezli ve uzun takip süreli çalışmaların detaylı bir şekilde incelenmesini içerir. İkincil amacımız, özellikle tanı algoritmasının, tedavi seçiminin ve takip prosedürlerinin geliştirilmesine odaklanmaktır.

Yöntemler: Kırk dört hasta retrospektif olarak analiz edildi. Otuz dokuz hasta çalışmaya dahil edildi. Demografik bilgiler, semptomlar, radyolojik muayeneler, paraganglioma tipleri, evreler ve ameliyat sonrası komplikasyonlar kaydedildi. 2010'dan bu yana yayınlanmış uzun takip süresi olan ve farklı tedavi yöntemlerini kullanan tek merkez deneyimlerini rapor eden makaleleri seçmek için bir literatür taraması da yapıldı.

Bulgular: Hastaların ortalama yaşı 54 ve kadın/erkek oranı 3,55:1 olarak bulundu. İncelenen 39 olgudan 18'i servikal paraganglioma ve 19'u temporal kemik paraganglioma olarak tanımlandı. Tüm olgular başlangıçta cerrahi rezeksiyon geçirdi. Ortalama takip süresi 5,42 yıl idi. Ameliyat sonrası dört kalıntı ve iki nüks tanımlandı ve ek tedavi olarak Gamma Knife kullanıldı. Daha sonra 17 makale seçildi ve özetlendi, ardından tanı, tedavi ve takip için bir akış şeması hazırlandı.

Sonuçlar: Preoperatif evreleme, cerrahi planlamada ve potansiyel intraoperatif komplikasyonları öngörmede esastır. Bulgularımıza ve makalelerin gözden geçirilmesine dayanarak, teşhis, tedavi ve baş boyun paragangliomalarının takibine yardımcı olmak için bütün olasılıkları ağırlıklandıran, tümör evresine bağlı bir akış şeması hazırladık.

Anahtar kelimeler: Baş boyun paragangliomu, cerrahi, radyaterapi, glomus tümörleri, paraganglioma evrelemesi

Address for Correspondence: Fazil Necdet Ardic, Pamukkale University Faculty of Medicine, Department of Otorhinolaryngology and Head and Neck Surgery, Denizli, Türkiye
E-mail: fnecdetardic@gmail.com **ORCID ID:** orcid.org/0000-0003-4230-3141

Presented in: The study will be partially presented at the 1st International Congress on Updates on Head and Neck Paragangliomas, September 2023, Piacenza, Italy.

Received: 18 July 2024
Accepted: 22 August 2024
Online First: 04 September 2024

Cite as: Aydemir G, Ardic FN, Kara CO, Bir F. Head and Neck Paragangliomas: 16-year Single-center Experience and Mini Review on Diagnosis, Treatment, and Follow-up. Medeni Med J. 2024;39:192-203

INTRODUCTION

Paragangliomas (PGL) are neuroendocrine tumors that develop from neural crest cells in sympathetic or parasympathetic ganglia. These types of tumor are infrequent in the head and neck region, accounting for approximately 0.6% of all head and neck cancers[1]. In general, they are characterized by slow growth and a benign nature. However, a small proportion of cases exhibit malignant behavior and may metastasize. Although catecholamine secretion is uncommon, it can lead to troublesome complications if it is present. PGL can arise sporadically or be associated with a genetic syndrome. In familial PGL, a succinate dehydrogenase (*SDHx*) gene mutation is commonly identified as an underlying cause[2].

PGL in the head and neck region can be classified into two anatomical categories: cervical PGL (carotid body and vagal) and temporal bone (tympanomastoid and tympanojuguler). The most common locations for head and neck PGL are the following: the carotid bifurcation (known as glomus carotid body), the superior vagal ganglion (known as glomus tympanojugular), the middle ear promontories (involving the auricular branch of the 10th cranial nerve, also known as Arnold's nerve, and the tympanic branch of the 9th cranial nerve, known as Jacobson's nerve, forming glomus tympanomastoid), and the inferior vagal ganglion (known as glomus vagale)[1,3]. In addition to the locations mentioned above, PGL rarely occur in the nasal cavity, orbit, oropharynx, and larynx[4].

Given their proximity to critical structures, deciding whether to prioritize preserving these structures or pursuing complete tumor removal can be a challenge for both patients and physicians. Treatment options, such as surgery, radiation therapy, a combination of both, and regular follow-up, are suggested. While there are consensus statements regarding the treatment of PGL, it is important to consider that each patient possesses unique characteristics that can influence the outcome of treatment[5].

Our aim was to thoroughly examine head and neck PGL treated at our medical center from 2007 to 2023 and to compare them with previously published studies that concentrated on the long-term outcomes of individual medical centers. Our additional goal is to improve our understanding of these cases, with a particular focus on refining the diagnosis, treatment selection, and follow-up algorithm.

MATERIALS and METHODS

This single-center retrospective study was conducted following the guidelines established in the Declaration of Helsinki and was approved by the Pamukkale University Non-Interventional Clinical Research Ethics Committee (no.: E-60116787-020-380730, date: 14.06.2023). All patients gave their written consent, including data usage before treatment. It is retrospectively registered on clinical trials.com (NCT05942482). This retrospective analysis examined data from 44 patients who underwent head and neck surgeries by the same surgical team at university hospital between 2007 and 2023, and a histopathological diagnosis of PGL. Five patients were excluded from the study due to limitations in accessing their data, leaving a total of 39 patients with a minimum follow-up period of 6 months who were included in the analysis.

The study recorded various demographic data, including age, sex, and any relevant medical history. Patients' complaints reported at the time of admission were documented along with the results of preoperative radiological examinations, such as contrast-enhanced computed tomography (CT), magnetic resonance imaging (MRI), and angiography. Pure tone audiometry results were also noted to assess any hearing-related issues.

The stages were determined by radiological examination and surgical notes. The surgical techniques were also recorded. The Shamblin classification system was used for carotid body PGL[6]. For vagal PGL, the staging system defined by Browne et al.[7] based on the relationship between the tumor and the jugular foramen was used. On the other hand, the modified Fisch classification was used to stage temporal bone PGL[8]. Postoperative complications after surgery and any recurrent PGL observed during follow-up were documented.

During the review phase, we conducted a comprehensive literature search and focused on articles presenting large series from single centers newer than 2010. Because they represented highly experienced centers. Subsequently, we extracted key data points, including age and sex distribution, familial, multiple, and functional case numbers, selected interventions, embolization options, complications, follow-up duration, residual or recurrence rates, and second-line treatments. These data were sourced from text, tables, and graphs.

Statistical Analysis

Descriptive analyses were performed to summarize the data. The results are reported as mean ± standard deviation, median, number, and percentage (%). The analyses were performed using IBM SPSS Statistics for Windows, Version 22.0 (IBM Corp., Armonk, NY).

RESULTS

The mean age of the patients was 54 years (range 18-79 years), and the female/male ratio was 3.55:1. Among the 39 cases examined, 18 were cervical, 19 were temporal, 1 was paranasal, and 1 was metastatic. The detailed classification and treatment results are shown in Figure 1. The mean follow-up duration was 5.42 years.

All cases, except metastatic PGL, demonstrated a non-functional and benign nature, accounting for 97.4% of the cases. In the 24 hour urine samples, only three individuals exhibited a slight elevation in vanillylmandelic acid levels. These PGL were also classified as nonfunctional. The most common complaint in patients with cervical PGL was the presence of a neck mass. Transcervical surgery was performed on all patients, leading to a successful total excision of the masses. Of the 18 lesions, 14 were carotid body tumors. No recurrence was observed in any of the patients with carotid body PGL cases (Figure 2). The probability of postoperative nerve palsy increased with increasing stage.

Patients with vagal PGL were classified into three stages according to the relative position of the tumor to the jugular foramen (Figure 3). Half of our four cases of vagal PGL (50%) were classified as stage 1, while the

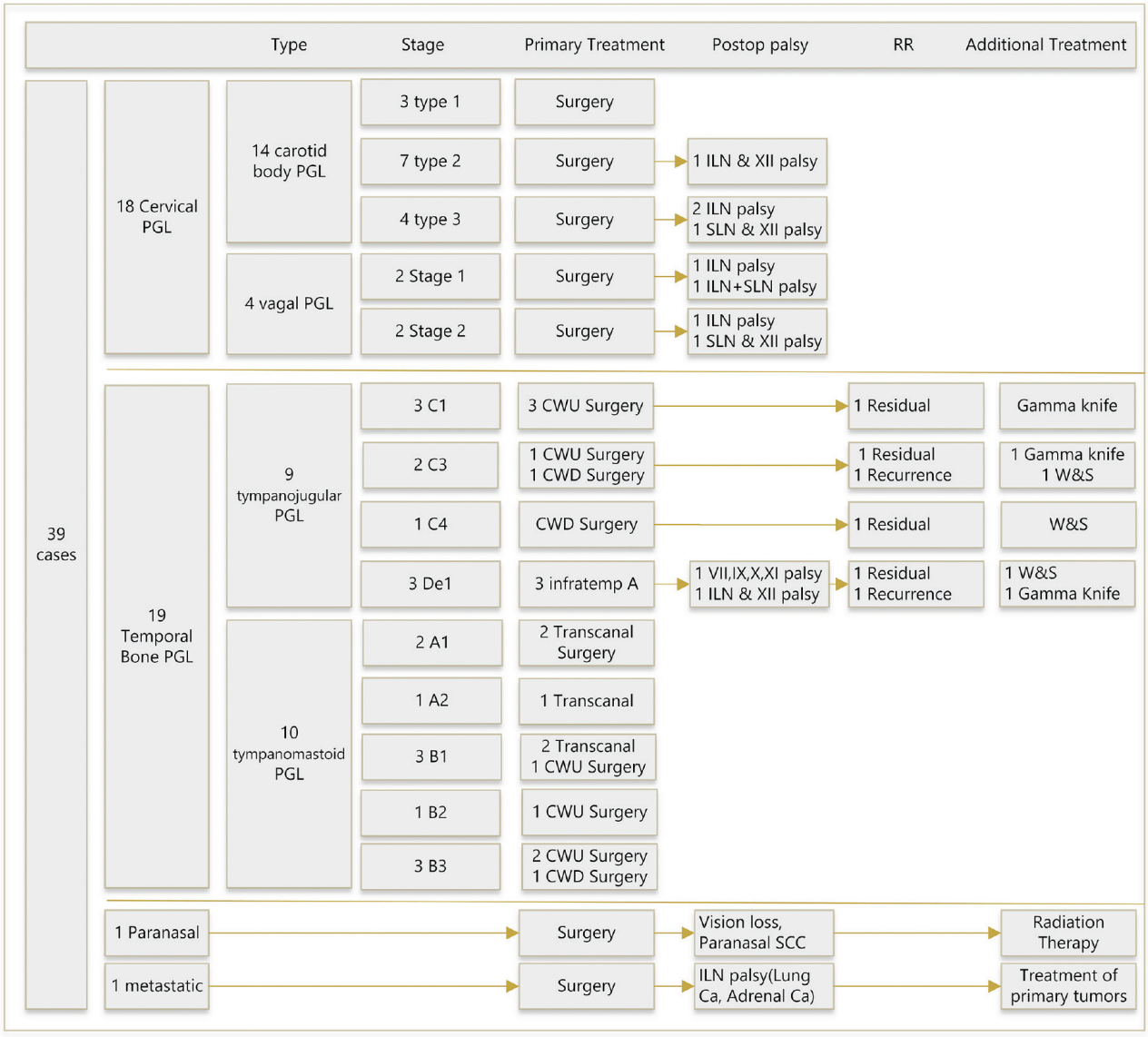

Figure 1. Our case summaries: Staging of PGL subtypes, surgical method, postoperative outcome.
CN paralysis. CN: Cranial nerve, PGL: Paragangliomas, CWU: Canal wall up, CWD: Canal wall down, RR: Residual/recurrence, SLN: Superior laryngeal nerve, ILN: Inferior laryngeal nerve, Ca: Cancer

remaining half (50%) were classified as stage 2. Hearing loss and pulsatile tinnitus were identified as the most common complaints in cases of temporal bone PGL. Detailed information about temporal bone PGL is presented in Figure 1.

Another PGL case involved a patient who underwent orbital exenteration and maxillectomy due to paranasal sinus squamous cell carcinoma. Interestingly, an incidental PGL was detected during the histopathological examination of the orbital tissue. In the second case, the patient was diagnosed with adrenal gland and lung cancers. Additionally, a metastatic PGL was discovered on histopathological examination, prompting us to perform surgery due to the presence of a neck mass.

Subsequently, 17 articles with extensive cohorts and long follow-up durations were selected. These studies included various treatment modalities, such as surgery, surgery combined with radiation therapy, radiation therapy alone, and a wait-and-scan policy. The data collected from these articles are presented in Table 1. Initially, information about the diagnosis was collected and subsequently merged. The focus then shifted to the preferred interventions and their outcomes. This information was used to design a diagnostic and therapeutic flowchart (Figure 4).

DISCUSSION

In this study, we conducted a retrospective review of 39 cases treated in our clinic. The average duration

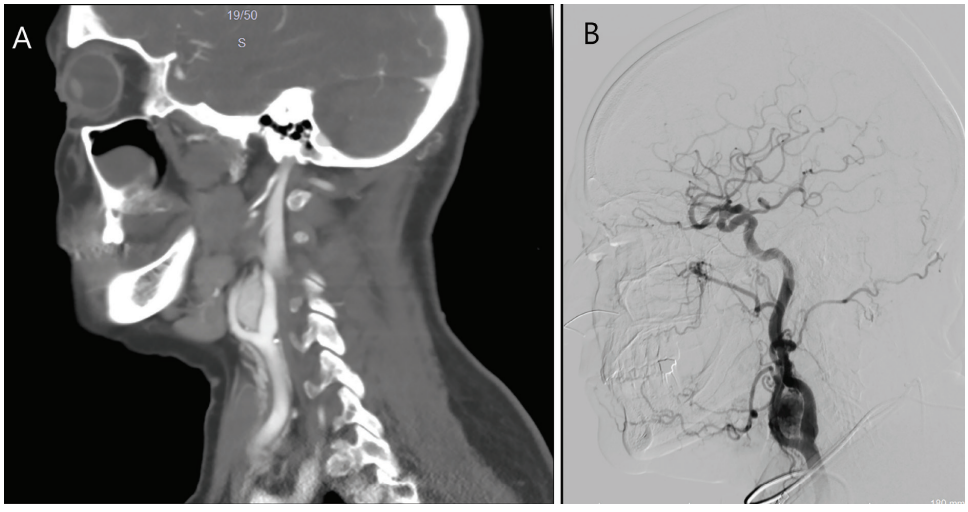

Figure 2. A 64-year-old woman with right Shamlin type 2 glomus caroticum [CT angiography, sagittal view **(A)**, conventional carotid angiography **(B)**].

CT: Computed tomography

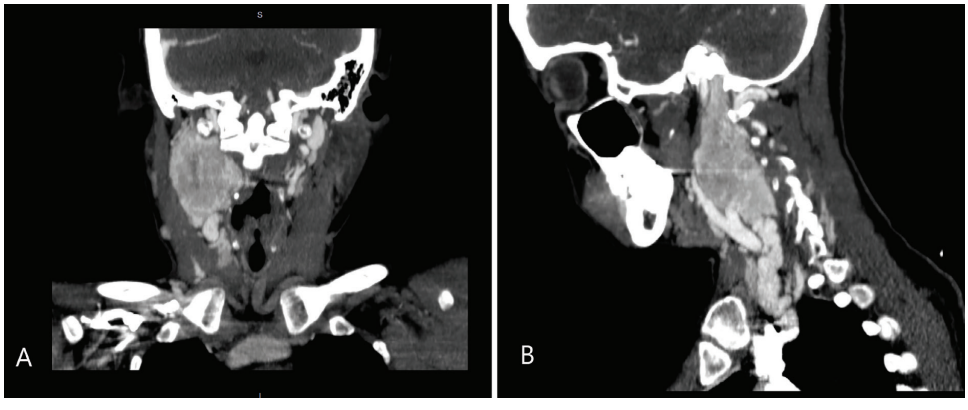

Figure 3. A 41-year-old woman with right stage 2 vagal glomus [CT angiography, coronal view **(A)**, and sagittal view **(B)**].

CT: Computed tomography

Table 1. The summary of cohorts from single center studies.

	Type	mAge	F:M	Fml	Mtpl	Func	Emb
Aydemir et al. (our series)	14 carotid	57.21	7:1	0	0	0	None
	4 vagal	55.75	1:1	0	0	0	None
	9 jugular	56	3.5:1	0	11%	0	100%
	10 tympanic	47.16	10:0	0	0	0	None
Rijken et al.[9] 2019	17 carotid	45.3	2.12:1	43%	54%	30%[c]	-
	10 vagal						-
	25 jugular						-
	15 tympanic						-
Ferrante et al.[17] 2015	44 carotid	55	3.71:1	20%	16%	-	50%
Merzouqi et al.[12] 2021	10 carotid	56.67	2.3:1	-	50%	10%	6%
	5 vagal	58.4	5:0		0	0	0
	6 jugular	54.72	2.7:1	-	0	0	50%
	5 tympanic					0	0
Nicoli et al.[13] 2017	18 jugular	55	2.6:1	-	-	-	44%
	18 tympanic			-	-	-	-
Castelhano et al.[10] 2022	24 carotid	56.5	1.92:1	37.5%	20.5%	14%	64.4%[c]
	22 vagal					16%	
	31 jugular					10%	
	9 tympanic						
Yildiz et al.[14] 2021	41 jugular	56	3.21:1	-			51%[c]
	18 tympanic					-	31%[c]
Valero et al.[20] 2020	68 carotid	49.1	1.51:1	14.6%	11.7%	1%[g]	6.8%
	24 vagal	52.9	2.5:1				30%
	8 jugular						
	2 tympanic						
Smith et al.[15] 2017	61 carotid	54	1.58:1	84%[f]	12.4%	-	51%[c]
	20 vagal	47.7	1:1.33			0	100%[c]
	41 jugular	52.5	2.72:1			16%	68%[c]
	22 tympanic	60.3	6.3:1			-	-
Jackson et al.[31] 2001	152 jugular	41	2.59:1	-	9%	9.7%	-
	27 vagal						
	3 carotid						
Anderson et al.[24] 2020	25 jugular	55	2:1	13.3%		-	23%
	3 carotid						
	1 tympanic						
	1 glomus vagale						

Table 1. Continued

	Intervention	Complication[a]	FU	Rce/Rsd	Second line[b]
Aydemir et al. (our series)	100% Srg	28% CNP	6.42	0	-
	100% Srg	100% CNP	4.62	0	-
	100% Srg	22% CNP	5.1	66%	50% GK, 50% W&S
	100% Srg	0	4.3	0	-
Rijken et al.[9] 2019	53% Srg, 47% W&S	?	11.2	11%[c]	?
	40% Srg, 10% RTA, 50% W&S	?	7.2	33%[c]	?
	32% Srg, 12% RTA, 48% W&S, 8% Srg + ART	?	8.7	36%[d]	?
	67% Srg, 33% W&S	?	3.1	0	-
Ferrante et al.[17] 2015	100% Srg	6.7% CNP, 2% bleeding	-	2%	100% Srg
Merzouqi et al.[12] 2021	100% Srg	10% CNP	3.6	10%	100% RTA
	100% Srg	100% CNP	2.4	0	-
	50% Srg, 50% RTA	36% CNP[e]	3.95	0	-
	100% Srg	-			-
Nicoli et al.[13] 2017	94% Srg, 6% RTA	53% CNP[c], 2% bleeding	6.1	60%[c]	22% Srg, 11% Srg + RTA, 55% RTA
		11% CNP		22%	25% Srg, 25% RTA, 50% Srg + ART
Castelhano et al.[10] 2022	66.3% Srg, 29.4% RTA, 4.4% W&S	33% CNP	7.6	52%[c]	32% W&S, 3.5% Srg, 50% RTA
		100% CNP			
		40% CNP			
		-			
Yildiz et al.[14] 2021	36% Srg, 34% Srg, 34% Srg + RTA, 24% RTA, 2.5% W&S, 2.5% none	23%[c] CNP, 3% bleeding	10.3	34%	50% RTA, 35% Srg
	88% Srg, 5% RTA, 5% W&S	0		5%	?
Valero et al.[20] 2020	16.2% W&S, 82.4% Srg + ART, 1.5% RTA	5.9% CNP	2	10.6%	18% Srg
	25.7% W&S, 54.3% Srg + ART, 20% RTA	71.4% CNP	4		
Smith et al.[15] 2017	80.3% Srg, 23% W&S	40.8%[c] CNP	1.58	3%	100% Srg
	52% Srg, 9.5% RTA, 38% W&S	100%[c] CNP	2	9.5%	50% Srg
	39% Srg, 26.8% RTA, 24.3% W&S	56%[c] CNP	3.84	36.5%	60% RTA
	86% Srg, 13.6% W&S	-	2	-	-
Jackson et al.[31] 2001	100% Srg	69% CNP	4.5	14.8%	22% Srg, 7% W&S, 3.5% RTA, 66% None[i]
		100% CNP			
		67% CNP			
Anderson et al.[24] 2020	20% ART, 20% salvage, 60% RTA (36.7% Srg before)	16.6% CNP	4.16	0	-

Table 1. Continued

	Type	mAge	F:M	Fml	Mtpl	Func	Emb
Alvarez-Morujo et al.[11] 2016	24 multicentric (37 carotid, 10 vagal, 13 jugular)	40.4	1:1	70.8%	100%	0	-
Dorobisz et al.[19] 2016	47 carotid	45	1:1.5	-	4%	-	-
Prasad et al.[16] 2016	236 jugular	46.7	1:1.06		14.6%	0	99%
Smee et al.[21] 2015	27 jugular 7 tympanic 9 cervical	54	1.78:1	20%	16%	-	-
Hong et al.[25] 2021	4 tympanic 21 jugular 3 carotid	50	1.07:1		7%	14%	
Gilbo et al.[26] 2014	131	55	2:1		15%		
Carlson et al.[27] 2015	16 jugular	64.2	4:1	-	20%	-	-
Langerman et al.[28] 2012	28 carotid 19 vagal	56	2.30:1	19%	25%		

Table 1. Continued

	Intervention	Complication[a]	FU	Rce/Rsd	Second line[b]
Alvarez-Morujo et al.[11] 2016	36 Srg (21 carotid, 9 jugular, 6 vagal) 9 RTA (1 carotid, 6 jugular, 2 vagal) 12 W&S (10 carotid, 1 jugular, 1 vagal)	83% CNP	3	20.8%	20% Srg, 80% RTA
Dorobıscz et al.[19] 2016	100% Srg	42% vascular work, 10% CNP	?	0	-
Prasad et al.[16] 2016	66.9% single-stage Srg, 11.4% two-stage Srg, 19.4% W&S, 0.4% RTA	23.2%[b] new facial 36%[b] new IX 32.9%[b] new X 48%[b] new XI 20%[b] new XII	3.8	12.4%[c]	30.4% RTA, 69.6% W&S
Smee et al.[21] 2015	23% Srg + RT (9% ART, 4.5% SRS, 7% SRT)	2% CNP	3.5	50%[c]	?
	77% RT (20% SRS, 38.6% SRT, 25% RTA)			0	
Hong et al.[25] 2021	10% adjuvant SRT 42% salvage SRT 48% primer SRT	3% facial palsy 3% cerebellar necrosis	5.25	59% PR 3% PRG	?
Gilbo et al.[26] 2014	55% RTA, 9% SRT, 36% IMRT, (14% treated before)	0	11.5	3.8%	20% RTA, 20% Srg, 20% Srg +ART, 40% None
Carlson et al.[27] 2015	100% W&S	38% hearing loss, 12.5% bloody otorhea, 37% CNP	6.85	33%	20% Srg, 20% RTA, 60% None
Langerman et al.[28] 2012	100% W&S	42% stable, 38% grew little, 20% reduced	5	0	-

Fml: Familial, Mtpl: Multiple, Embo: Embolization, FU: Mean follow-up (years), Rce: Recurrence, Rsd: Residual, mAge: Mean age in years, Srg: Surgery, GK: Gamma Knife, W&S: Wait and scan, RTA: Radiotherapy alone, ART: Adjuvant radiotherapy, SRS: Stereotactic radiosurgery, SRT: Stereotactic radiotherapy, PR: Partial response, PRG: Progressive, IMRT: Intensity-modulated radiation therapy. [a]New complications after intervention, [b]Ratio of treatment preference in residual and recurrent tumors, [c]Only in the surgery group, [d]Only in treated group, [e]Tumors that extended to the skull base were not included in this series, [f]Only 53 patients had genetic tests, 41 was positive

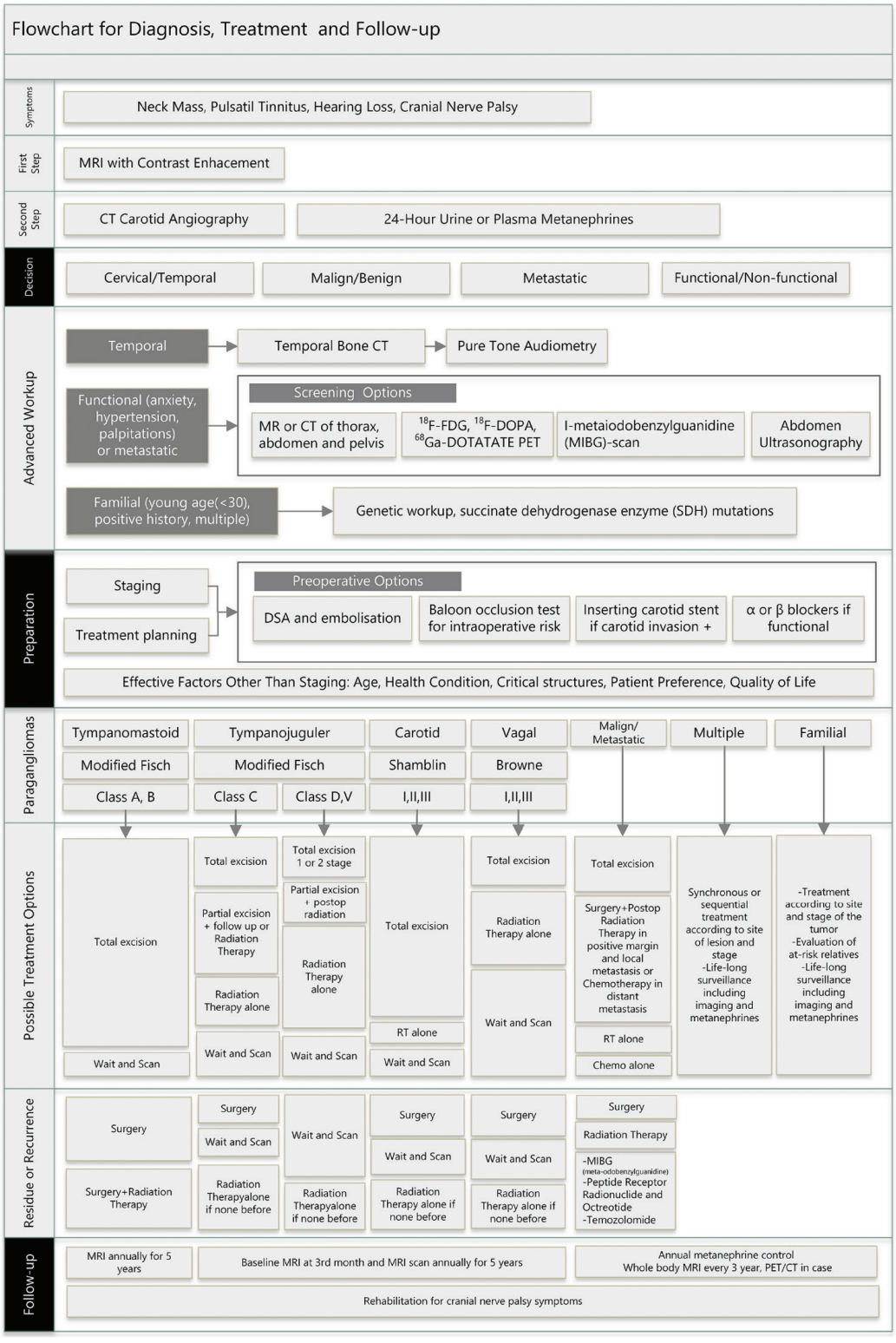

Figure 4. We combined all algorithms and the preferences of experienced centers in a simple flowchart. Our flowchart shows the possible treatment options. The size of the rectangles in the flowchart represents the power of the recommendations.

CT: Computed tomography, MRI: Magnetic resonance imaging, F-FDG: F-fluorodeoxyglucose, F-DOPA: F-deoxyphenyl-alanine, DSA: Digital subtraction angiography, RT: Radiotheraphy, PET/CT: Positron emission theraphy/computed tomography

of follow-up was 5.42 years. The main issues observed were cranial nerve palsy in cervical PGLs and residual/recurrence rates in tympanojugular PGLs. Diagnostic tools were generally sufficient and easily accessible, except for genetic testing, which was not as readily available. In our clinic, radiation therapy or Gamma Knife treatment was the secondary treatment. Most patients did not show signs of disease, whereas those with residual/recurrence lived with stable disease and underwent regular follow-up visits.

However, regardless of treatment, head and neck PGL can significantly affect quality of life. Hence, determining the treatment method is a challenging decision for doctors and patients. We selected 17 articles reporting single-center experiences with different treatment modalities (Table 1). Imaging techniques such as contrast-enhanced CT, MRI, and angiography were common. In addition, all functional tests were performed routinely. However, genetic studies were limited[9-11]. Staging procedures were performed for all cases, with a consensus among the authors on using the Fisch classification for temporal bone PGLs and the Shamblin classification for carotid PGLs. However, there was no unanimous decision on vagal PGLs.

The diversity of treatment modalities represents the initial step. Surgery was the predominant choice among the selected articles, possibly influenced by our selection bias. Surgical intervention for head and neck PGL presents distinct challenges because of their proximity to critical vascular structures and cranial nerves. To mitigate excessive bleeding and minimize brain tissue damage, certain patients favored alternative approaches, such as embolization, carotid stenting, and balloon occlusion tests. Embolization was predominantly preferred for tympanojugular PGL like us[10,12-16], but some authors also opted for this method for carotid and vagal PGLs[15,17]. In a retrospective study by Han et al.[18], a comparison was made between patients who underwent preoperative embolization and those who did not. The study did not reveal any differences in stroke rate, recurrence, cranial nerve injury, operation duration, and blood loss[18]. In our clinic, the balloon occlusion test, which provides vital information about the collateral circulation of brain vessels, was routinely used for cervical and tympanojugular PGLs.

The success of the surgical approach hinges on the utilization of meticulous techniques and the promotion of close collaboration among the surgical team. Although employing sophisticated methods and experienced surgeons may not always be possible, complete tumor removal may not always be possible, depending on tumor size, location, involvement of neighboring structures, and potential risks to vital components[11,16,19]. Alternative treatment options, such as partial resection or adjuvant therapy, may be considered in such cases. In addition to subtotal excision, radiotherapy, particularly Gamma Knife, plays a crucial role in the effective treatment of tumors, especially in stage 3-4 glomus tympanojugular tumors[9,14,20,21]. In our patient cohort, a considerable proportion (66.7%) of advanced-stage (class C-D) temporal bone PGL cases experienced recurrence over time, despite the absence of visible residual tumor during initial treatment or when residual tissue was deliberately retained during surgery to avoid potential complications. Recurrence of early-stage (class A-B) TBP was observed at a rate of 11.1%.

In 2018, Jansen et al.[22] proposed a combined radiation therapy and surgery for stage 3-4 tumors. They found the highest local control rate (100%) in TBP when combined therapy consisting of tumor debulking and postoperative radiotheraphy was performed. This approach aims to maximize treatment effectiveness by harnessing the benefits of radiation therapy and surgical intervention, particularly for advanced-stage tumors. Additionally, another study reported a tumor control rate of 84% in C1- 4 tumors after radiation therapy, while tumor control ranged from 80% to 95% after surgery within the same Fisch class group[23]. Yildiz et al.[14] also supported this approach, emphasizing the importance of total excision surgery for stage 1-2 temporal PGL and advocating a combination treatment approach with subtotal excision for stage 3-4 patients. In 88% of all Fisch A and B tumors that underwent surgical resection, successful tumor control was achieved. However, this percentage decreased to 83% for surgically resected Fisch C and D tumors, particularly in larger tumor sizes[14]. However, some authors preferred radiotherapy as the primary modality and reported high success rates[24-26].

The wait-and-scan approach was also reported as feasible in selected patients[27,28]. Carlson et al.[27] reported that the most common indications were advanced age (73%), patient preference (73%), and contralateral skull base or cervical lesions (13%) for this approach.

Suárez et al.[29] mentioned that the risk of vascular injury is low when using the transcervical approach for PGL surgery. However, the risk of vagus nerve damage is relatively high. They found that the vagus nerve was functionally preserved in only 4.3% of surgically treated patients[29]. The Shamblin classification can be modified to include the assessment of the vagal ganglia and jugular foramen. This modification allows a more comprehensive evaluation of the extent and involvement of vagus nerve

structures. In our study, we observed postoperative recurrent nerve paralysis in four patients with vagal PGL.

Glomus caroticum was the most common type of head and neck paraganglioma, which is consistent with previous findings in the literature[20,28]. We encountered inferior laryngeal nerve palsy (28.6%) and hypoglossal nerve palsy (14.3%) in high-grade patients. In one patient, arterial anastomosis was performed via cardiovascular surgery because of rupture of the internal carotid artery caused by tumor invasion.

Smith et al.[15] proposed an algorithm based on their experience with 194 patients. Hu and Persky[30] also published an algorithmic approach to head-neck PGLs based on a literature review. Published algorithms ended with a certain decision. However, many experienced centers use different approaches. We combined all algorithms and preferences of experienced centers with large cohorts into a simple flowchart[9-17,19-21,24-28,31]. Our flowchart shows the possible treatment options. The size of the rectangles in the flowchart represents the power of the recommendations by experienced centers (Figure 4).

Our study has several limitations, notably the small sample size and retrospective design, which may introduce biases and constraints in data collection. Additionally, the selection of articles predominantly focusing on surgery reflects our preference. More research is warranted to establish stronger evidence for managing head and neck paraganglioma. This future investigation should consider larger sample sizes, employ prospective designs, conduct a comprehensive evaluation of various treatment modalities according to tumor stage, and, importantly, use quality of life questionnaires.

CONCLUSION

The location primarily dictates the clinical presentation of paraganglioma. As the stages progress, there is an increased risk of postoperative complications and the possibility of residual tumors. Therefore, preoperative staging is essential in surgical planning to predict potential intraoperative complications. We strongly believe in considering the patient's quality of life when selecting a treatment modality. Based on our findings and review of the articles, we have decided to alter our approach and have proposed an algorithm for diagnosis, treatment, and follow-up that takes into account tumor staging.

Ethics

Ethics Committee Approval: Approval was granted by the Pamukkale University Non-Interventional Clinical Research Ethics Committee (no.: E-60116787-020-380730, date: 14.06.2023).

Informed Consent: All patients gave their written consent, including data usage before treatment.

Author Contributions

Surgical and Medical Practices: G.A., F.N.A., C.O.K., F.B., Concept: G.A., F.N.A., C.O.K., F.B., Design: G.A., F.N.A., C.O.K., F.B., Data Collection and/or Processing: G.A., F.N.A., Analysis and/or Interpretation: G.A., F.N.A., Literature Search: G.A., F.N.A., C.O.K., F.B., Writing: G.A., F.N.A., C.O.K., F.B.

Conflict of Interest: The authors have no conflict of interest to declare.

Financial Disclosure: The authors declared that this study has received no financial support.

REFERENCES

1. Sandow L, Thawani R, Kim MS, Heinrich MC. Paraganglioma of the Head and Neck: A Review. Endocr Pract. 2023;29:141-7.
2. Muth A, Crona J, Gimm O, et al. Genetic testing and surveillance guidelines in hereditary pheochromocytoma and paraganglioma. J Intern Med. 2019;285:187-204.
3. Tokgöz SA, Saylam G, Bayır Ö, et al. Glomus tumors of the head and neck: thirteen years' institutional experience and management. Acta Otolaryngol. 2019;139:930-3.
4. Mete O, Wenig BM. Update from the 5th Edition of the World Health Organization Classification of Head and Neck Tumors: Overview of the 2022 WHO Classification of Head and Neck Neuroendocrine Neoplasms. Head Neck Pathol. 2022;16:123-42.
5. Lloyd S, Obholzer R, Tysome J; BSBS Consensus Group. British Skull Base Society Clinical Consensus Document on Management of Head and Neck Paragangliomas. Otolaryngol Head Neck Surg. 2020;163:400-9.
6. Shamblin WR, ReMine WH, Sheps SG, Harrison EG Jr. Carotid body tumor (chemodectoma). Clinicopathologic analysis of ninety cases. Am J Surg. 1971;122:732-9.
7. Browne JD, Fisch U, Valavanis A. Surgical therapy of glomus vagale tumors. Skull Base Surg. 1993;3:182-92.
8. Shin SH, Sivalingam S, De Donato G, Falcioni M, Piazza P, Sanna M. Vertebral artery involvement by tympanojugular paragangliomas: management and outcomes with a proposed addition to the fisch classification. Audiol Neurootol. 2012;17:92-104.
9. Rijken JA, de Vos B, van Hest LP, et al. Evolving management strategies in head and neck paragangliomas: A single-centre experience with 147 patients over a 60-year period. Clin Otolaryngol. 2019;44:836-41.
10. Castelhano L, Correia F, Donato S, Ferreira L, Montalvão P, Magalhães M. Paragangliomas da Cabeça e Pescoço: A Experiência de um Centro Oncológico do Sul da Europa. Acta Med Port. 2022;35:789-97.
11. Álvarez-Morujo RJ, Ruiz MÁ, Serafini DP, Delgado IL, Friedlander E, Yurrita BS. Management of multicentric paragangliomas: Review of 24 patients with 60 tumors. Head Neck. 2016;38:267-76.

12. Merzouqi B, El Bouhmadi K, Oukesou Y, et al. Head and neck paragangliomas: Ten years of experience in a third health center. A cohort study. Ann Med Surg (Lond). 2021;66:102412.
13. Nicoli TK, Sinkkonen ST, Anttila T, Mäkitie A, Jero J. Jugulotympanic paragangliomas in southern Finland: a 40-year experience suggests individualized surgical management. Eur Arch Otorhinolaryngol. 2017;274:389-97.
14. Yildiz E, Dahm V, Gstoettner W, et al. Long-Term Outcome and Comparison of Treatment Modalities of Temporal Bone Paragangliomas. Cancers (Basel). 2021;13:5083.
15. Smith JD, Harvey RN, Darr OA, et al. Head and neck paragangliomas: A two-decade institutional experience and algorithm for management. Laryngoscope Investig Otolaryngol. 2017;2:380.
16. Prasad SC, Mimoune HA, Khardaly M, Piazza P, Russo A, Sanna M. Strategies and long-term outcomes in the surgical management of tympanojugular paragangliomas. Head Neck. 2016;38:871-85.
17. Ferrante AM, Boscarino G, Crea MA, Minelli F, Snider F. Cervical paragangliomas: single centre experience with 44 cases. Acta Otorhinolaryngol Ital. 2015;35:88-92.
18. Han T, Pu J, Tang H, et al. Retrospective, multicenter study of surgical treatment for carotid body tumors with or without preoperative embolization. Front Oncol. 2023;13:1123430.
19. Dorobisz K, Dorobisz T, Temporale H, et al. Diagnostic and Therapeutic Difficulties in Carotid Body Paragangliomas, Based on Clinical Experience and a Review of the Literature. Adv Clin Exp Med. 2016;25:1173-7.
20. Valero C, Ganly I, Shah JP. Head and neck paragangliomas: 30-year experience. Head Neck 2020;42:2486-95.
21. Smee RI, Jayasekara J, Williams JR, Hanna C. Paragangliomas: presentation and management by radiotherapy at the Prince of Wales Hospital. J Med Imaging Radiat Oncol. 2015;59:229-35.
22. Jansen TTG, Kaanders JHAM, Beute GN, Timmers HJLM, Marres HAM, Kunst HPM. Surgery, radiotherapy or a combined modality for jugulotympanic paraganglioma of Fisch class C and D. Clin Otolaryngol. 2018;43:1566-72.
23. Jansen TTG, Timmers HJLM, Marres HAM, Kaanders JHAM, Kunst HPM. Results of a systematic literature review of treatment modalities for jugulotympanic paraganglioma, stratified per Fisch class. Clin Otolaryngol. 2018;43:652-61.
24. Anderson JL, Khattab MH, Anderson C, et al. Long-term Outcomes for the Treatment of Paragangliomas in the Upfront, Adjuvant, and Salvage Settings With Stereotactic Radiosurgery and Intensity-modulated Radiotherapy. Otol Neurotol. 2020;41:133-40.
25. Hong S, Kagawa K, Sato K, Ichi S. The Long-Term Outcome of CyberKnife-Based Stereotactic Radiotherapy for Head and Neck Paragangliomas: A Single-Center Experience. World Neurosurg. 2021;155:382-90.
26. Gilbo P, Morris CG, Amdur RJ, et al. Radiotherapy for benign head and neck paragangliomas: a 45-year experience. Cancer. 2014;120:3738-43.
27. Carlson ML, Sweeney AD, Wanna GB, Netterville JL, Haynes DS. Natural history of glomus jugulare: a review of 16 tumors managed with primary observation. Otolaryngol Head Neck Surg. 2015;152:98-105.
28. Langerman A, Athavale SM, Rangarajan SV, Sinard RJ, Netterville JL. Natural history of cervical paragangliomas: outcomes of observation of 43 patients. Arch Otolaryngol Head Neck Surg. 2012;138:341-5.
29. Suárez C, Rodrigo JP, Bödeker CC, et al. Jugular and vagal paragangliomas: Systematic study of management with surgery and radiotherapy. Head Neck. 2013;35:1195-204.
30. Hu K, Persky MS. Treatment of Head and Neck Paragangliomas. Cancer Control. 2016;23:228-41.
31. Jackson CG, McGrew BM, Forest JA, Netterville JL, Hampf CF, Glasscock ME 3rd. Lateral skull base surgery for glomus tumors: long-term control. Otol Neurotol. 2001;22:377-82.

DOI: 10.4274/MMJ.galenos.2024.16098
Medeni Med J 2024;39:204-210

Original Article

Comparative Effects of Candesartan Versus Enalapril on Apelin, Visfatin, and Lipid Levels in Non-obese Hypertensive Patients

Obez Olmayan Hipertansif Hastalarda Kandesartan ve Enalaprilin Apelin, Visfatin ve Lipid Düzeyleri Üzerindeki Karşılaştırmalı Etkileri

Yaseen K. JUMAAH, Zainab H. FATHI, Jehan A. MOHAMMAD

University of Mosul, College of Pharmacy, Department of Pharmacognosy and Medicinal Plants, Mosul, Iraq

ABSTRACT

Objective: Apelin and visfatin are adipokines secreted from adipose tissue that play important roles in regulating blood pressure. Therefore, the current study aimed to investigate the effects of candesartan versus enalapril on apelin, visfatin, and lipid profiles in hypertensive patients.

Methods: In this case-control study, 120 participants were enrolled in four groups; Healthy people, newly diagnosed hypertensive patients, and enalapril- and candesartan-treated patients.

Results: Serum apelin levels were significantly lower and visfatin levels were significantly higher in newly diagnosed hypertensive patients compared with the control group (p=0.0015, p=0.0175 respectively). Moreover, apelin levels were higher and visfatin levels were lower in the candesartan-treated patients compared with the newly diagnosed group (p=0.0487, p<0.0001 respectively). Interestingly, apelin levels were non-significantly higher and visfatin levels were significantly lower in enalapril-treated patients compared with the newly diagnosed group (p<0.0001).

Conclusions: Lower apelin and higher visfatin levels are associated with newly diagnosed patients with hypertension. Interestingly, the findings suggest that ACE inhibition and angiotensin receptor blockade by enalapril and candesartan, respectively, positively regulate apelin and visfatin levels in hypertension. Specifically, candesartan regulates these adipokine to a greater extent than enalapril.

Keywords: Apelin, visfatin, lipid, hypertension, candesartan, enalapril

ÖZ

Amaç: Apelin ve visfatin, yağ dokusundan salgılanan ve kan basıncının düzenlenmesinde önemli rol oynayan adipokinlerdir. Bu nedenle, bu çalışmada hipertansif hastalarda kandesartan ve enalaprilin apelin, visfatin ve lipid profilleri üzerindeki etkilerinin araştırılması amaçlanmıştır.

Yöntemler: Bu olgu-kontrol çalışmasında 120 katılımcı dört gruba ayrıldılar; sağlıklı kişiler, yeni tanı konmuş hipertansif hastalar, enalapril ile tedavi gören hastalar ve kandesartan ile tedavi gören hastalar.

Bulgular: Yeni tanı konmuş hipertansif hastalarda, kontrol grubuna kıyasla, serum apelin düzeyleri anlamlı derecede düşük ve visfatin düzeyleri anlamlı derecede yüksekti (sırasıyla p=0,0015, p=0,0175). Ayrıca, kandesartan ile tedavi edilen hastalarda, apelin düzeyleri yeni tanı konulan gruba kıyasla daha yüksek ve visfatin düzeyleri daha düşüktü (sırasıyla p=0,0487, p<0,0001). İlginç bir şekilde, yeni tanı konulan grup ile kıyaslandığında, enalapril ile tedavi edilen hastalarda apelin düzeyleri anlamlı olmayan bir şekilde daha yüksek ve visfatin düzeyleri anlamlı bir şekilde daha düşüktü (p<0,0001).

Sonuçlar: Düşük apelin ve yüksek visfatin düzeyleri yeni tanı konmuş hipertansiyon hastalarıyla ilişkili bulunmuştur. İlginç bir şekilde, bulgular sırasıyla enalapril ve kandesartan ile ACE inhibisyonu ve anjiyotensin reseptör blokajının, hipertansiyonda apelin ve visfatin seviyelerini olumlu yönde düzenlediğini göstermektedir. Özellikle, kandesartan bu adipokinleri enalaprilden daha çok düzenlemektedir.

Anahtar kelimeler: Apelin, visfatin, lipid, hipertansiyon, kandesartan, enalapril

INTRODUCTION

Hypertension is a prevalent condition characterized by persistently elevated blood pressure that increases the risk of developing cardiovascular diseases (CVDs) and other serious health complications[1]. The main causes of hypertension include genetic predisposition, a sedentary lifestyle, high salt intake, alcohol consumption, psychological stress, and obesity. Alternative methods for treating hypertension should be considered due to

Address for Correspondence: Z. H. Fathi, University of Mosul, College of Pharmacy, Department of Pharmacognosy and Medicinal Plants, Mosul, Iraq
E-mail: zainabh@uomosul.edu.iq **ORCID ID:** orcid.org/0000-0003-0327-0914

Received: 12 June 2024
Accepted: 26 August 2024
Online First: 05 September 2024

Cite as: Jumaah YK, Fathi ZH, Mohammad JA. Comparative Effects of Candesartan Versus Enalapril on Apelin, Visfatin, and Lipid Levels in Non-obese Hypertensive Patients. Medeni Med J. 2024;39:204-210

its multifactorial etiology. One potential risk factor of hypertension in patients with obesity is chronic mild inflammation. Adipose tissues release adipokine in response to inflammation, and these molecules may be associated with hypertension.

Apelin, visfatin, and several other peptides have been recognized as adipokines[2]. By activating the G-protein-coupled receptor angiotensin II (AngII) protein J receptor (APJ), apelin increases diuresis by opposing arginine vasopressin, causing vasodilation with a corresponding reduction in blood pressure through a nitric oxide-dependent mechanism and has a positive inotropic effect on the myocardial[3]. Interestingly, apelin decreases the release of free fatty acids, increases the thickness of the perilipin layer around lipid vacuoles, and increases its stability against lipase[4]. Elevated low-density lipoprotein-cholesterol (LDL-c) levels are associated with lower apelin levels[5].

Visfatin was identified in 2005. It is unclear how visfatin contributes to hypertension pathophysiology. Visfatin produces oxidative pressure, which damages NO and increases endothelin factor 1 levels, possibly leading to atherosclerosis and vasoconstriction[6]. Interestingly, visfatin increases the synthesis of interleukin 6, which is a potential inhibitor of adipogenesis, and influences the metabolism of humane adipocytes by lowering lipoprotein lipase activity[7].

Low plasma apelin levels are associated with arterial hypertension and atherosclerosis. In contrast, elevated visfatin levels can induce vascular inflammation, destabilize atherosclerotic plaques, and serve as markers for determining the stages of essential hypertension[8].

Apelin and visfatin were previously reported to affect food intake and lipid metabolism. The salivary and serum levels of these adipocytokine have been extensively evaluated as biomarkers for the early diagnosis of CVDs[9,10]. Visfatin has a specific appeal for researchers due to its role in the pathogenesis of hypertension and the possibility of using its serum levels as a prognostic biomarker for hypertension detection. Visfatin may alter metabolic processes involved in lipid and glucose metabolism via its NAMPT enzyme-like activity. Furthermore, apelin has been reported to block lipolysis and enhance the stability of lipid vacuoles by rendering them resistant to lipases. Interestingly, apelin is related to higher lipid levels and can be used as an indicator of premature atherosclerosis in hypertensive patients[11].

There are conflicting studies on the comparative effects of candesartan and enalapril on adipokine levels in hypertensive patients[12]. Therefore, the aim of this study was to determine whether treatment with enalapril or candesartan influences plasma apelin, visfatin, and lipid profiles in non-obese hypertensive patients.

MATERIALS and METHODS

Subjects and Study Designs

This comparative case-control study included 120 subjects (controls and hypertensive of both sexes) aged between 38 and 65 years and was classified into four groups (30 samples each); group A: healthy subjects as controls, group B: hypertensive patients (newly diagnosed), group C: enalapril-treated patients (20 mg once daily) for 1 year, and group D: candesartan-treated patients (16 mg once daily) for 1 year. The current case-control study conducted between September 2023 and February 2024 in the Kirkuk governorate included the following hospitals (Hawija General Hospital, Azadi Teaching Hospital in Kirkuk, and Kirkuk General Hospital). The ethical integrity of this study was paramount and was conducted under ethical guidelines and with approval from the Kirkuk Health Province Department Knowledge Management and Research Division (approval no.: 631, date: 05/10/2023). Their endorsement for the study was documented in a letter dated October 5, 2023, bearing reference number 631, and informed consent was obtained from all participants. Pregnant and lactating women, patients taking drugs other than candesartan or enalapril, those taking dietary supplements, patients with acute or chronic health conditions other than hypertension, patients changing medications during the study year, smokers, patients with a history of drinking, and anyone unable to follow the study procedures were excluded from the study. Body mass index (BMI) was determined from anthropometric data (height and weight) for each group.

Collection of Specimens

Venous blood samples (5 mL) were collected after an overnight fast from the control and patient subjects. The blood samples were immediately transferred to gel tubes from each participant and incubated for 10 min at 37 °C in a water bath. After that, samples were centrifuged for 10 min at 2000-3000 xg to separate the serum. Serum samples were divided into 3 parts and transferred promptly by micropipette into Eppendorf tubes, labeled, and refrigerated at 20 °C for later analysis.

Estimation of Serum Apelin and Visfatin Levels

Apelin and visfatin hormone levels were estimated using the enzyme-linked immunosorbent assay technique

at 450 nm using a kit supplied by Bioassay Technology Laboratory (Shanghai Korain Biotech Company).

Estimation of Serum Lipid Profile

Cobas c311 was utilized to quantify serum total cholesterol (TC), high-density lipoprotein (HDL), and triglycerides by enzymatic colorimetric techniques using the detergent cholesterol esterase, cholesterol, and its esters are released from lipoprotein which formed H_2O_2 and hydrolyzes the esters.

LDL and very low-density lipoprotein (VLDL) were estimated using Friedewald's equation[13].

Statistical Analysis

GraphPad Prism software was used to conduct statistical analyses. The Mann-Whitney U and Kruskal-Wallis tests, which were followed by Dunn's multiple comparisons test, were used to conduct two or multiple comparisons. Apelin and visfatin levels were correlated with other laboratory parameters using Spearman rank correlation analysis. The statistical significance level was set at $p<0.05$, and all quantitative data were presented as medians (minimum-maximum). Version 10 of the GraphPad Prism software (San Diego, California, USA) was used in all experiments.

RESULTS

Demographic information for Study Groups

Table 1 shows the ages, sex, BMI, and systolic and diastolic blood pressures of the hypertensive patients and controls. No significant differences were found between the study groups.

Validation of Serum Apelin and Visfatin

Serum level of apelin was significantly lower in newly diagnosed hypertensive patients than in the control group with p-value 0.0015. The circulating level of apelin was significantly higher in the candesartan-treated patients compared with the newly diagnosed hypertensive group at p-value 0.0487. However, no statistically significant differences were observed in the enalapril-treated group compared with the other groups and the candesartan-treated group compared with the control group, as shown in Figure 1. Additionally, serum levels of visfatin showed significantly elevated in the newly diagnosed hypertensive patients compared with the control group (p=0.0175) and lower in both the candesartan- and enalapril-treated patients compared with the newly diagnosed hypertensive group with p-value <0.0001. However, compared with the control group, no statistical significance was found for enalapril- and candesartan-treated patients, as shown in Figure 2.

Table 2 shows the serum levels of apelin, visfatin, and lipids in the control, newly diagnosed, and hypertensive-treated groups. It was observed that serum TC, TG, LDL, and VLDL levels were significantly higher in newly diagnosed hypertensive patients with p-value, <0.0001, 0.001, 0.0003, 0.0001 respectively, along with low HDL-cholesterol (HDL-c) levels, compared with the control group with p-value 0.0146. Concomitant serum levels of TC and LDL-c were significantly lower in enalapril-treated patients with p-value 0.0095 for TC and 0.0182 for LDL-c, while serum levels of other lipid parameters were non-significantly lower compared with newly diagnosed hypertensive patients. Moreover, analysis of the results revealed that compared with newly diagnosed hypertensive groups, the candesartan-treated group had lower levels of TC (p=0.0187) and non-significantly lower levels of other lipid parameters.

Compared with the control group, enalapril-treated patients showed significantly higher levels of serum TG, VLDL with p-value 0.036, 0.0005 respectively, with no significant variations in other lipid parameters.

Our data showed that circulating levels of TC, TG, LDL, and VLDL were significantly higher in the candesartan-treated patients compared with the control group

Table 1. Demographic characteristics of hypertensive patients and control subjects.

Parameters	Control n (30)	Newly diagnosed HT n (30)	Enalapril n (30)	Candesartan n (30)
Age (years)	45 (38-54)	43 (39-65)	48 (40-62)	46 (39-65)
Sex (M, F)	16, 14	19, 11	15, 15	11, 19
BMI (kg/m^2)	24.62 (22.47-24.7)	24 (22.09-25)	24.36 (18.49-25)	24.75 (20.6-24.97)
Blood pressure				
SBP (mmHg)	120 (115-121)	155 (139-155)	123 (120-130)	120 (118-125)
DBP (mmHg)	79 (79-81)	95 (95-110)	82 (81-83)	80 (78-82)

Values are presented as medians (minimum-maximum) BMI: Body mass index, M: Male, F: Female, SBP: Systolic blood pressure, DBP: Diastolic blood pressure

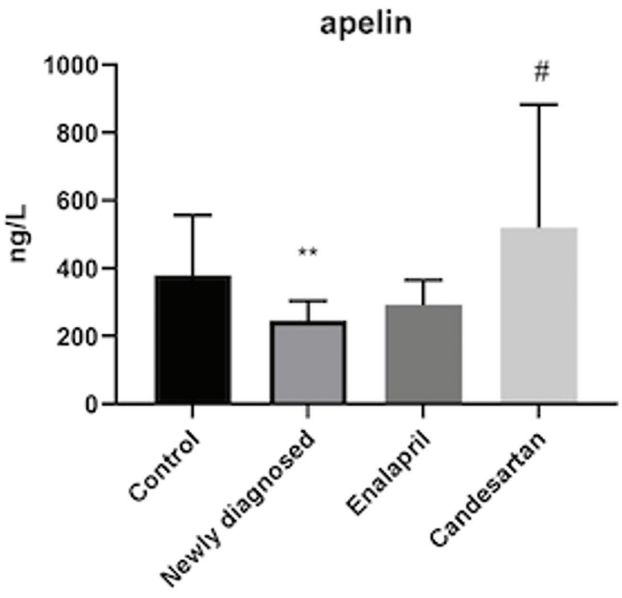

Figure 1. Effects of enalapril and candesartan on serum level of apelin. *Indicates statistically significant differences compared with the control group, and # indicates statistically significant differences compared with the newly diagnosed hypertensive group (#p<0.05, **p<0.01), as shown by Dunn's multiple comparisons post-hoc test upon completion of the Kruskal-Wallis test.

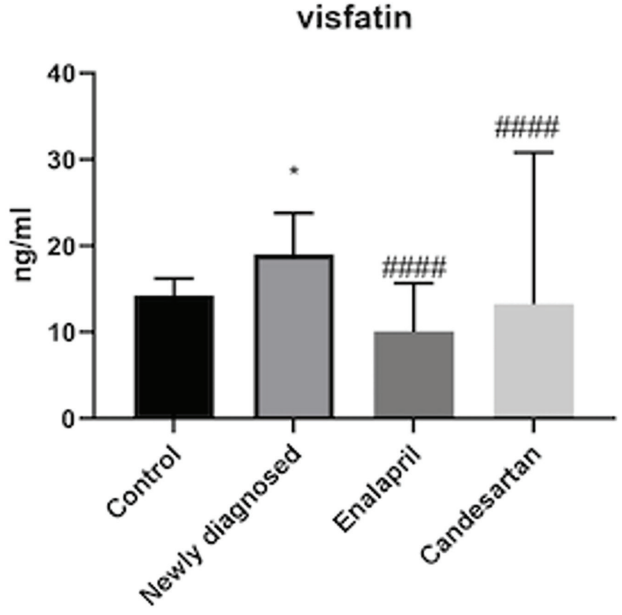

Figure 2. Effects of enalapril and candesartan on serum level of visfatin. *Indicates statistically significant differences compared with the control group, and # indicates statistically significant differences compared with the newly diagnosed hypertensive group (*p<0.05; ####p<0.0001), as shown by Dunn's multiple comparisons post-hoc test upon completion of the Kruskal-Wallis test.

(p=0.0189, 0.017, 0.001, and 0.0002), respectively, with no significant variations in the HDL-c levels. Furthermore, no statistical significance was observed between the candesartan- and enalapril-treated groups for any of the following parameters (Table 2).

DISCUSSION

While candesartan and enalapril have frequently been used for hypertension, studies focused on their effects on adipokine and lipids have shown conflicting results. Concerning apelin levels, our findings are consistent with those of Mahmoud Kadry et al.[14], which showed that apelin levels were lower in hypertensive patients than in the control. Furthermore, Derosa et al.[15] found elevated apelin levels after administration of candesartan in the animal model. In contrast, Skoczylas et al.'s[16] study showed no statistically significant difference in the apelin levels between candesartan-treated patients. Apelin is easily degraded by proteases, which limits its effectiveness. However, hypertension may be a result of elevated AngII and an increase in ACE2 expression as compensated, so there may be an increase in the metabolism of apelin[17]. However, the effect of apelin/APJ on hypertension. Concerning the enalapril group, our results disagreed with Ahmad et al.'s[18] study, which found that combining felodipine and enalapril for treating essential hypertension and coronary artery disease can reduce blood pressure, enhance their effectiveness, and improve peripheral blood circulation apelin.

Recent developments in the field suggest that visfatin could function as either a "friend" or a "foe", contingent upon the circumstances. Generally, arterial hypertension, obesity, and type 2 diabetes are associated with elevated visfatin levels[19]. Our findings were in agreement with the study by Yu et al.[20], which revealed higher visfatin levels in hypertensive participants than in healthy controls. This increase may partly explain the cardiovascular risk in the hypertensive group. In contrast, Dogru et al.[21] Did not find any significant variation in visfatin levels between the hypertensive and control groups. Although endothelial dysfunction may occur in essential hypertension and visfatin may cause endothelial dysfunction, the causal relationship between visfatin and essential hypertension remains unclear. Furuya et al.[22] revealed that candesartan can improve visfatin levels in patients undergoing peritoneal dialysis. Kärberg et al.[23] showed no significant effect on visfatin levels in patients with type 2 diabetes treated with candesartan. Candesartan's anti-inflammatory effect of candesartan was primarily produced by inhibiting AngII-induced reactive oxygen species production and blocking AT1R. Our findings revealed that serum visfatin levels were low after

Table 2. Clinical parameters in healthy and hypertensive patients.

Parameters	Control (a)	Newly diagnosed (b)	Enalapril (c)	Candesartan (d)	Significant	p-value
Apelin (ng/L)	323.3 (215.3-810)	257.3 (106-363.3)	263 (205.3-506.7)	268 (200.7-1146)	a & b** b & d*	(0.0015) (0.0487)
Visfatin (ng/mL)	14 (12-17)	18 (13-27)	10 (1-19)	9 (2-70)	a & b* b & c**** b & d****	(0.0175) (<0.0001) (<0.0001)
TC (mg/dL)	148.3 (124.6-179.2)	195.5 (133.3-250.8)	157.4 (118.1-227.3)	166.9 (100-228)	a & b**** a & d* b & c** b & d*	(<0.0001) (0.0189) (0.0095) (0.0187)
TG (mg/dL)	100.7 (67-185.2)	200.6 (124.7-340.7)	161.1 (111.9-935.3)	180 (90-380)	a & b** a & c* a & d*	(0.001) (0.036) (0.017)
LDL (mg/dL)	65.7 (49.9-75.4)	96.4 (41.9-158.1)	71.3 (22.2-126.3)	61.3 (49.4-95)	a & b*** b & c* b & d***	(0.0003) (0.0182) (0.0004)
HDL (mg/dL)	48.7 (40.5-56.9)	40.9 (28.8-46.4)	45.1 (28.9-61.4)	41.2 (25-70.7)	a & b*	(0.0146)
VLDL (mg/dL)	20.1 (13.4-37)	39.5 (14.3-68.1)	31.6 (22.4-65.9)	40 (21-76)	a & b*** a & c*** a & d***	(0.0001) (0.0005) (0.0002)

Values are presented as medians (minimum-maximum). *p<0.05; **p<0.01; ***p<0.001; ****p<0.0001 represented statistically significant variations, as set by the Kruskal-Wallis test followed by Dunn's multiple comparisons. TC: Total cholesterol, LDL: Low-density lipoprotein, TG: Triglyceride, VLDL: Very low-density lipoprotein, HDL: High-density lipoprotein.

treatment with enalapril for over 1 year. Bryniarski et al.'s[24] study showed that enalapril inhibits pro-inflammatory cytokine production.

Dyslipidemia and BMI are markers of human health that are frequently linked to hypertension. Tasci et al.[5] demonstrated that plasma apelin levels were lower in individuals with hypercholesterolemia that were non-obese, non-diabetic, and normotensive. Our results are consistent with Zhang et al.'s[25] study, indicating that overweight individuals with dyslipidemia are at a greater risk of developing hypertension. Dyslipidemia can alter the permeability of cell membranes by altering their structure, and it can also result in damage to the renal microvascular system, thereby inducing hypertension[26]. Moreover, our results are compatible with Dharwadkar's[27] findings that found serum levels of TC and LDL-c were lower in hypertensive patients treated with enalapril. Enalapril decreases AngII production, thereby reducing TC and LDL. Furthermore, dyslipidemia induces overexpression of the AT1 receptor. Keidar et al.[28] demonstrated that AngII significantly enhances cellular cholesterol biosynthesis following AngII injection. Both the AT1 receptor blocker and ACE inhibitor reduced the formation of cholesterol in response to AngII. Interestingly, AngII failed to increase cholesterol production in cells lacking AT1 receptors. However, candesartan blocks the AT1 receptor, resulting in decreased blood pressure and may affect lipid profiles[29]. Simultaneously, Quesada-Caballero et al.[30] found that the serum level of HDL-c was lower in hypertensive patients. It is unclear which processes underlie high HDL-c and low blood pressure. However, HDL-c may increase the availability of nitric oxide in the endothelial cells, thereby relaxing blood vessels and reducing blood pressure. However, it is possible that variations in blood pressure might have a reverse causal relationship with HDL-c levels. Interestingly, the possibility of a reverse causal relationship in which changes in blood pressure affect serum HDL cannot be ruled out[31].

CONCLUSION

In conclusion, apelin and visfatin appear to have clinical significance and promising diagnostic, prognostic, and therapeutic applications in CVDs. Additionally, we concluded that blocking of renin-Ang system may

represent a major positive regulator of apelin and visfatin actions in the vasculature and heart, unlocking novel potential therapeutic targets for these anti-inflammatory and proinflammatory adipokine in the treatment of hypertension. Specifically, candesartan regulates adipokine to a greater extent than enalapril.

Ethics

Ethics Committee Approval: The ethical integrity of this study was paramount and was conducted under ethical guidelines and with approval from the Kirkuk Health Province Department Knowledge Management and Research Division approval no.: 631, date: 05/10/2023).

Informed Consent: Informed consent was obtained from all participants.

Author Contributions

Surgical and Medical Practices: Y.K.J., J.A.M., Concept: Z.H.F., Design: Z.H.F., Data Collection and/or Processing: Y.K.J., Z.H.F., J.A.M., Analysis and/or Interpretation: Y.K.J., Z.H.F., J.A.M., Literature Search: Y.K.J., Writing: Y.K.J., J.A.M.

Conflict of Interest: The authors have no conflict of interest to declare.

Financial Disclosure: The authors declared that this study has received no financial support.

REFERENCES

1. Alzahrani SA, Bin Muammar MF, Bin Muammar AF, Alolah A, Almutawa M. The Adoption and Acceptance of mHealth Interventions for Self-Management of Hypertension Among Adult Patients: A Systematic Review. Cureus. 2022;14:e31484.
2. Mattu HS, Randeva HS. Role of adipokines in cardiovascular disease. J Endocrinol. 2013;216:17-36.
3. Przewlocka-Kosmala M, Kotwica T, Mysiak A, Kosmala W. Reduced circulating apelin in essential hypertension and its association with cardiac dysfunction. J Hypertens. 2011;29:971-9.
4. Bertrand C, Valet P, Castan-Laurell I. Apelin and energy metabolism. Front Physiol. 2015;6:115.
5. Tasci I, Dogru T, Naharci I, et al. Plasma apelin is lower in patients with elevated LDL-cholesterol. Exp Clin Endocrinol Diabetes. 2007;115:428-32.
6. Siddiqa A, Khadija H, Ahad A. Critical Analysis of Serum Visfatin Levels in Obese and Non-Obese Primary Hypertensive Subjects. Int J Adv Health Sci. 2022;9:10-6.
7. Yang CC, Deng SJ, Hsu CC, et al. Visfatin regulates genes related to lipid metabolism in porcine adipocytes. J Anim Sci. 2010;88:3233-41.
8. Dakroub A, A Nasser S, Younis N, et al. Visfatin: a possible role in cardiovasculo-metabolic disorders. Cells. 2020;9:2444.
9. Shokrollahi B, Jang SS, Lee HJ, et al. Exploring the potential roles of apelin, visfatin, and irisin in energy regulation in farm animals: an overview. Front Vet Sci. 2024;11:1435788.
10. Mohammed M, Mohammad J, Fathi Z, Al-Hamdany M, Alkazzaz N. Comparative evaluation of cystatin C and neutrophil gelatinase-associated lipocalin in patients with thalassemia major versus thalassemia intermedia. Pharmacia. 2021;68:741-6.
11. Akbari H, Hosseini-Bensenjan M, Salahi S, et al. Apelin and its ratio to lipid factors are associated with cardiovascular diseases: A systematic review and meta-analysis. PLoS One. 2022;17:e0271899.
12. Cuspidi C, Muiesan ML, Valagussa L, et al. Comparative effects of candesartan and enalapril on left ventricular hypertrophy in patients with essential hypertension: the candesartan assessment in the treatment of cardiac hypertrophy (CATCH) study. J Hypertens. 2002;20:2293-300.
13. Vargas-Vázquez A, Bello-Chavolla OY, Antonio-Villa NE, Mehta R, Cruz-Bautista I, Aguilar-Salinas CA. Comparative assessment of LDL-C and VLDL-C estimation in familial combined hyperlipidemia using Sampson's, Martin's and Friedewald's equations. Lipids Health Dis. 2021;20:46.
14. Mahmoud Kadry Z, Mahmoud Ahmed A, Khalifa Ahmed A, Hafez Abdelall A, Mahmoud Mohamed S, Ahmed AO. Association Between Apelin and Nitrous Oxide with Essential Hypertensive Patient and their Relation toSex. Sohag Medical Journal. 2022;26:19-24.
15. Derosa G, Maffioli P, Salvadeo SA, et al. Differential effects of candesartan and olmesartan on adipose tissue activity biomarkers in type II diabetic hypertensive patients. Hypertens Res. 2010;33:790-5.
16. Skoczylas A, Piecha G, Więcek A. Effects of antihypertensive treatment on plasma apelin, resistin, and visfatin concentrations. Pol Arch Med Wewn. 2016;126:243-53.
17. Mohammed MK, Fathi ZH, Mohammad JA. Effects of Angiotensin Receptor Blockers on Apelin and Visfatin in Hypertension. Al-Anbar Medical Journal. 2024;20:10-18.
18. Ahmad H, Khan H, Haque S, Ahmad S, Srivastava N, Khan A. Angiotensin-Converting Enzyme and Hypertension: A Systemic Analysis of Various ACE Inhibitors, Their Side Effects, and Bioactive Peptides as a Putative Therapy for Hypertension. J Renin Angiotensin Aldosterone Syst. 2023;2023:7890188.
19. Liakos CI, Sanidas EA, Perrea DN, et al. Apelin and visfatin plasma levels in healthy individuals with high normal blood pressure. Am J Hypertens. 2016;29:549-52.
20. Yu PL, Wang C, Li W, Zhang FX. Visfatin Level and The Risk of Hypertension and Cerebrovascular Accident: A Systematic Review and Meta-Analysis. Horm Metab Res. 2019;51):220-9.
21. Dogru T, Sonmez A, Tasci I, et al. Plasma visfatin levels in young male patients with uncomplicated and newly diagnosed hypertension. J Hum Hypertens. 2007;21:173-5.
22. Furuya R, Odamaki M, Kumagai H, Hishida A. Impact of angiotensin II receptor blocker on plasma levels of adiponectin and advanced oxidation protein products in peritoneal dialysis patients. Blood Purif. 2006;24:445-50.
23. Kärberg K, Forbes A, Lember M. Visfatin and Subclinical Atherosclerosis in Type 2 Diabetes: Impact of Cardiovascular Drugs. Medicina (Kaunas). 2023;59:1324.
24. Bryniarski P, Nazimek K, Marcinkiewicz J. Immunomodulatory Activity of the Most Commonly Used Antihypertensive Drugs-Angiotensin Converting Enzyme Inhibitors and Angiotensin II Receptor Blockers. Int J Mol Sci. 2022;23:1772.
25. Zhang FL, Guo ZN, Xing YQ, Wu YH, Liu HY, Yang Y. Hypertension prevalence, awareness, treatment, and control in northeast China:

a population-based cross-sectional survey. J Hum Hypertens. 2018;32:54-65.

26. Wautier JL, Wautier MP. Vascular Permeability in Diseases. Int J Mol Sci. 2022;23:3645.
27. Dharwadkar S. Comparative Effects of Enalapril and Amlodipine on the levels of Serum Angiotensin Converting Enzyme and Lipid Profile in Patients with Hypertension. Int J Biotechnol. 2011;1:444-50.
28. Keidar S, Attias J, Heinrich R, Coleman R, Aviram M. Angiotensin II atherogenicity in apolipoprotein E deficient mice is associated with increased cellular cholesterol biosynthesis. Atherosclerosis. 1999;146:249-57.
29. Jacobsen AP, Whelton SP, Blumenthal RS, Mcevoy JW. Dyslipidemia. Hypertension: Elsevier; 2024. p. 476-88.
30. Quesada-Caballero M, Carmona-García A, García-Lara RA, et al. Assessing the Risk of Hypertension in Chronic, Elderly Patients during the COVID-19 Pandemic: A Prospective Study. J Cardiovasc Dev Dis. 2024;11:21.
31. Yang G, Qian T, Sun H, et al. Adjustment for body mass index changes inverse associations of HDL-cholesterol with blood pressure and hypertension to positive associations. J Hum Hypertens. 2022;36:570-9.

DOI: 10.4274/MMJ.galenos.2024.82274
Medeni Med J 2024;39:211-220

Original Article

Alpha B-crystallin Ameliorates Imbalance of Redox Homeostasis, Inflammation and Apoptosis in an Acute Lung Injury Model with Rats

Alpha B-kristalin Sıçan Akut Akciğer Hasarı Modelinde Redoks Homeostazının Dengesizliğini, Enflamasyonu ve Apoptozu İyileştirir

Seda KOCAK[1], Ibrahim GUNER[2], Muhittin Onur YAMAN[3], Tugba EKIZ YILMAZ[4], Emine Elif GUZEL MEYDANLI[4], Nermin YELMEN[3], Gulderen SAHIN[5]

[1]Kirsehir Ahi Evran University Faculty of Medicine, Department of Physiology, Kirsehir, Türkiye
[2]Tekirdag Namik Kemal University Faculty of Medicine, Department of Physiology, Tekirdag, Türkiye
[3]Istanbul University-Cerrahpasa, Cerrahpasa Faculty of Medicine, Department of Physiology, Istanbul, Türkiye
[4]Istanbul University-Cerrahpasa, Cerrahpasa Faculty of Medicine, Department of Histology and Embriology, Istanbul, Türkiye
[5]Istanbul Aydin University Faculty of Medicine, Department of Physiology, Istanbul, Türkiye

ABSTRACT

Objective: Ischemia-reperfusion (IR) of the aorta is a significant contributor to the development of postoperative acute lung damage after abdominal aortic surgery. The aim of the present study was to examine the effect of alpha B-crystallin, a small heat shock protein (known as HspB5), on lung injury induced by abdominal aortic IR in rats.

Methods: Male Sprague-Dawley rats were divided into three groups: control, ischemia-reperfusion (IR, 90 min ischemia and 180 min reperfusion), and alpha B-crystallin +IR. Alpha B-crystallin (50 µg/100 g) was intraperitoneally administered 1 h before IR. Lung tissue samples were obtained for histological and biochemical analyses of oxidative stress and cytokine and apoptosis parameters in plasma, lung tissues, and bronchoalveolar lavage (BAL) fluid.

Results: The levels of malondialdehyde, reactive oxygen species, total oxidant status, tumor necrosis factor-alpha (TNF-α), interleukin-1 beta (IL-1β), nuclear factor kappa B (NFKβ), caspase-9 (CASP-9), 8-hydroxy-2′-deoxyguanosine, total antioxidant status, superoxide dismutase, and interleukin-10 levels in lung tissues, plasma, and BAL fluid ($p<0.05$ versus control) increased in Aortic IR. However, alpha B-crystallin significantly reduced the lung tissue levels of oxidative, inflamatuvar, and apoptotic parameters in the plasma, lung tissues, and BAL fluid ($p<0.05$ versus aortic IR). Histopathological results showed that alpha B-crystallin ameliorated the morphological changes related to lung injury ($p<0.001$).

Conclusion: Alpha B-crystallin substantially restored disrupted the redox balance, inflammation, and apoptotic parameters in rats exposed to IR. The cytoprotective effect of alpha B-crystallin on redox balance might be attributed to improved lung injury.

Keywords: Abdominal surgery, cytokines, inflammation, immunology, ischemia-reperfusion

ÖZ

Amaç: İskemi-reperfüzyon (IR) aortası, abdominal aort cerrahisi sonrası akut akciğer hasarının önemli bir nedenidir. Çalışmamızın amacı, sıçanlarda abdominal aort IR tarafından indüklenen akciğer hasarı üzerine küçük ısı şok proteinlerinden biri olan alfa B-kristalinin (HspB5 olarak da bilinir) etkisini incelemektir.

Yöntemler: Erkek Sprague Dawley sıçanları üç gruba ayrıldı: kontrol, IR (IR, 90 dakika iskemi ve 180 dakika reperfüzyon) ve alfa B-kristalin+IR. Alfa B-kristalin (50 µg/100 g), IR'den bir saat önce intraperitoneal olarak verildi. Akciğer dokusu örnekleri histolojik analiz ve oksidatif stres parametreleri, sitokinler, apoptoz parametreleri açısından biyokimyasal analiz için alındı. Plazma, akciğer dokusu ve bronkoalveoler lavaj (BAL) sıvısında parametreler incelendi.

Bulgular: Aortik IR, akciğer dokularında malondialdehit, reaktif oksijen türleri, toplam oksidan durum, tümör nekroz faktörü-alfa (TNF-α), interleukin-1 beta (IL-1β), nükleer faktör kappa B (NFKβ), kaspaz-9 (CASP-9), 8-hidroksi-2′-deoksiguanozin, total antioksidan durum, süperoksit dismutaz, interleukin-10 seviyelerini anlamlı olarak artırırken ($p<0,05$, kontrol grubuna göre), alfa B-kristalin, plazma, akciğer dokusu ve BAL sıvısındaki oksidatif, enflamatuar ve apoptotik parametreleri anlamlı olarak azalmıştır ($p<0,05$, aortik IR'ye göre). Histopatolojik değerlendirme, alfa B-kristalinin akciğer hasarı ile ilişkili morfolojik değişiklikleri iyileştirdiğini göstermiştir ($p<0,001$).

Sonuçlar: Alfa B-kristalin, IR'ye maruz kalan sıçanlarda bozulmuş redoks dengesi, enflamasyon ve apoptotik parametreleri önemli ölçüde düzeltmiştir. Bu antioksidan etki, alfa B-kristalinin akciğer hasarı üzerindeki koruyucu etkisine bağlanabilir.

Anahtar Kelimeler: Abdominal cerrahi, sitokinler, enflamasyon, immünoloji, iskemi-reperfüzyon

Address for Correspondence: S. Kocak, Kirsehir Ahi Evran University Faculty of Medicine, Department of Physiology, Kirsehir, Türkiye
E-mail: seda.kocak@ahievran.edu.tr **ORCID ID:** orcid.org/0000-0003-1183-4847

Received: 15 June 2024
Accepted: 09 September 2024

Cite as: Kocak S, guner I, Yaman MO, Ekiz Yilmaz T, Guzel Meydanlı EE, Yelmen N, Sahin G. Alpha B-crystallin Ameliorates Imbalance of Redox Homeostasis, Inflammation and Apoptosis in an Acute Lung Injury Model with Rats. Medeni Med J. 2024;39:211-220

INTRODUCTION

Infrarenal abdominal aortic clamping and declamping after coronary artery surgery cause ischemia-reperfusion[1,2]. Distant organ damage is often associated with ischemia-reperfusion (IR) injury. The lungs are one of the distant organs that are damaged. IR inflammation exacerbates ischemic trauma and necessitates the maintenance of blood supply to prevent cell death[3]. Although the exact pathophysiological mechanisms of distant organ injury remain unclear, damage is attributed to oxidative, inflammatuvar, and apoptotic mediators released after IR[2,4].

Oxidative stress is an early and important symptom of acute lung injury. After reoxygenation of the lungs, a number of intricate events may take place, including oxidative damage to deoxyribonucleic acid (DNA) and proteins, peroxidation of membrane lipids, release of intracellular enzymes, increase in intracellular calcium, and neutrophil buildup in ischemic tissue[5,6]. Clinical and experimental studies have shown that IR in the lungs induces proinflammatory cytokines and apoptosis. In this condition, lung tissue are affected by oxidative, inflammatory, and apoptotic pathways[7,8]. The cause of lung injury as a result of IR following aortic surgery can be attributed to the release of cytokines, immune cells, various mediators secreted by immune cells, and their accumulation in the lungs[9]. Additionally, reactive oxygen species that cause DNA damage and apoptosis may lead to increased levels of proinflammatory cytokines and decreased expression of anti-inflammatory cytokines.

Heat shock proteins comprise a group of proteins including subfamilies. Their expressions are elevated under stress conditions. The subfamily includes small heat shock proteins. Alpha B-crystallin (known as HspB5) is one of the main lens proteins in vertebrates and a member of the small heat shock protein family[10]. The roles of alpha B-crystallin have been reported in different IR models. A retinal rat IR model showed that alpha B-crystallin decreased ischemic retinal damage, oxidative stress, iNOS, and nuclear factor kappa B (NFKβ) levels, and improved retinal function[11]. In addition, an experimental anterior ischemic optic neuropathy model in mice showed that both short-term treatment with alpha B-crystallin decreased inflammation and long-term treatment improved optic neuropathy function[12]. Kirbach et al.[13] demonstrated that HspB5 was upregulated in a rat cerebral ischemia model. In this study, HspB5 was one of the most significant HspBs in the neuronal stress response to IR injury. There are no articles in the literature about the expression of alpha B-crystallin after aortic IR-induced acute lung injury or its effect in a lung aortic IR model.

In addition, alpha B-crystallin has been used therapeutically for stroke and spinal cord contusion of mice studies[14,15]. In the first study, HspB5 decreased both the volume of stroke and inflammatory cytokines related to stroke pathology. In the second study, mice treated with HspB5 showed improvement of locomotor capabilities and a reduction in secondary tissue injury. In another study, the administration of alpha B-crystallin chronically improved cardiac function in a mouse myocardial infarction model. Mice treated with HspB5 exhibited increased left ventricular ejection fraction[16]. Different studies have shown that alpha B-crystalline decreases plasma interleukin (IL)-6[17], increases IL-10[18], inhibits NF-κB activation, suppress tumor necrosis factor-alpha (TNF-α) induced apoptosis[19], and reduces lipid peroxidation and the protective role of reactive oxygen against lung injury through its role in immune, inflammatory, and ischemic processes.

To our knowledge, no research has been conducted on the antioxidant, anti-inflammatory, and anti-apoptotic regulatory effects of alpha B-crystalline on aortic IR-induced lung damage *in vivo*. In the present study, we demonstrated that exogenous administration of alpha B-crystalline reduced lung tissue oxidative stress and cellular injury by inhibiting oxidative and proinflammatory responses, including cytokines.

MATERIALS and METHODS

Animals

Adult 24 male Sprague-Dawley rats (12 weeks-average weight: 320 grams) were housed in separate cages in a standardized temperature and light-dark cycle controlled environment. Animals had free access to standard feed and water. The animal studies were conducted after receiving approval from the Institutional Animal Care and Istanbul University Animal Experiments Local Ethics Committee (decision no: 2014/62 date: 29.05.2014).

Sprague-Dawley rats were divided into three groups. 1) Control (C; n=8) group: the control group underwent midline laparotomy and dissection of infrarenal abdominal aorta (IAA) without occlusion. 10 mL physiological serum was administered to this group into the peritoneal cavity during the procedure. IR procedure was not applied. 2) Ischemia-Reperfusion (IR; n=8) group: 10 mL physiological serum was administered into the peritoneal cavity during the procedure. In addition, 90 min of ischemia and 180 min of reperfusion were performed. 3) Alpha B-crystallin+Ischemia-Reperfusion (Alpha B-crystallin+IR; n=8) group: 10 mL physiological serum was administered during the procedure. Intraperitoneal

alpha B-crystallin administration (50 µg /100 g) were performed for 1 h before ischemia, 90 min of ischemia, and 180 min of reperfusion. We used the dosage of alpha B-crystallin according to its nontoxic effects[18,20].

Ischemia-reperfusion Procedure

All animals were anesthetized intraperitoneally with thiopental sodium (60 mg/kg). Tracheotomy was performed after anesthesia; trachea was intubated with a polyvinylchloride cannula. Animals were placed on a heating plate to maintain body temperature at 37 ˚C during experiment. A 22-gauge catheter was inserted to draw blood from the carotid artery and monitor blood pressure. After the skin of rats was prepared aseptically, a midline laparotomy was performed, and the intestines were pulled to the left with wet gauze. Heparin was mixed with physiological serum 50 U/kg (500 mL volume), (Nevpar's; MN Pharmaceutical, Istanbul, Türkiye) before the ischemia protocol to prevent clotting. The area called the IAA just below the right and left kidney arteries was isolated, and dissection of IAA was performed in the IR and alpha B-crystallin+IR groups. A non-traumatic microvascular clamp (vascu-statts II, midi straight 1001-532; Scanlan Int, St Paul, MN) was placed to perform the 90 min ischemia protocol. 10 mL of physiological serum adjusted to body temperature was administered to the peritoneal cavity. After suturing the incision area with surgical thread, the area was covered with moist gauze to minimize fluid and heat loss. After 90 min of ischemia, the incision was reopened, and the microvascular clamp from the infrarenal aortic area was removed[21]. These changes were also confirmed using a computerized system (PowerLab, 16 SP, ADInstruments, Castle Hill, Australia) with systemic arterial blood pressure records from the carotid artery. At the end of 180 min of reperfusion, a high dose of intravenous thiopental sodium (150 mg/kg) was administered for euthanasia after collecting bronchoalveolar lavage (BAL) fluid samples from the lungs and blood from the carotid artery. The lung was removed together with the trachea, and the lower right lung lobe was stored in the formol for histological examination. The lung, BAL fluid, and plasma samples were stored at -80 ˚C for biochemical analyses.

Bronchoalveolar Lavage (BAL) Procedure

The left main bronchus was cannulated and secured. Saline (5 mL) was injected into three quick aliquots (5 mL) each, with each aliquot withdrawn slowly. The BAL specimen was collected with a fluid recovery of 90% or greater[22]. The fluid was centrifuged at 1500 rpm for 8 minutes at +4 ˚C. The supernatant was then stored at -80 ˚C until biochemical analysis.

Lung Tissue, Plasma, and BAL Fluid Biochemical Analysis

Lung tissue samples were washed in physiological serum and phosphate buffer and then crushed by freezing in liquid nitrogen. After thawing, phosphate buffer was added, and the tissues were homogenized. Homogenates were centrifuged (3000 rpm, 20 min, +4 ˚C), and the resulting supernatants were used for biochemical analysis. BAL fluid and plasma samples were collected after reperfusion. Levels of malondialdehyde (MDA), reactive oxygen species (ROS), total oxidant status (TOS), total antioxidant status (TAS), superoxide dismutase (SOD), IL-10, TNF-α, IL-1β, NF-κB, CASP-9, and 8-OHdG were quantified using Sunred ELISA kits.

Histological Evaluation

The middle lobe of the right lung was fixed in 10% neutral formalin, embedded in paraffin, and sectioned into 5 µm slices. After deparaffinization and staining with hematoxylin and eosin, the sections were evaluated histologically by two independent pathologists using a light microscope (Olympus BX61, Japan). Histologic injury scores were determined based on five parameters: alveolar wall thickness, intra-alveolar edema-infiltration, intra-alveolar hemorrhage, capillary blood collection, and alveolar damage, each scored on a scale from 0 to 4 (0: absent and normal appearance, 1: mild, 2: moderate, 3: severe, 4: intense). Additionally, the total lung injury score was calculated for each animal group[23].

Statistical Analysis

The data was processed by the statistical analysis software GraphPad Prism version 5.0 for Windows. The Bonferroni test was used to assess significant variations between groups using one-way analysis of variance (ANOVA). Statistical significance was set as $p<0.05$. The histological data was processed by the statistical analysis software Sigma Stat for Windows, version 3.0 (Jandel Scientific, San Rafael, CA) and one-way ANOVA. The Holm-Sidak test was used to assess group variations. Statistical significance was set as $p\leq0.001$. All the data are shown as the mean values±standard deviation.

RESULTS

Oxidative Stress Parameters

When the ELISA results for oxidative stress markers were analyzed in all animal groups, lung tissue, BAL, and plasma results were similar. ROS, TOS, and MDA levels increased in the IR group compared with the control group. Alpha B-crystallin application decreased these parameters in alpha B-crystallin+IR group compared

to IR group. Table 1 shows the p-values, which are the statistically significant differences between means of groups. SOD and TAS values increased in the alpha B-crystallin+IR group compared with the IR group (Figures 1 and 2).

Inflammation Parameters

When inflammation parameters in all animal groups were compared, TNF-α, IL-1β and NF-κB levels differed between the IR and control groups. TNF-α, IL-1β and NF-κB were higher in the IR group. Compared with the

Table 1. Oxidative stress marker levels in lung tissue, plasma, and bronchoalveolar lavage fluid of all groups.

		Control (n=8)	Ischemia-reperfusion (n=8)	Alpha B-crystallin+ischemia reperfusion (n=8)	p-value
MDA	Tissue (nM/mg)	15.31±0.86	26.12±1.39^{a***}	18.54±0.71^{b***}	^{a}p<0.001 ^{b}p<0.001
	Plasma (nmol/mL)	9.94±0.38	14.90±0.73^{a***}	10.70±0.44^{b***}	^{a}p=0.001 ^{b}p=0.004
	BAL fluid (nmol/mL)	14.68±0.21	27.99±1.69^{a***}	15.45±0.44^{b***}	^{a}p=0.000 ^{b}p=0.000
ROS	Tissue (U/mg)	3905,66±211.35	5540,10±234.76^{a***}	4496,93±221.86^{b**}	^{a}p<0.001 ^{b}p<0.001
	Plasma (U/mL)	1919,61±201.83	2842,11±112.01^{a**}	1989.91±152.94^{b**}	^{a}p=0.008 ^{b}p=0.006
	BAL fluid (U/mL)	2721,36±50.21	3866,93±103.60^{a***}	2986,14±241.18^{b**}	^{a}p=0.002 ^{b}p=0.004
TOS	Tissue (nM/mg)	5.21±0.41	7.70±0.34^{a***}	5.62±0.30^{b**}	^{a}p<0.001 ^{b}p<0.001
	Plasma (nM/mL)	3.17±0.09	4.13±0.17^{a***}	3.33±0.17^{b**}	^{a}p=0.005 ^{b}p=0.012
	BAL fluid (nM/mL)	4.07±0.16	6.66±0.54^{a***}	4.66±0.16^{b**}	^{a}p=0.001 ^{b}p=0.012

Data are expressed as mean±standard deviation. *p<0.05, **p<0.01, ***p<0.001, ^{a}: Comparisons between the control and IR groups, ^{b}: Comparisons between the IR and alpha B-crystallin+IR groups, MDA: Malondialdehyde, ROS: Reactive oxygen species TOS: Total oxidant status BAL: Bronchoalveolar lavage

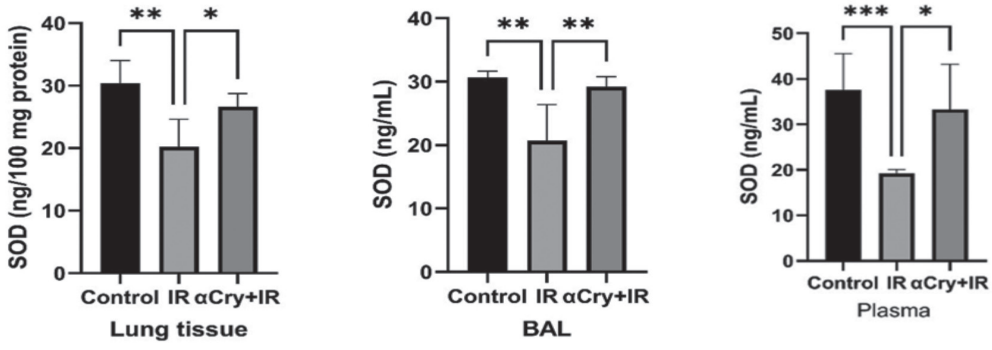

Figure 1. Lung tissue, BAL, and plasma SOD levels of groups. Experimental groups: Control, IR, IR administered alpha B-Crystallin (aCry+IR) group.

*p<0.05, **p<0.01, ***p<0.001, BAL: Bronchoalveolar lavage, SOD: Superoxide dismutase, IR: Ischemia-reperfusion

IR group, the levels of these parameters in the alpha B-crystallin+IR group decreased. Table 2 shows the means of groups and p-values. When we looked at the IL-10 levels, IL-10 was significantly decreased in the IR group. However, when the IR and alpha B-crystallin+IR groups were compared, IL-10 levels increased significantly in the alpha B-crystallin+IR group (Figure 3).

Apoptotic Parameters

When we analyzed apoptotic parameters in the rat lung and plasma of all groups, CASP-9 and 8-OHdG levels were significantly higher in the IR group than in the control group. Alpha B-crystallin application reduced these parameters in alpha B-crystallin+IR group

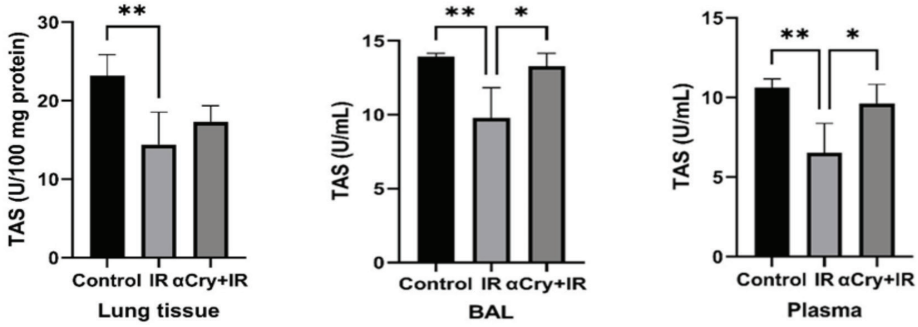

Figure 2. Lung tissue, BAL, and plasma TAS levels of groups. Experimental groups: Control, ischemia-reperfusion (IR), IR administered alpha B-Crystallin (aCry+IR) group.

Control, ischemia-reperfusion (IR), IR administered alpha B-Crystallin (aCry+IR) group.

TAS: Total Antioxidant Capacity, BAL: Bronchoalveolar lavage,*p< 0.05 **p< 0.001,

Table 2. Inflammation marker levels in lung tissue, plasma, and bronchoalveolar lavage fluid of the groups.

		Control (n=8)	Ischemia-Reperfusion (n=8)	Alpha B-crystallin+ Ischemia-Reperfusion (n=8)	p-value
TNF-α	Tissue (ng/mg)	269.81±15.10	422.49±14.74^{a***}	321.27±5.18^{b**}	^{a}p=0.000 ^{b}p=0.045
	Plasma (ng/L)	152.55±7.94	269.20±14.55^{a***}	175.26±4.85^{b***}	^{a}p=0.002 ^{b}p=0.001
	BAL fluid (ng/L)	192.23±6.22	294.55±4.88^{a***}	219.64±19.33^{b***}	^{a}p<0.0001 ^{b}p=0.012
IL-1β	Tissue (pg/mg)	2101,22±185.70	2887,22±150.56^{a**}	2247.28±53.82^{b*}	^{a}p=0.032 ^{b}p=0.033
	Plasma (pg/L)	1127,82±19.71	1514,79±46.80^{a***}	1181.54±33.03^{b***}	^{a}p=0.000 ^{b}p=0.004
	BAL fluid (pg/L)	1795,68±19.05	2513,64±129.67^{a***}	1941,38±36.79^{b***}	^{a}p=0.002 ^{b}p=0.007
NF-κB	Tissue (ng/mg)	5.23±0.38	9.31±0.56^{a***}	6.77±0.38^{b**}	^{a}p=0.000 ^{b}p=0.012
	Plasma (ng/mL)	3.07±0.19	5.11±0.28^{a***}	3.59±0.14^{b***}	^{a}p=0.000 ^{b}p=0.003
	BAL fluid (ng/mL)	4.54±0.10	6.05±0.09^{a***}	5.04±0.31	^{a}p=0.000

Control group, IR Ischemia-Reperfusion group, Alpha B-crystallin+IR Alpha B-crystallin+Ischemia-Reperfusion group. Data are expressed as mean±standard deviation. *p<0.05, **p<0.01, ***p<0.001, ^{a}: comparisons between the Control and IR group, ^{b}: comparisons between the IR and Alpha B-crystallin+IR group, TNF-α: Tumor necrosis factor-alpha, IL-1β: interleukin 1 beta, NF-κβ: Nuclear factor kappa beta BAL: Bronchoalveolar lavage

compared to IR group. Figures 4 and 5 show the CASP-9 and 8-OHdG parameters in the specimens.

Histopathologic Results

Histopathological examination of the right lung lobe was performed in all animal groups. Total lung injury was the least in the control group and the most severe IR group. The lung injury score was significantly higher in the IR group (9.0±0.8 p<0.001) than in the control group (2.286±0.714 p<0.001). Lung injury parameters in the IR group included intra-alveolar macrophage, neutrophil infiltration, alveolar damage, and alveolar wall thickening. Application of alpha B-crystallin before IR significantly reduced IR damage, and the total lung injury score decreased significantly in the alpha B-crystallin+IR group [5.56±0.56 p<0.001] compared with the IR group (9.0±0.8 p<0.001). Lung injury parameters observed in the alpha B-crystallin+IR group were less evident (Figure 6).

DISCUSSION

Our study showed that 90 min of infrarenal aortic occlusion followed by 180 min of reperfusion resulted in acute lung damage, including destruction of the alveolar architecture and inflammatory cell infiltration. The levels of MDA, ROS, TOS, TNF-α, IL-1β, NF-κB,, CASP-9, and 8-OHdG increased, whereas the levels of SOD, TAS, and IL-10 decreased in plasma, BAL fluid, and lung tissue samples. Interestingly, pre-administration of alpha B-crystallin 1 h before ischemia mitigated these effects, improving oxidative, inflammatory, and apoptotic

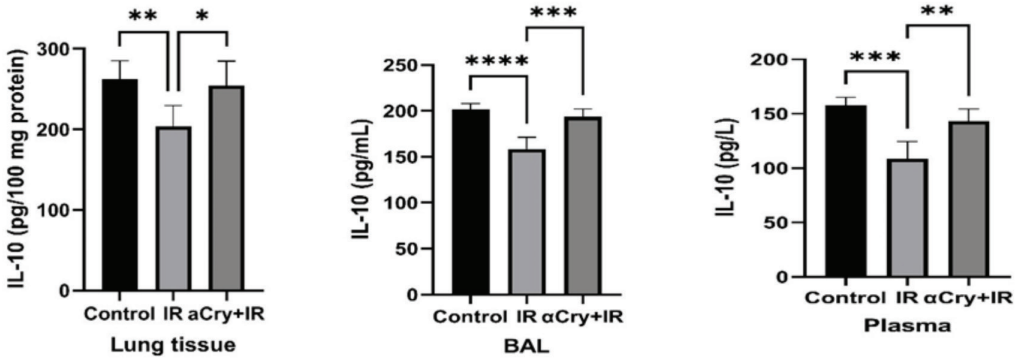

Figure 3. IL-10 Lung tissue, BAL, and plasma IL-10 levels of groups. Experimental groups: control, IR administered alpha B-Crystallin (aCry+IR) group.

*p<0.05, **p<0.01, ***p<0.001, ****p<0.0001, IL-10: interleukin, BAL: Bronchoalveolar lavage IR: Ischemia-reperfusion

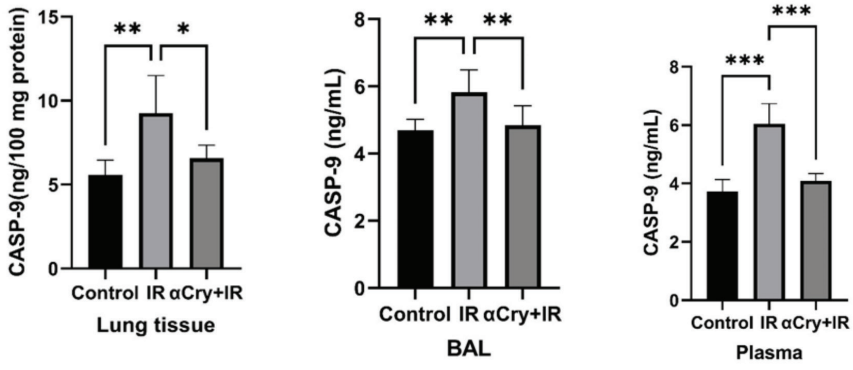

Figure 4. Lung tissue, BAL, and plasma CASP-9 levels of groups. Experimental groups: control, IR administered alpha B-Crystallin (aCry+IR) group.

*p< 0.05 , **p< 0.01, ***p< 0,001, CASP-9: caspase-9, BAL: Bronchoalveolar lavage, IR: Ischemia-reperfusion

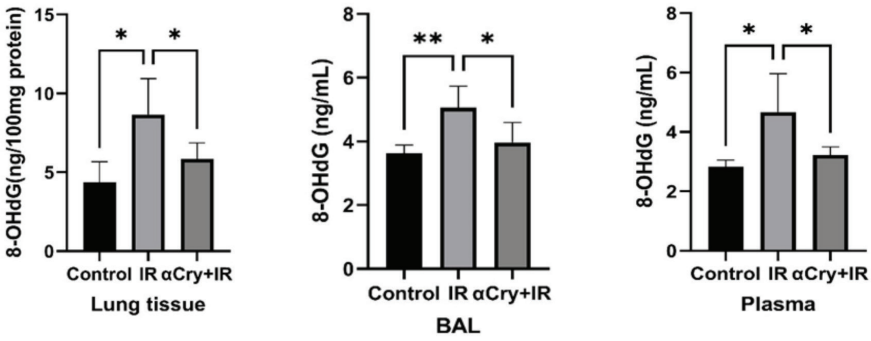

Figure 5. 8-OHdG Lung tissue, BAL, and 8-OHdG plasma levels of groups. Experimental groups: control, IR administered alpha B-Crystallin (aCry+IR) group.

*p< 0.05, **p< 0.01, 8-OHdG: 8-hydroxy-2′ -deoxyguanosine, BAL: Bronchoalveolar lavage, IR: Ischemia-reperfusion

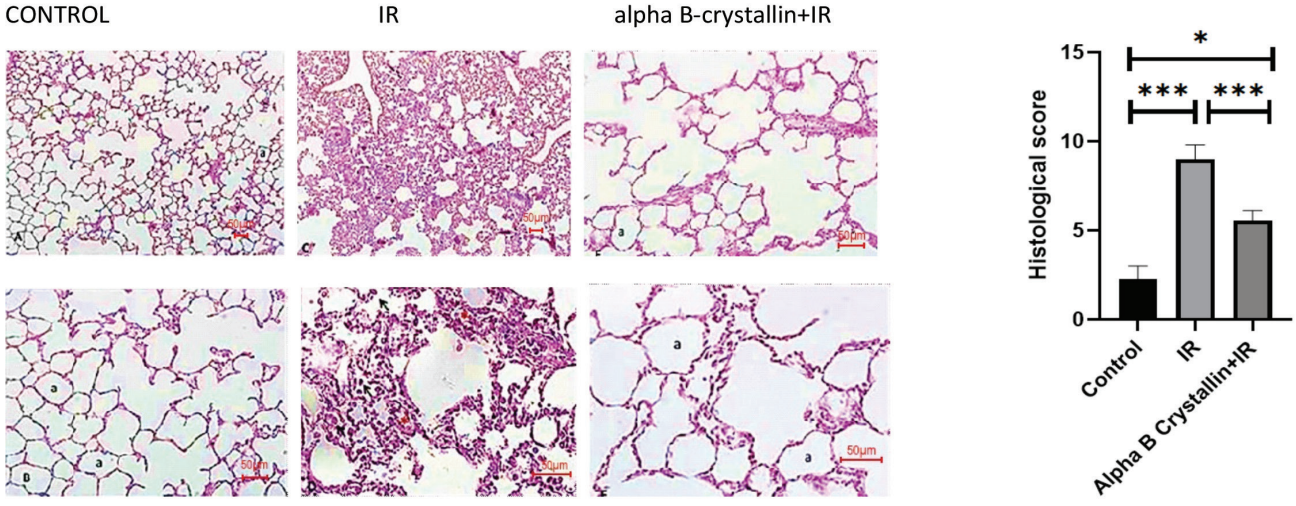

Figure 6. Histological sections of lung tissues from different experimental groups: control **(A, B)**, IR **(C, D)**, and alpha B-crystallin+IR **(E, F)** groups; histological scoring graph. In panels A and B, minimal histological changes with thin alveolar walls are observed. Panels C and D exhibit significant lung damage characterized by intra-alveolar infiltration (black arrow) and alveolar damage. Panels E and F, in contrast, show mild alveolar damage. The effects of alpha B-crystallin on histopathological changes in the lung tissue of rats with IR-induced acute lung injury are shown in panels E and F. Statistical significance is denoted as *p< 0.05, ***p< 0,001. (H&E A and C x10, B and E x20, D and F x40), IR: Ischemia-reperfusion

parameters in plasma, lung tissue, and BAL fluid samples and enhancing cellular structure.

Lung injury, IR, and systemic inflammation are clinically interrelated. Physiopathological mechanisms describing the interaction of these three titles are not fully understood. Various mediators are released by immune cells after IR injury, and these mediators seem to be important in the development of pulmonary damage[24]. Increase in biochemically triggered cytokine levels after aortic aneurysm treatment causes death with fever, tissue destruction, and even septic shock postoperatively[2].

Aortic IR injury causes pulmonary dysfunction[21]. IR injury is the result of a sequence of biochemical processes in which unbalanced ROS scavenging[25]. Increased ROS

levels can lead to protein, DNA, and lipid peroxidation, as well as mitochondria-induced cell death, which can contribute to IR injury[26]. One of the related therapies for IR injury is antioxidant therapy. Antioxidants have been shown to reduce cellular and tissue damage by lowering intracellular ROS levels and reducing oxidative stress[27].

Tural et al.[28] determined that aortic occlusion contributes to the increase in lung tissue MDA levels. Similarly, we observed that aortic occlusion increased pulmonary tissue MDA levels. There was a significant positive correlation between reactive oxygen species and MDA, a marker of lipid peroxidation. Further analysis showed that the application of alpha B-crystallin before IR decreased the production of reactive oxygen species and lipid peroxidation. It was also found that the SOD and TAS parameters increased. This implies that alpha B-crystallin systematically exerts an antioxidant effect.

Changes in the processes following IR can cause pulmonary apoptosis. Morphologically, apoptosis can also be characterized by DNA fragmentation[29]. Caspase-9 and 8-OhDG analyses were performed to demonstrate apoptosis and DNA damage. According to our results, the value of these parameters increased significantly not only in the lungs but also in plasma and BAL fluid in the IR group. 8-OHdG is the dominant form of oxidative damage caused by free radical species in nuclear and mitochondrial DNA and is used as a biomarker for oxidative stress[30]. Increased 8-OHdG levels of oxidative stress in the aortic IR-induced lung injury group indicates nuclear or mitochondrial DNA damage occurred. A significant reduction in 8-OHdG was detected in all samples from the alpha B-crystallin-treated group compared with the IR group. In addition, a significant decrease in caspase-9 expression was observed following alpha B-crystallin treatment. Initial studies have shown that alpha B-crystallin is effective against proapoptotic proteins and stops the translocation of Bax and Bcl-Xs[31]. Another anti-apoptotic role of alpha B-crystallin is its ability to prevent caspase-3 activation regardless of intrinsic or extrinsic pathway[32,33]. In light of this information, we can state that alpha B-crystallin affects apoptosis through different mechanisms and prevents apoptosis by inhibiting caspases. The effect of alpha B-crystallin on caspase-9 levels probably occurs via two mechanisms. One of the possible explanations for this is that alpha B-crystallin connects Bax and prevents the transfer of Bax from mitochondrial membrane from the cytosol[32]. Kamradt et al.[34] confirmed that alpha B-crystallin disrupts the proteolytic activation of caspase-3. In light of this information, another possible explanation is that alpha B-crystallin prevents the transition of procaspase-9 from an inactive to an active form, caspase-9. The secondary pathway can be more possible due to the proteolytic activation of caspase 9.

Histopathological examination of lung tissues in the control group showed less severe disease than that in the IR group. Intra-alveolar macrophages, neutrophil infiltration, alveolar damage, and alveolar wall thickening were observed in the lung tissues of the IR group. These injuries were less evident in rats administered alpha B-crystallin than in the IR group. Our analysis found that in rats treated with alpha B-crystallin, total histological injury was substantially reduced. Different studies showed that TNF-α and IL-1β play an important role in IR damage. These proinflammatory cytokines damage vascular beds, activate neutrophils, and migrate to the alveolar area[35]. Activated neutrophils release free radicals, proteolytic enzymes and peroxidase. Activated neutrophils can also lead to acute lung injury by increasing pulmonary vascular permeability[36].

Our experiments showed that TNF-α and IL-1β levels increased, whereas IL-10 levels decreased, in rats exposed to IR. This decrease may have resulted from the suppression of activity of IL-10 by TNF-α and IL-1β [37]. The transcription factor NF-κB, which promotes the expression of proinflammatory cytokines such as TNF-α and IL-1β, is also linked to neutrophil infiltration into the lungs and lipid peroxidation[38,39]. In our study, the increase of TNF-α and IL-1β together with NF-κβ suggests that inflammation in acute lung injury is increased by NF-κβ-mediated proinflammatory cytokines. Based on our results of decreasing TNF-α and IL-1β levels and increasing IL-10 levels in rats, we conclude that alpha B-crystallin reduces acute inflammation. This effect of alpha B-crystallin may inhibit the activity of proinflammatory cytokines by inhibiting the suppression of IL-10. Levels of NF-κβ decreased in all alpha B-crystallin+IR groups compared to IR group. Lentsch et al.[40] showed that the inflammatory-suppressing effect of IL-10 occurs by inhibiting the translocation of NF-κβ from cytoplasm to the nucleus in rat lung tissues. However, this study has some limitations. First, the unavailability of resources for immunohistochemical staining may limit the representation of apoptotic DNA fragmentation in TUNEL assays. Second, western blotting could be used to identify proteins, but insufficient resources limits this.

CONCLUSION

Based on our findings, alpha B-crystallin has the potential to prevent acute lung injury caused by aortic IR, mainly because of its antioxidant and anti-inflammatory properties. It also appears to mitigate DNA damage and

cell apoptosis associated with IR. Preadministration of alpha B-crystallin before aortic surgery could potentially mitigate IR injury. The present study underscores the potential of alpha B-crystallin as a novel treatment for IR-induced lung injury, marking its debut in this therapeutic context.

Ethics

Ethics Committee Approval: Approval was received from the Istanbul University Animal Experiments Local Ethics Committee (decision no: 2014/62 date: 29.05.2014).

Informed Consent: Because this article is based on animal studies, patient consent is not required.

Author Contributions

Surgical and Medical Practices: S.K., I.G., M.O.Y., G.S., Concept: S.K., I.G., G.S., Design: S.K., I.G., G.S., Data Collection and/or Processing: S.K., I.G., M.O.Y., T.E.Y., E.E.G.M., N.Y., G.S., Analysis and/or Interpretation: S.K., I.G., M.O.Y., T.E.Y., E.E.G.M., N.Y., G.S., Literature Search: S.K., I.G., E.E.G.M., G.S., Writing: S.K., I.G., E.E.G.M., G.S.

Conflict of Interest: The authors have no conflict of interest to declare.

Financial Disclosure: This study was supported by Istanbul University Scientific Research Projects under Grant (project number: 46006) and Council of Higher Education Faculty Member Training Program.

REFERENCES

1. Rossi M, Delbauve S, Roumeguère T, et al. HO-1 mitigates acute kidney injury and subsequent kidney-lung cross-talk. Free Radic Res. 2019;53:1035-43.
2. Erbel R, Aboyans V, Boileau C, et al. 2014 ESC Guidelines on the diagnosis and treatment of aortic diseases: Document covering acute and chronic aortic diseases of the thoracic and abdominal aorta of the adult. The Task Force for the Diagnosis and Treatment of Aortic Diseases of the European Society of Cardiology (ESC). Eur Heart J. 2014;35:2873-926.
3. Kalogeris T, Baines CP, Krenz M, Korthuis RJ. Cell biology of ischemia/reperfusion injury. Int Rev Cell Mol Biol. 2012;298:229-317.
4. Nieuwenhuijs-Moeke GJ, Pischke SE, Berger SP, et al. Ischemia and Reperfusion Injury in Kidney Transplantation: Relevant Mechanisms in Injury and Repair. J Clin Med. 2020;9:253.
5. de Perrot M, Liu M, Waddell TK, Keshavjee S. Ischemia-reperfusion-induced lung injury. Am J Respir Crit Care Med. 2003;167:490-511.
6. Bezerra FS, Lanzetti M, Nesi RT, et al. Oxidative Stress and Inflammation in Acute and Chronic Lung Injuries. Antioxidants (Basel). 2023;12:548.
7. Fischer S, Cassivi SD, Xavier AM, et al. Cell death in human lung transplantation: apoptosis induction in human lungs during ischemia and after transplantation. Ann Surg. 2000;231:424-31.
8. Forgiarini Junior LA, Holand AR, Forgiarini LF, et al. Endobronchial perfluorocarbon reduces inflammatory activity before and after lung transplantation in an animal experimental model. Mediators Inflamm. 2013;2013:193484.
9. Fadanni GP, Calixto JB. Recent progress and prospects for anti-cytokine therapy in preclinical and clinical acute lung injury. Cytokine Growth Factor Rev. 2023;71-72:13-25.
10. Bakthisaran R, Tangirala R, Rao ChM. Small heat shock proteins: Role in cellular functions and pathology. Biochim Biophys Acta. 2015;1854:291-319.
11. Yan H, Peng Y, Huang W, Gong L, Li L. The Protective Effects of αB-Crystallin on Ischemia-Reperfusion Injury in the Rat Retina. J Ophthalmol. 2017;2017:7205408.
12. Pangratz-Fuehrer S, Kaur K, Ousman SS, Steinman L, Liao YJ. Functional rescue of experimental ischemic optic neuropathy with αB-crystallin. Eye (Lond). 2011;25:809-17.
13. Bartelt-Kirbach B, Slowik A, Beyer C, Golenhofen N. Upregulation and phosphorylation of HspB1/Hsp25 and HspB5/αB-crystallin after transient middle cerebral artery occlusion in rats. Cell Stress Chaperones. 2017;22:653-63.
14. Arac A, Brownell SE, Rothbard JB, et al. Systemic augmentation of alphaB-crystallin provides therapeutic benefit twelve hours post-stroke onset via immune modulation. Proc Natl Acad Sci U S A. 2011;108:13287-92.
15. Klopstein A, Santos-Nogueira E, Francos-Quijorna I, et al. Beneficial effects of αB-crystallin in spinal cord contusion injury. J Neurosci. 2012;32:14478-88.
16. Velotta JB, Kimura N, Chang SH, et al. αB-crystallin improves murine cardiac function and attenuates apoptosis in human endothelial cells exposed to ischemia-reperfusion. Ann Thorac Surg. 2011;91:1907-13.
17. Rothbard JB, Kurnellas MP, Brownell S, et al. Therapeutic effects of systemic administration of chaperone αB-crystallin associated with binding proinflammatory plasma proteins. J Biol Chem. 2012;287:9708-21.
18. Masilamoni JG, Vignesh S, Kirubagaran R, Jesudason EP, Jayakumar R. The neuroprotective efficacy of alpha-crystallin against acute inflammation in mice. Brain Res Bull. 2005;67:235-41.
19. Adhikari AS, Singh BN, Rao KS, Rao ChM. αB-crystallin, a small heat shock protein, modulates NF-κB activity in a phosphorylation-dependent manner and protects muscle myoblasts from TNF-α induced cytotoxicity. Biochim Biophys Acta. 2011;1813:1532-42.
20. Masilamoni JG, Jesudason EP, Baben B, Jebaraj CE, Dhandayuthapani S, Jayakumar R. Molecular chaperone alpha-crystallin prevents detrimental effects of neuroinflammation. Biochim Biophys Acta. 2006;1762:284-93.
21. Guner I, Yaman MO, Aksu U, et al. The effect of fluoxetine on ischemia-reperfusion after aortic surgery in a rat model. J Surg Res. 2014;189:96-105.
22. Yaman OM, Guner I, Guntas G, et al. Protective Effect of Thymosin β4 against Abdominal Aortic Ischemia-Reperfusion-Induced Acute Lung Injury in Rats. Medicina (Kaunas). 2019;55:187.
23. Murakami K, Katahira J, McGuire R, et al. Heparin nebulization attenuates acute lung injury in sepsis following smoke inhalation in sheep. Shock. 2002;18:236-41.
24. Ferrari RS, Andrade CF. Oxidative Stress and Lung Ischemia-Reperfusion Injury. Oxid Med Cell Longev. 2015;2015:590987.

25. Naito H, Nojima T, Fujisaki N, et al. Therapeutic strategies for ischemia reperfusion injury in emergency medicine. Acute Med Surg. 2020;7:e501.

26. Auten RL, Davis JM. Oxygen toxicity and reactive oxygen species: the devil is in the details. Pediatr Res. 2009;66:121-7.

27. Zhou T, Prather ER, Garrison DE, Zuo L. Interplay between ROS and Antioxidants during Ischemia-Reperfusion Injuries in Cardiac and Skeletal Muscle. Int J Mol Sci. 2018;19:417.

28. Tural K, Ozden O, Bilgi Z, et al. The protective effect of betanin and copper on heart and lung in end-organ ischemia reperfusion injury. Bratisl Lek Listy. 2020;121:211-7.

29. Liu J, Wang J, Xiong A, et al. Mitochondrial quality control in lung diseases: current research and future directions. Front Physiol. 2023;14:1236651.

30. Valavanidis A, Vlachogianni T, Fiotakis C. 8-hydroxy-2′ -deoxyguanosine (8-OHdG): A critical biomarker of oxidative stress and carcinogenesis. J Environ Sci Health C Environ Carcinog Ecotoxicol Rev. 2009;27:120-39.

31. Mao YW, Liu JP, Xiang H, Li DW. Human alphaA- and alphaB-crystallins bind to Bax and Bcl-X(S) to sequester their translocation during staurosporine-induced apoptosis. Cell Death Differ. 2004;11:512-26.

32. Hu W-F, Gong L, Cao Z, et al. αA- and αB-crystallins interact with caspase-3 and Bax to guard mouse lens development. Curr Mol Med. 2012;12:177-87.

33. Ikeda R, Yoshida K, Ushiyama M, et al. The small heat shock protein alphaB-crystallin inhibits differentiation-induced caspase 3 activation and myogenic differentiation. Biol Pharm Bull. 2006;29:1815-9.

34. Kamradt MC, Lu M, Werner ME, et al. The small heat shock protein alpha B-crystallin is a novel inhibitor of TRAIL-induced apoptosis that suppresses the activation of caspase-3. J Biol Chem. 2005;280:11059-66.

35. Khimenko PL, Bagby GJ, Fuseler J, Taylor AE. Tumor necrosis factor-alpha in ischemia and reperfusion injury in rat lungs. J Appl Physiol (1985). 1998;85:2005-11.

36. Pararajasingam R, Weight SC, Bell PR, Nicholson ML, Sayers RD. Endogenous renal nitric oxide metabolism following experimental infrarenal aortic cross-clamp-induced ischaemia-reperfusion injury. Br J Surg. 1999;86:795-9.

37. Akdis CA, Blaser K. Mechanisms of interleukin-10-mediated immune suppression. Immunology. 2001;103:131-6.

38. Lingappan K. NF-κB in Oxidative Stress. Curr Opin Toxicol. 2018;7:81-6.

39. Miskolci V, Rollins J, Vu HY, Ghosh CC, Davidson D, Vancurova I. NFkappaB is persistently activated in continuously stimulated human neutrophils. Mol Med. 2007;13:134-42.

40. Lentsch AB, Shanley TP, Sarma V, Ward PA. In vivo suppression of NF-kappa B and preservation of I kappa B alpha by interleukin-10 and interleukin-13. J Clin Invest. 1997;100:2443-8.

DOI: 10.4274/MMJ.galenos.2024.09382
Medeni Med J 2024;39:221-229

Original Article

Clinical Characteristics of Children with Acute Post-Streptococcal Glomerulonephritis and Re-Evaluation of Patients with Artificial Intelligence

Akut Post-Streptokokal Glomerülonefritli Çocukların Klinik Özellikleri ve Hastaların Yapay Zeka ile Yeniden Değerlendirilmesi

Emre LEVENTOGLU, Mustafa SORAN

Konya City Hospital, Clinic of Pediatric Nephrology, Konya, Türkiye

ABSTRACT

Objective: Acute post-streptococcal glomerulonephritis (APSGN) is a common cause of acute glomerulonephritis in children. The condition may present as acute nephritic and/or nephrotic syndrome and rarely as rapidly progressive glomerulonephritis. ChatGPT (OpenAI, San Francisco, California, United States of America) has been developed as a chat robot supported by artificial intelligence (AI). In this study, we evaluated whether AI can be used in the follow-up of patients with APSGN.

Methods: The clinical characteristics of patients with APSGN were noted from patient records. Twelve questions about APSGN were directed to ChatGPT 3.5. The accuracy of the answers was evaluated by the researchers. Then, the clinical features of the patients were transferred to ChatGPT 3.5 and the follow-up management of the patients was examined.

Results: The study included 11 patients with an average age of 9.08±3.96 years. Eight (72.7%) patients had elevated creatinine and 10 (90.9%) had hematuria and/or proteinuria. Anti-streptolysin O was high in all patients (955±353 IU/mL) and C3 was low in 9 (81.8%) patients (0.56±0.34 g/L). Hypertensive encephalopathy, nephrotic syndrome, and rapidly progressive glomerulonephritis were observed in three patients. Normal creatinine levels were achieved in all patients. Questions assessing the definition, epidemiologic characteristics, pathophysiologic mechanisms, diagnosis, and treatment of APSGN were answered correctly by ChatGPT 3.5. All patients were diagnosed with APSGN, and the treatment steps applied by clinicians were similarly recommended by ChatGPT 3.5.

Conclusions: The insights and recommendations offered by ChatGPT for patients with APSGN can be an asset in the care and management of patients. With AI applications, clinicians can review treatment decisions and create more effective treatment plans.

Keywords: Acute postinfection glomerulonephritis, artificial intelligence, ChatGPT

ÖZ

Amaç: Akut post-streptokokal glomerülonefrit (APSGN) çocuklar arasında akut glomerülonefritin önde gelen nedenidir. Akut nefritik sendrom, nefrotik sendrom ve hızlı ilerleyen glomerülonefrit şeklinde ortaya çıkabilir. ChatGPT (OpenAI, San Francisco, California, Amerika Birleşik Devletleri) yapay zeka destekli bir sohbet robotu olarak geliştirilmiştir. Bu çalışmada, yapay zekanın APSGN'nin tanı, tedavi ve takibinde kullanılıp kullanılamayacağı ilk kez değerlendirilmiştir.

Yöntemler: APSGN tanısı alan hastaların klinik özellikleri hasta dosyalarından not edildi. APSGN hakkında genel bilgileri sorgulayan on iki soru ChatGPT 3.5'e yöneltildi. Cevapların doğruluğu iki araştırmacı tarafından değerlendirildi. Daha sonra hastaların klinik ve laboratuvar özellikleri ChatGPT 3.5'e aktarılarak hastaların takibinin yapay zeka tarafından nasıl yönetileceği incelendi.

Bulgular: Çalışmaya toplam 11 hasta dahil edildi. Hastaların yaş ortalaması 9,08±3,96 yıldı. Sekiz (%72,7) hastada kreatinin yüksekliği ve 10 (%90,9) hastada hematüri ve/veya proteinüri vardı. Anti-streptolisin O tüm hastalarda yüksek (955±353 IU/mL) ve C3 9 (%81,8) hastada düşüktü (0,56±0,34 g/L). Üç farklı hastada hipertansif ensefalopati, nefrotik sendrom ve hızlı ilerleyen glomerülonefrit gözlendi. Tüm hastalarda normal kreatinin değerlerine ulaşıldı. APSGN'nin tanımı, epidemiyolojik özellikleri ve patofizyolojik mekanizmaları, tanı ve tedavisini değerlendiren sorular chatGPT 3.5 tarafından doğru yanıtlandı. Ayrıca, tüm hastalara APSGN tanısı konmuş ve klinisyenler tarafından uygulanan tedavi adımları ChatGPT 3.5 tarafından benzer şekilde önerilmiştir.

Sonuçlar: ChatGPT tarafından APSGN için sağlanan bilgi ve rehberlik, hastaların bakım ve yönetiminde değerli bir kaynak olabilir. Yapay zeka uygulamaları ile klinisyenler kararlarını gözden geçirebilir ve daha etkili tedavi planları oluşturabilirler.

Anahtar kelimeler: Akut postenfeksiyon glomerülonefrit, yapay zeka, ChatGPT

Address for Correspondence: E. Leventoglu, Konya City Hospital, Clinic of Pediatric Nephrology, Konya, Türkiye
E-mail: dremrelevent@gmail.com **ORCID ID:** orcid.org/0000-0002-0504-7911

Received: 30 March 2024
Accepted: 29 August 2024
Online First: 6 September 2024

Cite as: Leventoglu E, Soran M. Clinical Characteristics of Children with Acute Post-Streptococcal Glomerulonephritis and Re-Evaluation of Patients with Artificial Intelligence. Medeni Med J. 2024;39:221-229

INTRODUCTION

Acute post-streptococcal glomerulonephritis (APSGN) is the leading cause of acute glomerulonephritis in children resulting from group A beta-hemolytic streptococcal infection[1]. It is frequently observed in children aged 4-12 years[2]. Enhancements in socioeconomic conditions, sanitation practices, healthcare systems, and the rational use of antibiotics for group A streptococcal infections have reduced the prevalence of APSGN in high-income nations. Nevertheless, it remains a significant public health issue in developing countries[3].

APSGN typically occurs 1-2 weeks after a throat infection and 3-6 weeks after skin infections[4]. It shows seasonal variation, with pharyngeal infections being more prevalent in winter and skin infections in summer[5]. APSGN may be subclinical or may be observed in severe clinical spectra, including acute nephritic and/or nephrotic syndrome and rarely as rapidly progressive glomerulonephritis. Edema, tea/cola-colored urine, decreased urine output, and hypertension may be present at presentation. In addition to general measures such as rest, fluid, and salt restriction, immunosuppressive therapies, and renal replacement therapies may be necessary in some cases[4].

ChatGPT (Chat Generative Pre-trained Transformer, OpenAI, San Francisco, California, United States of America), which has gained momentum in the medical field and started to be used daily in many branches, was developed as a chat robot supported by artificial intelligence (AI)[6]. Trained on vast Internet text, it can generate human-like language and cover various topics[7,8]. In medicine, ChatGPT can help identify research topics, assist with clinical and lab assessments, and keep healthcare professionals updated on new developments[9].

Pediatrics focuses on the health of infants, children, and adolescents. Early diagnosis and appropriate management are vital, and effective clinical decision-making is crucial for patient outcomes[10]. Evaluating ChatGPT's ability to support clinical decision-making in pediatrics is essential because of the unique challenges in this field[11].

In this study, the clinical characteristics, laboratory parameters, complications, and prognosis of pediatric patients diagnosed with APSGN were evaluated. We also examined whether ChatGPT can be used for APSGN management.

MATERIALS and METHODS

Research Framework and Participant Group

This was a retrospective observational study with a cross-sectional design in which the demographic, clinical, and laboratory characteristics of patients aged 0-18 years who were followed up with a diagnosis of APSGN in the department of pediatric nephrology between September 2023 and March 2024 were analyzed from patient records.

Demographic characteristics such as age and sex, history of streptococcal infection, presence of macroscopic hematuria, and physical examination findings such as edema and blood pressure at presentation were analyzed. Complete urinalysis, spot urine protein-to-creatinine ratio, serum creatinine, estimated glomerular filtration rate (eGFR), serum albumin, and electrolyte levels (Na, K, Ca and P) were noted to evaluate renal function. Throat culture results, anti-streptolysin O (ASO) titer, and complement levels of C3 and C4 were analyzed. Urinary system ultrasonography was performed for increased renal parenchymal echogenicity and corticomedullary differentiation. If available, a renal biopsy report was obtained. Treatments and medications administered to the patients were noted. Posttreatment hematuria, proteinuria, blood pressure, serum creatinine, and complement C3 levels were analyzed.

Definitions

Blood pressure was measured using a manual auscultation device after a 10-min rest, with two measurements taken in the same arm using the appropriate cuff. The average of these readings was recorded. All measurements were performed by the same pediatric nephrologist during each outpatient visit. Hypertension was diagnosed based on the 2017 guidelines[12]. The presence of more than 5 erythrocytes per high-power field (HPF) in centrifuged urine indicates microscopic hematuria, whereas dark brown urine, resembling cola or tea, indicates macroscopic hematuria. Macroscopic hematuria lasting longer than 4 weeks is defined as persistent macroscopic hematuria. A spot urine protein-to-creatinine ratio >0.2 mg/mg indicates proteinuria, whereas a ratio exceeding 2 mg/mg is considered nephrotic-level proteinuria[13]. Nephrotic-level proteinuria accompanied by edema, hypoalbuminemia (less than 2.5 g/dL), and hypercholesterolemia (greater than 200 mg/dL) is defined as nephrotic syndrome[14]. eGFR was determined using a modified Schwartz formula[15]. Nephritic syndrome has been defined as the sudden onset of glomerular damage features manifested as hematuria, proteinuria, oliguria, edema, hypertension, and elevated creatinine. Moreover, nephritic syndrome,

which is characterized by a rapid decline in kidney function over a matter of days, has been defined as rapidly progressive glomerulonephritis[16].

AI

Using the local internet network of Konya City 12 open-ended questions about APSGN were directed to ChatGPT 3.5 in English (Table 1). No additional training was provided to the AI before the questions and clinical information of the cases were routed to it. No query was made to APSGN or any other subject, and the application was used immediately after the computer was turned on. The accuracy of the AI answers to the questions was evaluated by two researchers according to internationally accepted publications and guidelines. Each answer was categorized as "incorrect", "missing information", "correct" according to the evaluation result. Then, the characteristics of the patients included in the study were transferred to ChatGPT 3.5, and diagnosis and follow-up of the patients were managed using AI was examined. We evaluated whether there was a difference between the clinicians and AI follow-up.

The study received approval from the KTO-Karatay University Rectorate Dean of the Faculty of Medicine non-Drug and non-Medical Device Research Ethics Committee Presidency (decision no: 2024/57, date: 16.01.2024).

Statistical Analysis

In presenting descriptive statistics, continuous data were reported as mean±standard deviation, whereas categorical data were presented as counts (percentages). The Shapiro-Wilk test was used to assess the normality of the numerical data in the groups. Statistical analyses were performed using International Business Machines Statistical Package for Social Sciences statistics version 22.

RESULTS

Clinical and Laboratory Characteristics of Patients

The study included 11 patients, with a male-to-female ratio of 1.2. The mean age was 9.08±3.96 years (range, 5-16.3 years). The present complaints included bloody urine (n=7, 63.6%), edema (n=3, 27.3%), and headache/seizure (n=1, 9.1%). All patients had upper respiratory tract infection (URTI) before the onset of symptoms. The mean duration after URTI until the onset of symptoms was 10.1±2.8 (7-15) days.

At the time of presentation, the mean systolic and diastolic blood pressure z-score was 1.21±0.43 (0.56-2.33) and the mean diastolic blood pressure Z-score was 1.39±0.37 (0.67-2.33), and approximately half of the patients (n=5, 45.5%) had hypertension. Malignant hypertension was detected in one patient. Mean creatinine was 1.12±1.1 mg/dL (0.48-2.42) and mean eGFR was 78.7±31.8 mL/min/1.73m^2 (50.6-117.2). The mean serum albumin was 3.46±0.60 g/dL (2.3-4.1) and hypoalbuminemia was found in 3 (27.2%) patients. Throat culture samples were obtained from all patients, and group A β hemolytic streptococcus was grown in 4 (36.3%) patients. ASO was high in all patients [mean 955±353 IU/mL (488-1614)]. The mean complement C3 level was 0.56±0.34 g/L (0.19-1.17) and 9 (81.8%) patients had low complement levels. All patients had varying degrees of hematuria. The mean erythrocyte count was 525±915.4/HPF (10-3171) and spot urine protein/creatinine value was 2.85±2.16 mg/mg (0.19-6.94). Proteinuria was present in 10 patients (90.9%). In addition to rest, fluid, and salt restriction, angiotensin-converting enzyme inhibitors were started in 5 (45.5%) patients with hypertension associated with proteinuria (Table 2).

Table 1. Questions directed to ChatGPT 3.5.

	Questions
1.	What is the definition of acute post streptococcal glomerulonephritis?
2.	What is the epidemiology of acute post streptococcal glomerulonephritis?
3.	How is the pathophysiology of acute post streptococcal glomerulonephritis?
4.	What is the relationship between acute post streptococcal glomerulonephritis and complement system?
5.	What are the clinical manifestations of acute post streptococcal glomerulonephritis?
6.	How is acute post streptococcal glomerulonephritis diagnosed?
7.	What are the indications for renal biopsy in acute post streptococcal glomerulonephritis?
8.	How is the treatment of acute post streptococcal glomerulonephritis?
9.	What are the drugs that can be used in the treatment of acute post streptococcal glomerulonephritis?
10.	What are additional immunosuppressives other than steroids in acute post streptococcal glomerulonephritis?
11.	How should clinical and laboratory findings be monitored in the follow-up of acute post streptococcal glomerulonephritis?
12.	What is the prognosis of acute post streptococcal glomerulonephritis?

Table 2. Demographic and clinical features of the study group.			
	n (%)	**Mean ± SD**	**Min-max**
Sex			
Male	6 (54.5)		
Age (years)		9.08±3.96	5-16.3
URTI history	11 (100)		
Time after URTI (days)		10.1±2.8	7-157-15
At presentation			
Complaints			
Hematuria	7 (63.6)		
Edema	3 (27.3)		
Headache/seizure	1 (9.1)		
Blood pressure			
SBP (z-score)		1.21±0.43	0.56-2.33
DBP (z-score)		1.39±0.37	0.67- 2.33
HT	5 (45.2)		
Laboratory results			
Blood			
Creatinine (mg/dL)		1.12±1.1	0.48-2.42
eGFR (mL/min/1.73m^2)		78.7±31.8	50.6-117.2
Albumin (g/dL)		3.46±0.6	2.3-4.1
Hypoalbuminemia	3 (27.2)		
ASO (IU/mL)		955±353	488-1614
Complement C3 (g/L)		0.56±0.34	0.19-1.17
Low	9 (81.8)		
Na (mEq/L)		137.2±3.8	131-143
K (mEq/L)		5.10±0.62	4.0-6.2
Ca (mg/dL)		8.84±0.40	7.9-9.3
P (mg/dL)		5.02±0.87	3.8-6.6
Urine			
Erythrocye (/HPF)*		525±915	10-3171
Hematuria	11 (100)		
Protein/creatinine (mg/mg)		2.85±2.16	0.19-6.94
Proteinuria	10 (90.9)		
Throat culture			
A group β hemolytic streptococcus	4 (36.3)		
Treatments			
Drugs			
ACEi	5 (45.5)		
Esmolol	1 (9.1)		
Diuretics	1 (9.1)		
Steroids	2 (18.2)		
Cyclophosphamide	2 (18.2)		
RRT			
HD	1 (9.1)		
At last control			
Blood			
Creatinine (mg/dL)		0.54±0.15	0.38-0.89
Complement C3 (g/L)		1.13 ± 0.21	0.94 - 1.39
Low	0 (0)		
Na (mEq/L)		138.3±2.73	135-144
K (mEq/L)		4.77±0.67	4.0-6.0
Ca (mg/dL)		9.26±0.49	8.1-10.0
P (mg/dL)		4.85±0.53	3.7-5.6
Urine			
Erythrocye (/HPF)*		27±72	1-271
Hematuria	8 (72.2)		
Protein/creatinine (mg/mg)		0.71±2.38	0.10-8.39
Proteinuria	7 (63.6)		

*Since the results were not homogeneously distributed for urine erythrocytes, the median value was given instead of the mean. URTI: Upper respiratory tract infection, SBP: Systolic blood pressure, DBP: Diastolic blood pressure, HT: Hypertension, eGFR: Estimated glomerular filtration rate, ASO: Anti-streptolysin-O, ACEi: Angiotensin converting enzyme inhibitor, RTT: Renal replacement therapy, HD: Hemodialysis, Na: Sodium, K: Potassium, Ca: Calcium, P: Phosphorus

A patient with malignant hypertension presented to the emergency department because of headache and seizures. Cranial imaging showing posterior reversible encephalopathy syndrome. In the intensive care unit, intravenous esmolol and diuretics were initiated, and no hypertensive need remained during follow-up. Renal biopsy was performed in a patient whose serum creatinine was 2.42 mg/dL at admission and increased to 5.35 mg/dL within 4 days was thought to have rapidly progressive glomerulonephritis. The biopsy showed intense mesangial proliferation, matrix increase, and increased interstitial inflammation. Immunofluorescence staining revealed C3 and immunoglobulin G deposition in glomeruli. Crescent formation was observed in 55.5% and fibrinoid necrosis in 12.5% of the evaluated glomeruli. The patient received intravenous pulse methylprednisolone for 3 days, followed by oral prednisolone at a dose of 2 mg/kg/day, with a maximum dose of 60 mg/day. Intermittent hemodialysis was performed for a total of 14 days because of uremia. Pulse cyclophosphamide was started in a patient who did not have the expected creatinine decrease with hemodialysis, 3 doses have been administered so far, and it is planned to complete a total

Table 3. Clinical and laboratory characteristics of three patients and responses given by artificial intelligence.

Case presentation	Diagnosis	Treatment
5.4-year-old girl presents to the emergency department due to seizures following a headache for a few days. Eyelid edema is noted in the postictal period. It is learned that she had an upper respiratory tract infection about 14 days ago. On examination, her blood pressure is 145/89 mmHg (above 99th percentile for both). Laboratory findings show serum creatinine 1.32 mg/dL, serum albumin 3.3 g/L, Na 133 mmol/L, K 5.9 mmol/L, Ca 8.7 mg/dL, and P 5.3 mg/dL. Urinalysis reveals a red blood cell-count of 211 /HPF and a spot urine protein/creatinine ratio of 2.07 mg/mg. Complement C3 level is 0.19 g/L, and anti-streptolysin O (ASO) level is 1322 IU/mL. The throat culture shows no growth.	Based on the provided clinical information, the diagnosis of this patient is likely posterior reversible encephalopathy syndrome (PRES) with hypertension and seizure. The causes of PRES appears to be acute poststreptococcal glomerulonephritis (APSGN). This diagnosis is supported by the history of upper respiratory tract infection, significantly elevated ASO titer, low serum C3 level, and hematuria.	Hospitalization: Given the severity of the presentation, the patient should be hospitalized in intensive care unit for close monitoring and management. Management of hypertension: Aggressive control of hypertension is essential to prevent complications. Intravenous antihypertensive medications are commonly used in PRES to help lower blood pressure. Management of hyperkalemia: Given the high serum potassium level (6.9 mEq/L), measures to lower potassium levels should be initiated promptly, such as dietary restriction of potassium and possibly administration of potassium-lowering medications like loop diuretics or potassium binders. Inhaled salbutamol and insulin treatments can also be used if hyperkalemia persists.
14.4-year-old boy presents with complaints of bloody urine. It is learned that he had an upper respiratory tract infection about 10 days ago. On examination, his blood pressure is 145/91 mmHg (above 99th percentile for both). Laboratory findings show serum creatinine 2.42 mg/dL, serum albumin (2.3 g/L, Na 135 mmol/L, K 6.2 mmol/L, Ca 7.9 mg/dL, and P 6.6 mg/dL. Urinalysis reveals a red blood cell-count of 237 /HPF and a spot urine protein/creatinine ratio of 6.94 mg/mg. Complement C3 level is 0.52 g/L, and ASO level is 1614 IU/mL. The throat culture shows no growth. The patient's serum creatinine rises to 5.35 mg/dL within 4 days.	Based on the provided clinical information, the diagnosis of this patient is likely rapidly progressive glomerulonephritis (RPGN) with severe kidney impairment and hypertension. The causes of RPGN appears to be APSGN. This diagnosis is supported by the history of upper respiratory tract infection, significantly elevated ASO (anti-streptolysin O) titer, low serum C3 level, and hematuria.	Hospitalization: Given the severity of the presentation, the patient should be hospitalized for close monitoring and management. Management of hypertension: Aggressive control of hypertension is essential to prevent further kidney damage. Antihypertensive medications such as angiotensin-converting enzyme inhibitors (ACE inhibitors) or angiotensin receptor blockers (ARBs) are commonly used in RPGN to help reduce proteinuria and lower blood pressure. Management of hyperkalemia: Given the high serum potassium level (6.2 mEq/L), measures to lower potassium levels should be initiated promptly, such as dietary restriction of potassium and possibly administration of potassium-lowering medications like loop diuretics or potassium binders. Inhaled salbutamol and insulin treatments can also be used if hyperkalemia persists. Renal replacement therapy: With severe kidney impairment (serum creatinine 5.35 mg/dL), renal replacement therapy such as hemodialysis or peritoneal dialysis may be required to manage uremia and electrolyte abnormalities. Corticosteroids or immunosuppressive therapy: In cases of RPGN, particularly if there is evidence of crescentic glomerulonephritis on renal biopsy, corticosteroids and immunosuppressive agents such as cyclophosphamide may be initiated to suppress inflammation and prevent further kidney damage.

Table 3. Continued		
Case presentation	**Diagnosis**	**Treatment**
7.9-year-old girl presents with complaints of bloody urine. It is learned that she had an upper respiratory tract infection 12 days ago. On examination, her blood pressure is 132/92 mmHg (above 99th percentile for both). Laboratory findings show serum creatinine 0.48 mg/dL, serum albumin 2.6 g/L, Na 131 mmol/L, K 5.5 mmol/L, Ca 8.5 mg/dL, and P 5.7 mg/dL. Urinalysis reveals a red blood cell-count of 588 / HPF and a spot urine protein/creatinine ratio of 6.02 mg/mg. Complement C3 level is 1.07 g/L, and ASO level is 988 IU/mL. The throat culture shows no growth. ACE inhibitors were started for the patient, and blood pressure returned to normal, but hematuria and proteinuria persisted. During follow-up, significant edema develops in the face and legs, and serum albumin levels drop to 1.5 g/L. A kidney biopsy was performed, which showed mesangial IgG and C3 deposits, no IgA deposits, a starry sky appearance, and endocapillary proliferation.	Based on the provided clinical information, the diagnosis of this patient is likely nephrotic syndrome with hypoalbuminemia, proteinuria and edema. The causes of nephrotic syndrome appears to be APSGN. This diagnosis is supported by the history of upper respiratory tract infection, significantly elevated ASO titer, hematuria and a starry sky appearance in biopsy.	Hospitalization: Given the severity of the presentation, the patient should be hospitalized for close monitoring and management. Management of hypertension: Aggressive control of hypertension is essential to prevent further kidney damage. Antihypertensive medications such as angiotensin-converting enzyme inhibitors (ACE inhibitors) or ARBs are commonly used in APSGN to help reduce proteinuria and lower blood pressure. Management of hyperkalemia: Given the high serum potassium level (6.2 mEq/L), measures to lower potassium levels should be initiated promptly, such as dietary restriction of potassium and possibly administration of potassium-lowering medications like loop diuretics or potassium binders. Inhaled salbutamol and insulin treatments can also be used if hyperkalemia persists. Corticosteroids or immunosuppressive therapy: In cases of nephrotic syndrome, corticosteroids such as prednisolone for 6-8 weeks may be initiated to suppress inflammation and prevent further kidney damage.
ACE: Angiotensin converting enzyme, IgG: Immunoglobulin G, Na: Sodium, K: Potassium, Ca: Calcium, P: Phosphorus		

of 6 doses. Daily treatment with 10 mg of prednisolone is continued. Another patient who had hypoalbuminemia (2.3 g/dL) on admission and developed nephrotic syndrome during follow-up underwent renal biopsy. Unlike the first patient, no evidence of crescent or necrosis was observed. Treatment was continued with oral 2 mg/kg/day of pulse methylprednisolone. A patient with decreased proteinuria and improved hypoalbuminemia is being treated with a steroid taper. The clinical characteristics of the AI for these three patients and their responses are shown in Table 3.

In all patients with elevated serum creatinine levels, normal serum creatinine levels were reached after a mean of 12.5±4.9 days. At the last follow-up, the mean serum creatinine level of the study population was 0.54±0.15 mg/dL (0.38-0.89). Complement C3 levels returned to normal in all patients. Microscopic hematuria persisted in 8 patients (72.7%) (median 27±72/HPF erythrocytes on urinalysis). Except for the patient with rapidly progressive glomerulonephritis, proteinuria levels decreased significantly in all patients compared with baseline (median spot urine protein/creatinine 0.71±2.38 mg/mg). In a patient with rapidly progressive glomerulonephritis, the spot urine protein/creatinine ratio was 8.39 mg/mg (Table 2).

Evaluations Using AI

ChatGPT 3.5 answered questions evaluating the definition, epidemiologic characteristics, pathophysiologic mechanisms, diagnosis, and treatment of APSGN as "correct". Questions directed to ChatGPT and responses provided by ChatGPT are presented in Supplemental File 1.

When the clinical and laboratory characteristics of all patients were directed to the program, they were diagnosed with APSGN using ChatGPT 3.5. In terms of treatment and follow-up, the practices performed by ChatGPT 3.5 and clinicians were highly similar. Rest, fluid, and salt restriction were recommended to all patients by ChatGPT 3.5. The initiation of an angiotensin-converting enzyme inhibitor is recommended for hypertension and/or proteinuria. In patients with malignant hypertension, intravenous anti-hypertensives were initiated, and the patient was recommended to be followed up in the intensive care unit. In patients with hyperkalemia, a potassium-poor diet, inhaled salbutamol, and oral potassium binders are recommended. Steroid treatment was recommended for patients with nephrotic syndrome, but no recommendation was made regarding the route of administration or dosage. The patient with a rapid creatinine increase was also diagnosed with rapidly

progressive glomerulonephritis by ChatGPT 3.5 and was recommended to start steroid and cyclophosphamide treatments without any opinion on the dose and route of administration. No kidney biopsy was advised for any patient. Except for those presented in Table 2, the clinical characteristics of other patients referred to ChatGPT and the responses provided by ChatGPT are presented in Supplemental File 2.

DISCUSSION

APSGN is the most common glomerulonephritis in childhood caused by some strains of group A β-hemolytic streptococci following urticaria or skin infection, and develops with immune complex deposition in the kidney. Patients may experience sudden onset of bloody urination, edema, hypertension, and clinical findings of acute renal failure[17]. In our study, all patients had URTI before kidney involvement. Group A β-hemolytic streptococcus positivity was demonstrated in throat culture in some patients, but all patients had markedly elevated ASO levels, which is a marker of previous infection. Although macroscopic hematuria was seen in 63.6% of the patients who presented with hematuria, all patients had hematuria. Although nephrotic syndrome was observed in one patient and rapidly progressive glomerulonephritis in another, most patients presented with acute nephritic syndrome.

Precautions should be taken for acute renal failure due to APSGN. Penicillin is recommended for streptococcal infections. However, antibiotic treatment had no impact on the progression of the disease[18]. In our study, only penicillin was used in patients with a history of throat culture. Activity should not be restricted except in the acute period. Salt restriction should be performed during kidney impairment and hypertension. In selected cases, antihypertensive drugs, such as an angiotensin-converting enzyme inhibitor and/or calcium channel blockers, may be used[18]. Although normotension can be achieved with oral antihypertensives, malignant hypertension and related complications that may require the use of intravenous antihypertensives may also develop[19]. In our study, one of our patients presented to the hospital with headache, seizures, mild periorbital edema, and significantly elevated blood pressure according to age, sex, and height. The patient was diagnosed with posterior reversible encephalopathy on magnetic resonance imaging. Although serum creatinine was normal at presentation, the patient had a history of URTI, elevated ASO, and low complement C3. On follow-up, laboratory findings normalized, and normotension was achieved without the need for long-term antihypertensives. It was thought that the patient had acute renal failure with oliguria before presentation to the hospital and presented to the hospital with seizure in the late period when renal function started to improve. Apart from general recommendations and antihypertensive drugs for APSGN, immunosuppressive treatments may be indicated for patients with a noisy picture[20]. In our study, two patients who developed nephrotic syndrome and rapidly progressive glomerulonephritis were initiated on steroids and cyclophosphamide, respectively.

Among patients with APSGN, 95% recover without developing permanent problems. If the acute phase has a very severe course and glomerular hyalinization is caused, kidney failure may be observed in 5% of the cases[18]. In our study, except for the patient diagnosed with rapidly progressive glomerulonephritis, the hematuria level decreased significantly, and improvement was observed in the proteinuria levels in other patients. Even in our patient with severe initial findings due to rapidly progressive glomerulonephritis, serum creatinine levels regressed to normal values, but nephrotic proteinuria persisted.

ChatGPT is a language model developed by OpenAI. It is an AI system that is highly skilled in natural language processing and specializes in understanding, analyzing, and generating text data. It can interact with users in a natural language and generate meaningful responses[21]. The design and development phases of ChatGPT are complex. It is based on an architecture called "Generative Pre-trained Transformer". This architecture was pre-trained on datasets containing large amounts of text. These datasets are obtained from diverse sources, including books, articles, web pages, and forums. ChatGPT can be customized to specific tasks or datasets, typically by tweaking a pre-trained model. This fine-tuning process allows the model to produce more specific and accurate answers on a given topic[22].

Thanks to rapid technological advancement, ChatGPT versions have been rapidly updated in recent years as ChatGPT-3.0, 3.5, 4.0, and 4.0-Turbo, respectively. While ChatGPT-3.5 offers higher accuracy and consistency than ChatGPT-3.0, ChatGPT-4.0 can be trained with a larger training dataset and more parameters, resulting in more complex and nuanced responses. ChatGPT-4.0 also gained the ability to process text and visual inputs simultaneously. ChatGPT-4.0 Turbo is optimized for speed and cost, offering faster response times, especially in real-time applications. Although ChatGPT 4.0 and 4.0-turbo require a monthly fee, the previous versions can be used free of charge by anyone[23]. For this reason, ChatGTP 3.5, which is publicly and freely available,

was used in this study, and the economic burden associated with the use of AI was avoided. However, since ChatGPT-3.5 is trained on data up to September 2021, the accuracy of answers given after this date may be affected, especially in cases that query more recent developments in medical issues[24]. It is indisputable that the answers given by AI would contain much more up-to-date information if ChatGPT 4.0 or the 4.0-Turbo versions had been used in our study.

ChatGPT is used in many medical departments. In the field of pediatric dentistry, ChatGPT is used to identify caries lesions, improve diagnostic imaging accuracy and efficiency, improve treatment esthetics, simulate outcomes, and predict oral diseases. The ability to provide immediate feedback and clarify doubts has been shown to help improve health status and oral hygiene by providing patients with relevant information. However, it should be noted that ChatGPT is not completely free of errors or limitations, and the plausibility of incorrect answers can be surprising. Therefore, it is emphasized that ChatGPT outputs should be checked manually by clinicians[25]. However, in our study, questions evaluating the definition, epidemiologic characteristics, pathophysiologic mechanisms, diagnosis, and treatment of APSGN were answered correctly by ChatGPT 3.5. Answers to these questions can also be obtained using traditional search engines such as Google or medical/scientific databases such as PubMed or UpToDate. However, ChatGPT provides general medical information derived from various sources and responds very quickly[23]. Both PubMed and UpToDate present pages of data when information on a medical topic is sought, which may take users hours to sift through to find the desired information. Thus, ChatGPT saves users significant time. In a study in which ChatGPT asked junior and senior specialist questions about the thyroid, ChatGPT was shown to produce responses quickly[26]. However, unlike these search engines, ChatGPT does not provide references. This lack of citations is a potential weakness of ChatGPT. In a study comparing ChatGPT and UptoDate, ChatGPT could not provide references for some questions. In addition, the accuracy score of the responses provided by ChatGPT in this study was significantly lower than that of UptoDate[27].

There are some studies stating that the use of ChatGPT in the medical field is beneficial. For example, ChatGPT can play a role in various fields, including pediatric radiology. In this study, various case scenarios related to pediatric radiological imaging methods were directed to ChatGPT, and the responses of AI were evaluated. ChatGPT provided suggestions about imaging modalities that could be applied for each clinical scenario. It was able to provide information on whether imaging techniques that do not use radiation can be used in the current scenario. If radiation is to be used, it provides information on the optimum dose. It has been pointed out that ChatGPT can provide valuable information, but the final interpretation and diagnosis should always be made by a radiologist[22]. In another medical field, the integration of AI into the field of pediatrics has the potential to transform healthcare with new and effective approaches for supporting diagnoses, treatment plans, and specific clinical decisions[28]. This study explored ChatGPT's effectiveness as a decision-making tool in pediatrics by posing 8 clinical symptom-related questions. Two pediatricians independently assessed ChatGPT's open-ended responses. The findings indicated that ChatGPT could enhance clinical workflows and support decision-making in pediatrics[11]. In our study, when the features of the cases were assessed, treatments administered by clinicians to all patients with a diagnosis of APSGN and the ChatGPT recommendations. However, it did not mention the route of administration or dosage of the recommended drugs. In the field of pediatrics, the route of administration and dosage of each drug are of great importance. Although this situation seems to be a limitation of ChatGPT, ChatGPT will be used by medical specialists, as in this study. In any event, it is suggested to use ChatGPT's recommendations with questioning. It should be used together with the clinician and should be considered as an assistant to the clinician. Therefore, we believe that the lack of ChatGPT's information about drug administration routes and dosages is an acceptable deficiency.

CONCLUSION

Further investigations and advancements in ChatGPT's capabilities related to pediatric care could potentially enhance patient management and healthcare delivery. In our study, the information and guidance provided by ChatGPT on APSGN may be a valuable resource for patient care and management. However, under current conditions, the recommendations provided by ChatGPT applications must be manually checked and evaluated by clinicians. New updates and developments are required for AI to be routinely used.

Ethics

Ethics Committee Approval: The study received approval from the KTO-Karatay University Rectorate Dean of the Faculty of Medicine non-Drug and non-Medical Device Research Ethics Committee Presidency (decision no: 77998, date: 16.01.2024).

Informed Consent: This was a retrospective observational study with a cross-sectional design in which the demographic, clinical, and laboratory characteristics of patients aged 0-18 years who were followed up with a diagnosis of APSGN in the Department of Pediatric Nephrology between September 2023 and March 2024 were analyzed from patient records.

Author Contributions

Surgical and Medical Practices: E.L., Concept: E.L., M.S., Design: E.L., M.S., Data Collection and/or Processing: E.L., Analysis and/or Interpretation: E.L., M.S., Literature Search: E.L., M.S., Writing: E.L., M.S.

Conflict of Interest: The authors have no conflict of interest to declare.

Financial Disclosure: The authors declared that this study has received no financial support

REFERENCES

1. Steer AC, Danchin MH, Carapetis JR. Group A streptococcal infections in children. J Paediatr Child Health. 2007;43:203-13.
2. Balasubramanian R, Marks SD. Post-infectious glomerulonephritis. Paediatr Int Child Health. 2017;37:240-7.
3. Rodriguez-Iturbe B, Musser JM. The current state of poststreptococcal glomerulonephritis. J Am Soc Nephrol. 2008;19:1855-64.
4. Dhakal AK, Shrestha D, Singh SK, Acharya S. Clinical profile of children with acute post-streptococcal glomerulonephritis. Pediatr Nephrol. 2023;38:3327-36.
5. Hunt EAK, Somers MJG. Infection-Related Glomerulonephritis. Pediatr Clin North Am. 2019;66:59-72.
6. Liu J, Wang C, Liu S. Utility of ChatGPT in Clinical Practice. J Med Internet Res. 2023;25:e48568.
7. Curtis N; ChatGPT. To ChatGPT or not to ChatGPT? The Impact of Artificial Intelligence on Academic Publishing. Pediatr Infect Dis J. 2023;42:275.
8. Biswas S. ChatGPT and the Future of Medical Writing. Radiology. 2023;307:e223312.
9. Dave T, Athaluri SA, Singh S. ChatGPT in medicine: an overview of its applications, advantages, limitations, future prospects, and ethical considerations. Front Artif Intell. 2023;6:1169595.
10. Small PM. Improving Collaborative Decision-making in the Pediatric Setting. AACN Adv Crit Care. 2019;30:189-92.
11. Kao HJ, Chien TW, Wang WC, Chou W, Chow JC. Assessing ChatGPT's capacity for clinical decision support in pediatrics: A comparative study with pediatricians using KIDMAP of Rasch analysis. Medicine (Baltimore). 2023;102:e34068.
12. Flynn JT, Kaelber DC, Baker-Smith CM, Blowey D, Carroll AE, Daniels SR, et al. Clinical Practice Guideline for Screening and Management of High Blood Pressure in Children and Adolescents. Pediatrics. 2017;140:e20171904.
13. Viteri B, Reid-Adam J. Hematuria and Proteinuria in Children. Pediatr Rev. 2018;39:573-87.
14. Downie ML, Gallibois C, Parekh RS, Noone DG. Nephrotic syndrome in infants and children: pathophysiology and management. Paediatr Int Child Health. 2017;37:248-58.
15. Schwartz GJ, Work DF. Measurement and estimation of GFR in children and adolescents. Clin J Am Soc Nephrol. 2009;4:1832-43.
16. Asinobi AO, Ademola AD, Nwankwo AF. Childhood acute glomerulonephritis in Ibadan Nigeria. Nigerian journal of paediatrics. 2020;47:345-52.
17. Brant Pinheiro SV, de Freitas VB, de Castro GV, et al. Acute Post-Streptococcal Glomerulonephritis in Children: A Comprehensive Review. Curr Med Chem. 2022;29:5543-59.
18. Ong LT. Management and outcomes of acute post-streptococcal glomerulonephritis in children. World J Nephrol. 2022;11:139-45.
19. Soylu A, Kavukçu S, Türkmen M, Akbaş Y. Posterior leukoencephalopathy syndrome in poststreptococcal acute glomerulonephritis. Pediatr Nephrol. 2001;16:601-3.
20. Zaffanello M, Cataldi L, Franchini M, Fanos V. Evidence-based treatment limitations prevent any therapeutic recommendation for acute poststreptococcal glomerulonephritis in children. Med Sci Monit. 2010;16:RA79-84.
21. Hill-Yardin EL, Hutchinson MR, Laycock R, Spencer SJ. A Chat(GPT) about the future of scientific publishing. Brain Behav Immun. 2023;110:152-4.
22. Biswas SS. Role of ChatGPT in radiology with a focus on pediatric radiology: proof by examples. Pediatr Radiol. 2023;53:818-22.
23. Rojas M, Rojas M, Burgess V, Toro-Pérez J, Salehi S. Exploring the Performance of ChatGPT Versions 3.5, 4, and 4 With Vision in the Chilean Medical Licensing Examination: Observational Study. JMIR Med Educ. 2024;10:e55048.
24. Rahsepar AA, Tavakoli N, Kim GHJ, Hassani C, Abtin F, Bedayat A. How AI Responds to Common Lung Cancer Questions: ChatGPT vs Google Bard. Radiology. 2023;307:e230922.
25. Maltarollo TFH, Shitsuka C, Sivieri-Araújo G. ChatGPT and its use in paediatric dentistry. Eur Arch Paediatr Dent. 2023;24:675-6.
26. Guo S, Li R, Li G, et al. Comparing ChatGPT's and surgeon's responses to thyroid-related questions from patients. J Clin Endocrinol Metab. 2024:dgae235.
27. Karimov Z, Allahverdiyev I, Agayarov OY, Demir D, Almuradova E. ChatGPT vs UpToDate: comparative study of usefulness and reliability of Chatbot in common clinical presentations of otorhinolaryngology-head and neck surgery. Eur Arch Otorhinolaryngol. 2024;281:2145-51.
28. Andykarayalar R, Mohan Surapaneni K. ChatGPT in Pediatrics: Unraveling its Significance as a Clinical Decision Support Tool. Indian Pediatr. 2024;61:357-8.

DOI: 10.4274/MMJ.galenos.2024.78380
Medeni Med J 2024;39:230-234

Case Report

Revisiting the Muscles and Nerves of Anterior Compartment of the Arm: A Case Report

Kolun Ön Kompartman Kasları ve Sinirlerinin Yeniden Değerlendirilmesi: Bir Olgu Takdimi

Busra ANACUR[1], Eren OGUT[2], Cagatay BARUT[2]

[1]Bahçeşehir University Faculty of Medicine, Department of Anatomy, Istanbul, Türkiye
[2]Istanbul Medeniyet University Faculty of Medicine, Department of Anatomy, Istanbul, Türkiye

ABSTRACT

During routine dissection of the anterior compartment of the arm region, we encountered several variations in the muscular and neural structures in the right upper extremity of a female cadaver. We observed one superiorly positioned extramuscular head with fibers originating from both the biceps brachii (BB) and coracobrachialis (CB) muscles and one inferiorly positioned extramuscular head with fibers solely from the BB muscle. The musculocutaneous nerve did not penetrate the CB muscle, but instead provided a muscular branch that communicated with the median nerve (MN). Both the MN and brachial artery (BA) flow beneath the extra head. This case suggests that the described variations may contribute to the entrapment of the MN and compression of the BA. Understanding these variations is crucial before surgical intervention. The failure to recognize such anatomical nuances could lead to inadvertent nerve injury or compromised vascular perfusion, emphasizing the need for preoperative planning and intraoperative vigilance.

Keywords: Arm, musculocutaneous nerve, median nerve, brachial artery, upper extremity, muscle

ÖZ

Kol bölgesinin ön kompartmanının rutin disseksiyonu sırasında, kadavranın sağ üst ekstremitesinde kas ve sinir yapıları ile ilgili birkaç varyasyonla karşılaşıldı. Biceps brachii (BB) ve coracobrachialis'den (CB) köken alan bir adet üst konumlu ekstra kas başı ve sadece BB kasından liflerle köken alan bir adet alt konumlu ekstra kas başı gözlemlendi. Nervus musculocutaneus CB kasını delmiyordu, ancak bu kasa bir dal verdikten sonra ve nervus medianus'a (NM) bağlandı. Hem NM hem de arteria brachialis (AB) ekstra başların altından geçiyordu. Bu olguda, tanımlanan bu varyasyonların MN ve AB tuzaklanmasına katkıda bulunabileceği düşünülmektedir. Bu varyasyonların anlaşılması, cerrahi girişimler öncesinde kritiktir. Anatomideki bu varyasyonların tanınmaması, iyatrojenik sinir yaralanmasına veya vasküler perfüzyonun bozulmasına yol açabilir, bu da cerrahi girişim öncesi planlamanın önemini vurgular.

Anahtar kelimeler: Kol, nervus musculocutaneus, nervus medianus, arteria brachialis, üst ekstremite, kas

INTRODUCTION

The biceps brachii (BB) and coracobrachialis (CB) muscles are essential components of the anterior compartment of the arm and are crucial for various upper-limb movements. The musculocutaneous nerve (MCN), a branch of the brachial plexus, plays an integral role in the flexion and stabilization of the arm[1]. The CB muscle primarily originates from the coracoid process (CP) of the scapula, often in conjunction with the short head of the biceps brachii (SHBB)[2]. Interestingly, primates exhibit both superficial and deep CB muscles traversed by the MCN. In humans, this anatomical relationship manifests as a compound muscle composed of distinct components[2]. Conversely, the BB typically manifests as a dual-headed structure comprising short and long heads. Originating from the CP and supraglenoid tubercle of the scapula, this muscle exhibits considerable variability[2]. The MCN supplies the muscles of the anterior arm compartment and skin of the anterolateral forearm, traversing the CB as it descends into the arm[1]. However, the spatial relationship between the MCN, neighboring structures such as the CB muscle, and the median nerve (MN) exhibits notable

Address for Correspondence: C. Barut, Istanbul Medeniyet University Faculty of Medicine, Department of Anatomy, Istanbul, Türkiye
E-mail: cagbarut@yahoo.com **ORCID ID:** orcid.org/0000-0001-6999-5980

Received: 28 June 2024
Accepted: 12 August 2024
Online First: 03 September 2024

Cite as: Anacur B, Ogut E, Barut C. Revisiting the Muscles and Nerves of Anterior Compartment of the Arm: A Case Report. Medeni Med J. 2024;39:230-234

variability[2]. During limb development, the musculature arises directly from the mesoderm of the limb bud. In early embryonic stages, the BB, CB, and brachialis muscles exhibit close fusion, likely stemming from a common premuscle mass that undergoes subsequent regression[3]. The two heads of the BB originated from separate sources as the scapula developed. The common muscle mass differentiates later than the proximal end, which could explain the presence of the CB muscle and additional heads due to premature termination of this regression process[4]. The CB originates from the lateral mesoderm, similar to other muscles of the upper limb. It is speculated that muscle primordia combine to form a single body that subsequently undergoes regression as muscle layers develop. The presence of additional muscles can be attributed to the premature termination of regression. A split in the scapula might result from the in utero displacement of one ossification center or the presence of more than two ossification centers, in which case one forms a supernumerary head[5].

Deviations from this developmental trajectory, such as the appearance of muscular variations, such as extra heads, may result from incomplete regression processes. Therefore, our objective was to comprehensively identify and characterize multiple variations within a single case and elucidate their embryological underpinnings. By examining the embryonic origins and developmental processes governing these muscular variations, we aimed to contribute to a deeper understanding of limb musculature variability and its clinical implications.

CASE REPORT

During routine dissection of the anterior compartment of the arm region, we performed an in-depth examination of the muscular and neural structures within the right upper extremity of an 81-year-old female cadaver. The primary cause of death was Wernicke's encephalopathy, which is associated with alcoholism. In accordance with the ethical principles outlined in the Declaration of Helsinki, our investigation aimed to uncover and document any anatomical variations. This study was approved by the Bahcesehir University Clinical Research Ethics Committee on 21.09.2022, protocol no.: 2022-13/01. All measurements were performed twice using digital calipers to ensure precision and accuracy. We identified two additional heads of the BB during the examination (Figure 1). The first superiorly positioned muscular head originated from the SHBB and the lower fibers of the CB muscles (Figure 2). The length and transverse diameter at the center were measured at 164.3±0.71 mm and 11.1±0.28 mm, respectively. This superior additional head was inserted into the medial brachial intermuscular septum, with a distance of 134.69±0.11 mm noted between its insertion point and the medial epicondyle. The second additional head, situated more inferiorly, originated from the medial border of the SHBB and was inserted into the medial brachial intermuscular septum. It measured 106.47±0.41 mm in length, with a transverse diameter at the center of 9.83±0.3 mm and a distance of 81.11±0.89 mm between its insertion point and the medial epicondyle (Figure 2). The MCN did not penetrate the CB muscle but instead provided a muscular branch to supply the muscle, passing beneath the superior additional head before descending between the BB and brachialis muscles (Figure 2). In addition, the MCN issued a branch to the MN from behind the superior head. The MN and brachial artery (BA) traversed beneath these additional heads (Figure 1).

DISCUSSION

The incidence of an additional head of the BB ranged from 2.3% to 16.66%. Awareness of these anatomical variations is essential to avoid complications during tendon reconstructive surgery and repair in cases of avulsion[6]. One study reported that the supernumerary BB head originated from the anteromedial surface of the humerus just beyond the insertion of the CB and was inserted into the conjoined tendon of the BB. This muscular variant is associated with duplicated MCN. The proximal MCN followed a normal pattern in the proximal region, terminating after innervating the CB and BB muscles. The distal MCN nerve arose from the MN in the lower arm and passed laterally between the supernumerary BB head and the brachialis muscle, supplying both and terminating as the lateral cutaneous nerve of the forearm[7]. However, in our study, two additional heads were observed, and the MCN did not penetrate the CB. The MCN, through its muscular branches, innervated the BB and its extra heads and then provided a communicating branch to the MN before passing under the superior head of the BB and inferior head of the BB. The additional heads were located at different levels, and the nerve distribution patterns differed from those in previous reports. This variation may be attributed to developmental insufficiency during the embryological development of the upper limb. Embryologically, the upper limb develops from somites that migrate to form a limb bud. Through differential growth and apoptosis, somites give rise to muscle formation under complex regulation. Variations in muscle anatomy, such as the absence, presence, or abnormal orientation of muscles

or their parts, typically arise from the uneven expression of *Hox* genes and associated developmental processes[8].

The present case demonstrates two extra heads (with different origins) that contain more muscular fibers with the same insertion. The most common variation in the BB is related to the number of muscle bellies[2]. Rodríguez-Niedenführ et al.[9] divided the supernumerary heads of the BB into three types: inferomedial, superior, and inferolateral humeral head. These supernumerary heads originate from different structures but are inserted into various parts of the BB[9]. However, in our case, the origin and insertion site of the inferior extra head differed from those in the previous study.

These anatomical variations can influence muscle function and may lead to the compression of adjacent neurovascular structures. The additional heads of the BB can induce strong flexion and supination of the forearm, but they may also cause compression of the BA and MN. The presence of a communicating branch between the MCN and MN increases the risk of intermuscular compression, leading to various neural symptoms, such as tingling and weakness. A musculotendinous slip located above the MN and BA can compress these structures, and the additional head can be injured during shoulder joint surgery. These anatomical variations may lead to iatrogenic injuries. Therefore, it is crucial to have knowledge about these variations to prevent such injuries[6].

Slips originating from the BB and inserted into the internal intermuscular septum have been described previously[2]. As mentioned previously, the inferior

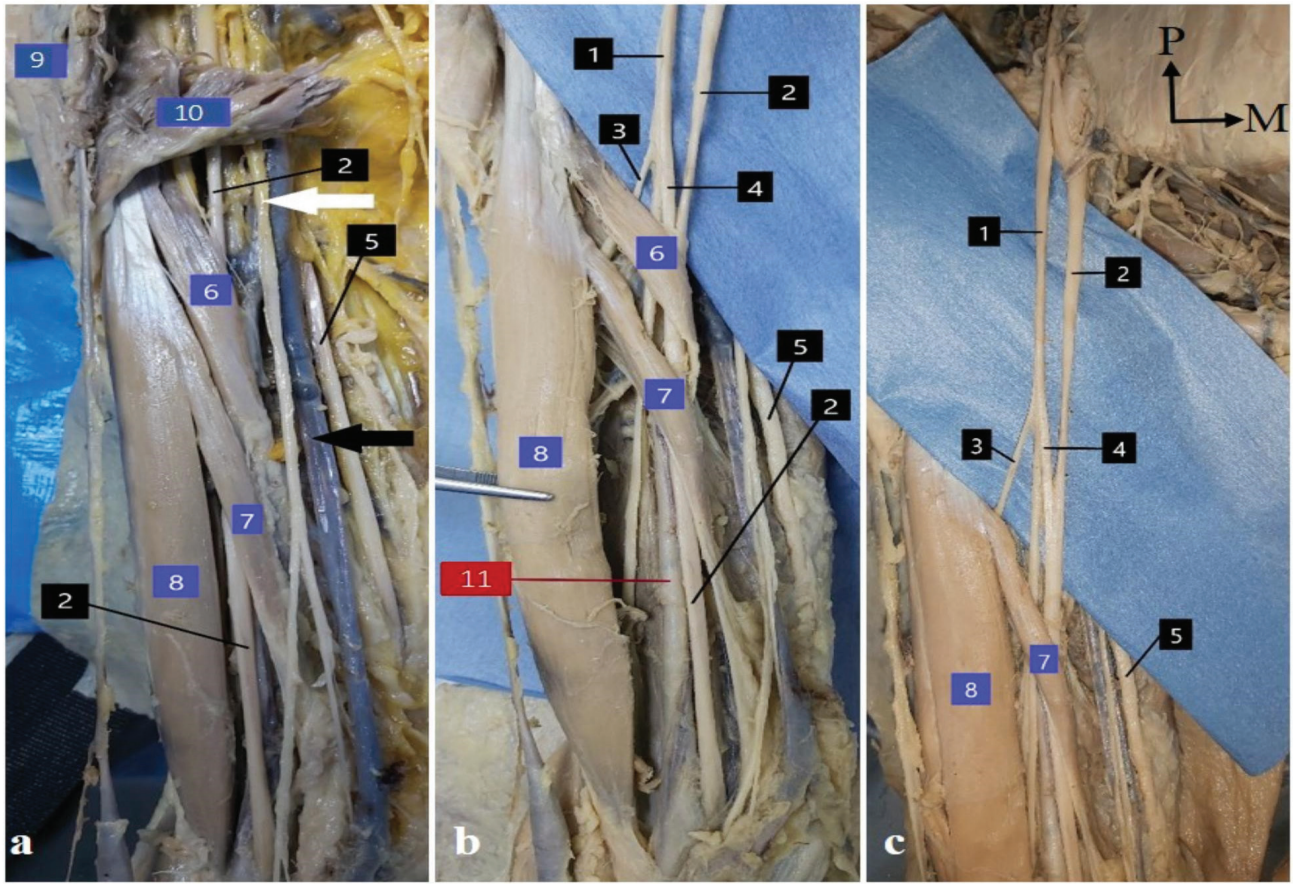

Figure 1. a. Variations in structures in the anterior compartment of right arm **b.** Figure shows both the superior (6) and inferior (7) extra heads of the biceps brachii (BB). **c.** Figure shows the nervous arrangement (1, 2, 3 and 4) under the level of the superior extra head. 1: Musculocutaneous nerve; 2: Median nerve; 3: Muscular branch; 4: Communicating branch; 5: Ulnar nerve; 6: Superior extra head of the BB; 7: Inferior extra head of the BB; 8: Short head of the BB; 9: Deltoid muscle; 10: Pectoralis major muscle; 11: Brachial artery. The white arrow shows the medial antebrachial cutaneous nerve; the black arrow indicates the basilic vein.

M: Medial, P: Proximal

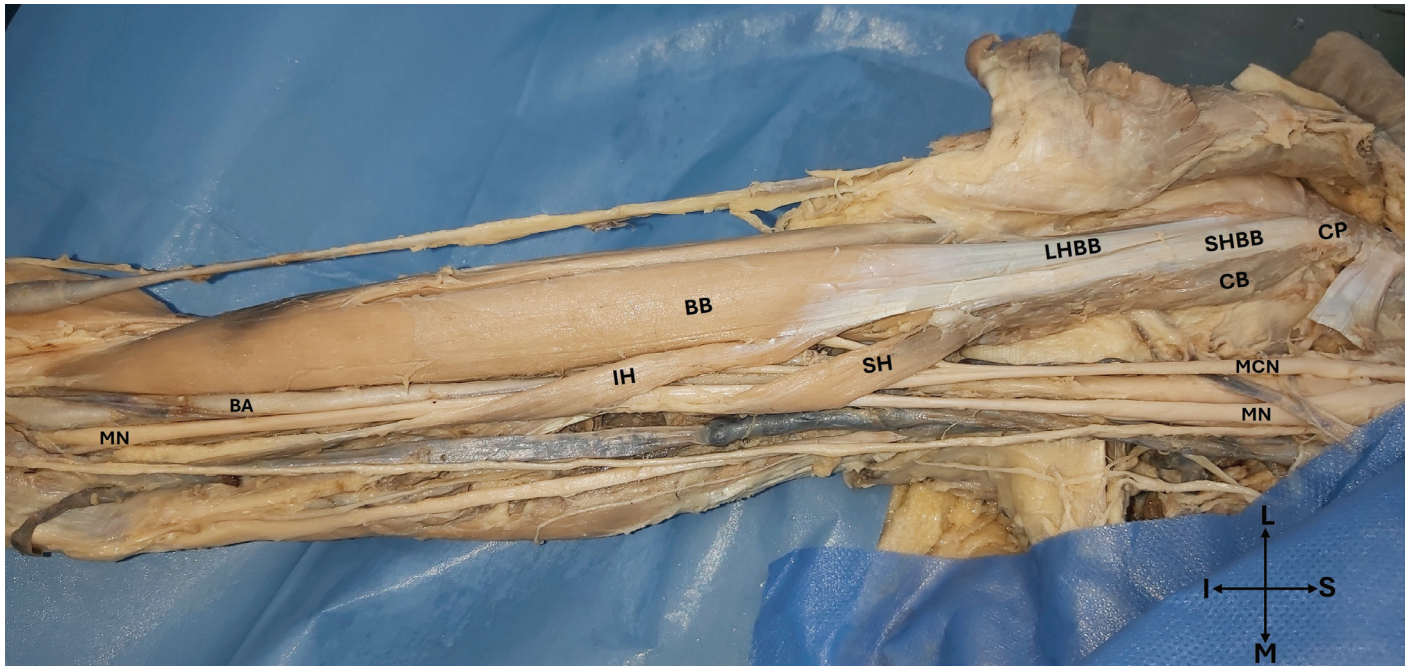

Figure 2. The CB and SHBB muscles originate from the CP, as shown in the figure. The CB muscle is located medial to the SHBB. The MCN did not penetrate the CB. Instead, the MCN passed beneath the SH, providing muscular branches to the BB. The MN traverses beneath the SH and IH. The SH separated from the SHBB at the proximal part of the humerus, corresponding to the insertion point of the CB. On the other hand, the IH separates from the body of the BB in the upper-middle part of the humerus.

BA: Brachial artery, BB: Biceps brachii, CB: Coracobrachialis muscle, CP: Coracoid process, IH: Inferior head of the biceps brachii, LHBB: Long head of the biceps brachii, MCN: Muscular nerve, MN: Median nerve, SH: Superior head of the biceps brachii, SHBB: Short head of the biceps brachii. S: Superior, I: Inferior, M: Medial, L: Lateral

extra head presented here has a large muscle mass that cannot be described as a slip and may be more likely to cause entrapment or compression while the muscle is functioning. Paraskevas et al.[10] encountered a variant muscle that arose from the medial border of the brachialis muscle, passed over the MN, BA, and brachial vein, and eventually fused with the medial intermuscular septum. They suggested that this variant muscle is an accessory fascicle of the brachialis and an embryonic remnant of the brachialis[10]. Therefore, if we apply their opinion to our case, the inferior extra head may be an embryological remnant of the BB muscle. Alternatively, it could be an insertion variation in the BB. The relationship between the MCN and CB muscles is variable[2]. Kervancioglu et al.[11] investigated the motor branching patterns of the MCN in human fetuses. Five of the 20 upper limbs of the fetuses had a communicating branch between the MCN and MN, and in two of them, the MCN did not penetrate the CB but provided a motor branch to supply it. In our case, however, we observed these two distinct variations in the same upper limb, as well as muscular variations in the same region. MCN variations were classified by Guerri-Guttenberg and Ingolotti[12] based on the presence or absence of the MCN, whether it penetrated the CB muscle, the presence and quantity of communication between the MCN and MN, and the level of communication (proximal/distal). According to this classification, our case presents as a 1B1 type of MCN, which implies that the MCN is present but does not perforate the CB muscle and that there is one communication between the MCN and MN. This communication occurs behind the level of the superior extra head and emerges distal to the emerging point of the muscular branch. Therefore, it is crucial to consider the accessory head of the muscle before performing coracoid mobilization to perform surgical procedures, such as hardware fixation, precise drill hole placement, and proper prosthetic alignment. MCN lesions can arise during coracoid bone block abutments and can be prevented by mobilizing and retracting the muscle inserted into the CP when performing coracoid abutment transfer using the Latarjet technique via a deltopectoral approach. However, this can lead to MCN injury, which is a common complication of procedures involving the

anterior shoulder. In addition, transient MCN lesions may occur owing to the elongation and modification of its angle of penetration into the muscle[13]. The presence of split CP may have hindered the latarjet procedure. Therefore, it is crucial to consider the anatomical variations in this region. Therefore, preoperative planning should involve the use of magnetic resonance imaging and computed tomography of the target region. These scans are essential for evaluating both anatomical and pathological shoulder and upper limb lesions as well as identifying any anatomical variations that may affect the success of the procedure[14]. In addition to its usefulness as a component of flap surgery, the BB is also important for its knowledge of the innervation of the accessory head, as well as its ability to compress the vasculature. This is crucial for surgeons who perform such procedures.

CONCLUSION

Variations in anatomical structures serve as crucial elements that enhance our understanding of orthopedics and traumatology. Clinicians rely on recognizing these variations to optimize diagnostic precision, effectively interpret radiographic data, and strategize surgical interventions. The intricate exploration of this case report highlights the significance of acknowledging anatomical diversity and offering insights into potential embryological or genetic influences. Such variations may stem from developmental anomalies, reinforcing the need for comprehensive anatomical examination. Moreover, the present case emphasizes the likelihood that the discovery of one variation may indicate the presence of additional variations across diverse anatomical regions.

Acknowledgements

The authors sincerely thank those who donated their bodies to the science for anatomical research. The results of such research could potentially increase the overall knowledge of mankind and improve patient care. Therefore, these donors and their families deserve the greatest gratitude.

Ethics

Financial Disclosure: This study was approved by the Bahcesehir University Clinical Research Ethics Committee on 21.09.2022, protocol no.: 2022-13/01.

Informed Consent: The study does not require patient consent.

Author Contributions

Surgical and Medical Practices: B.A., E.O., C.B., Concept: B.A., E.O., C.B., Design: B.A., E.O., C.B., Data Collection and/or Processing: B.A., E.O., C.B., Analysis and/or Interpretation: B.A., E.O., C.B., Literature Search: B.A., E.O., C.B., Writing: B.A., E.O., C.B.

Conflict of Interest: The authors have no conflict of interest to declare.

Financial Disclosure: The author declared that this study has received no financial support.

REFERENCES

1. Strandring S. Gray's Anatomy Churchill Livingstone: Elsevier; 2008.
2. Tubbs RS, Shoja MM, Loukas M. Bergman's comprehensive encyclopedia of human anatomic variation. Hoboken, New Jersey: Wiley Blackwell; 2016.
3. Keibel F, Mall F. Manual of Human Embryology. Philadelphia: JB Lippincott Company; 1910. p. 423.
4. Szewczyk B, Polguj M, Paulsen F, et al. A proposal for a new classification of coracobrachialis muscle morphology. Surg Radiol Anat. 2021;43:679-88.
5. el-Naggar MM. A study on the morphology of the coracobrachialis muscle and its relationship with the musculocutaneous nerve. Folia Morphol (Warsz). 2001;60:217-24.
6. Agarwal J, Gopal K. Variations of Biceps Brachii Muscle and its Clinical Importance. J Clin Diagn Res. 2020:4.
7. Abu-Hijleh MF. Three-headed biceps brachii muscle associated with duplicated musculocutaneous nerve. Clin Anat. 2005;18:376-9.
8. Mooney EK. Hand Embryology Gross Morphologic Overview of Upper Limb. Medscape. 2021.
9. Rodríguez-Niedenführ M, Vázquez T, Choi D, Parkin I, Sañudo JR. Supernumerary humeral heads of the biceps brachii muscle revisited. Clin Anat. 2003;16:197-203.
10. Paraskevas G, Natsis K, Ioannidis O, Papaziogas B, Kitsoulis P, Spanidou S. Accessory muscles in the lower part of the anterior compartment of the arm that may entrap neurovascular elements. Clin Anat. 2008;21:246-51.
11. Kervancioglu P, Orhan M, Kilinc N. Patterns of motor branching of the musculocutaneous nerve in human fetuses and clinical significance. Clin Anat. 2011;24:168-78.
12. Guerri-Guttenberg RA, Ingolotti M. Classifying musculocutaneous nerve variations. Clin Anat. 2009;22:671-83.
13. Clavert P, Lutz JC, Wolfram-Gabel R, Kempf JF, Kahn JL. Relationships of the musculocutaneous nerve and the coracobrachialis during coracoid abutment procedure (Latarjet procedure). Surg Radiol Anat. 2009;31:49-53.
14. Olewnik Ł, Zielinska N, Karauda P, Duparc F, Georgiev GP, Polguj M. The co-occurrence of a four-headed coracobrachialis muscle, split coracoid process and tunnel for the median and musculocutaneous nerves: the potential clinical relevance of a very rare variation. Surg Radiol Anat. 2021;43:661-9.

DOI: 10.4274/MMJ.galenos.2024.95994
Medeni Med J 2024;39:235-236

Letter to the Editor Regarding "Clinical and Sonographic Evaluation of the Effectiveness of Extracorporeal Shock Wave Therapy in Patients with Lateral Epicondylitis"

Editöre Mektup "Lateral Epikondilitli Hastalarda Ekstrakorporeal Şok Dalga Tedavisinin Etkinliğinin Klinik ve Sonografik Olarak Değerlendirilmesi" Hakkında

Yuhan GONG, Xinjie WANG

Jining Medical University, Department of Clinic Medicine, Jining, China

Keywords: Lateral epicondylitis, extracorporeal shock wave therapy (ESWT), sonographic assessment
Anahtar kelimeler: Lateral epikondilit, ekstrakorporeal şok dalga tedavisi (ESWT), sonografik değerlendirme

Dear Editor,

We read with great interest the paper by Murat et al.[1] entitled "Clinical and Sonographic Evaluation of the Effectiveness of Extracorporeal Shock Wave Therapy in Patients with Lateral Epicondylitis". They conducted a clinical trial designed to evaluate and compare the clinical and sonographic outcomes between extracorporeal shock wave therapy (ESWT) and lateral epicondylitis (LE). The study demonstrated that ESWT is a promising treatment modality for LE, with benefits in terms of improved grip strength and pain relief. We thank the authors for their valuable contribution in evaluating the effectiveness of ESWT for the treatment of LE. However, after extensive discussions with our professional peer group, we have identified several salient and pertinent questions that we hope you will address:

1. In this study, the visual analog scale was used to assess the level of pain without providing the reader with the position that the patient was in at the time of pain assessment, e.g., forearm pronation, natural droop, or wrist extension. Epicondylitis is an attachment point disorder related to the origin of the short extensor carpi radialis brevis muscle, which triggers or exacerbates pain when the forearm extensor muscles are tight or pulled[2]. Given this situation, we are concerned that inconsistencies in patient status during pain assessment may have confounded the primary outcome assessment in this study. Therefore, I was eager to obtain specific clarification from the authors regarding this issue because it has the potential to significantly impact the measurement of pain outcomes.

2. Correct diagnostic terminology is important for appropriate treatment. There is a plethora of terms used to describe LE, including tennis elbow, epicondylalgia, tendinitis, tendon degeneration, and tendinopathy. These terms often have the prefix extensor or lateral elbow,

Address for Correspondence: X. Wang, Jining Medical University, Department of Clinic Medicine, Jining, China
E-mail: wxj17854254607@163.com **ORCID ID:** orcid.org/0000-0002-9328-0114

Received: 01 July 2024
Accepted: 07 July 2024
Online First: 08 August 2024

Cite as: Gong Y, Wang X. Letter to the Editor Regarding "Clinical and Sonographic Evaluation of the Effectiveness of Extracorporeal Shock Wave Therapy in Patients with Lateral Epicondylitis". Medeni Med J. 2024;39:235-236

which refer to inappropriate etiological, anatomical, and pathophysiological terms. Therefore, in clinical practice, "lateral elbow tendinopathy" seems to be the most appropriate diagnostic term for the condition commonly referred to as LE[3].

3. Regarding the basic characteristics of the subjects, the results showed no statistically significant difference between the two groups in terms of age, gender, side, and pain pressure threshold. However, some important baseline information related to LE risk factors was not considered, such as occupation, lifestyle habits, smoking history, and dominant and affected sides, which may affect the accuracy and applicability of the findings[4]. Therefore, multidimensional baseline information is necessary to ensure the accuracy of the results, and we suggest that the authors discuss this in depth in subsequent studies, which could contribute to a more nuanced and nuanced interpretation of the data, promote safer clinical application, and avoid potential misuse of the study findings.

In conclusion, we would again like to sincerely thank Murat et al.[1] for this important study. We hope that these insights will further provide additional information to the field of ESWT for the treatment of LE, help researchers improve the design of subsequent studies, improve the interpretation of the results of the article, and inspire future research.

Keywords: Lateral epicondylitis, extracorporeal shock wave therapy (ESWT), sonographic assessment

Anahtar kelimeler: Lateral epikondilit, ekstrakorporeal şok dalga tedavisi (ESWT), sonografik değerlendirme

Ethics

Author Contributions

Concept: X.W., Writing: Y.G., X.W.

Conflict of Interest: The authors have no conflict of interest to declare.

Financial Disclosure: The authors declared that this study has received no financial support.

REFERENCES

1. Murat S, Dogruoz Karatekin B, Zengin M. Clinical and Sonographic Evaluation of the Effectiveness of Extracorporeal Shock Wave Therapy in Patients with Lateral Epicondylitis. Medeni Med J. 2024;39:109-116.
2. Ahmad Z, Siddiqui N, Malik SS, Abdus-Samee M, Tytherleigh-Strong G, Rushton N. Lateral epicondylitis: a review of pathology and management. Bone Joint J. 2013;95-B:1158-64.
3. Stasinopoulos D, Johnson MI. 'Lateral elbow tendinopathy' is the most appropriate diagnostic term for the condition commonly referred-to as lateral epicondylitis. Med Hypotheses. 2006;67:1400-2.
4. Sayampanathan AA, Basha M, Mitra AK. Risk factors of lateral epicondylitis: A meta-analysis. Surgeon. 2020;18:122-8.

DOI: 10.4274/MMJ.galenos.2024.80932
Medeni Med J 2024;39:237-238

Letter to the Editor

Comment on "Solitary Submandibular Schwannoma Mimicking a Salivary Gland Tumor in a Child"

"Bir Çocukta Tükürük Bezi Tümörünü Taklit Eden Soliter Submandibular Schwannoma" Üzerine Yorum

Rajesh KUMAR[1], Dibakar BORTHAKUR[2]

[1]All India Institute of Medical Sciences, Department of Anatomy, Patna, India
[2]All India Institute of Medical Sciences, Department of Anatomy, New Delhi, India

Dear Editor,

We read the article titled "Solitary Submandibular Schwannoma Mimicking a Salivary Gland Tumor in a Child" with utmost interest[1]. The authors have described a benign peripheral nerve sheath tumor in the submandibular space. They have described histopathological confirmation of their findings. We appreciate the authors' dedicated efforts.

Histopathological examination of the specimen shown in figures 4 and 5 did not reveal any labeling. Hypercellular (Antoni A), hypocellular areas (Antoni B), and Verocay bodies should be marked with arrows. Magnification of histopathological images was not mentioned, and both images are without any scale bar. Additionally, authors could have mentioned whether immunohistochemical evaluation for S-100 was performed or not which ideally shows diffuse S-100 positivity of the schwannoma cells and helps confirm the diagnosis of schwannoma[2].

Further, since it was detected in a 7-year-old child, a familial history for the presence of peripheral nerve sheath tumor should have been recorded and genetic testing should have been advised. Young adults with sporadic schwannoma may have heritable predisposing mutations[3]. Therefore, genetic testing may be a useful opportunity to detect the propensity for future additional tumor occurrence in young adults with sporadic schwannomas. The NF2, SMARCB1, and LZTR1 genes have been found to be associated with the occurrence of schwannomas[4,5].

We would appreciate the author response to this letter.

Thank you for your consideration.

Keywords: Schwannoma, peripheral nerve sheath tumor, submandibular gland neoplasms, neurilemmoma, salivary gland neoplasms

Anahtar kelimeler: Schwannoma, periferik sinir kılıfı tümörü, submandibular bez neoplazmları, nörilemmoma, tükürük bezi neoplazmları

Ethics

Author Contributions

Concept: R.K., Design: R.K., Analysis or Interpretation: R.K., Literature Search: R.K., D.B., Writing: R.K., D.B.

Conflict of Interest: The authors have no conflict of interest to declare.

Financial Disclosure: The authors declared that this study has received no financial support.

Address for Correspondence: R. Kumar, All India Institute of Medical Sciences, Department of Anatomy, Patna, India
E-mail: dr.rajesh11314@aiimspatna.org **ORCID ID:** orcid.org/0000-0002-8743-7541

Received: 06 July 2024
Accepted: 16 July 2024
Online First: 24 July 2024

Cite as: Kumar R, Borthakur D. Comment on "Solitary Submandibular Schwannoma Mimicking a Salivary Gland Tumor in a Child". Medeni Med J. 2024;39:237-238

REFERENCES

1. Wong KYR, Hakim I, Sawali H, Lim RCA, Mohd Mohsin NK. Solitary Submandibular Schwannoma Mimicking a Salivary Gland Tumor in a Child. Medeni Med J. 2024;39:132-5.
2. Rath S, Sasmal PK, Saha K, et al. Ancient Schwannoma of Ansa Cervicalis: A Rare Clinical Entity and Review of the Literature. Case Rep Surg. 2015;2015:578467.
3. Pathmanaban ON, Sadler KV, Kamaly-Asl ID, et al. Association of Genetic Predisposition With Solitary Schwannoma or Meningioma in Children and Young Adults. JAMA Neurol. 2017;74:1123-9.
4. Evans DG, Bowers NL, Tobi S, et al. Schwannomatosis: a genetic and epidemiological study. J Neurol Neurosurg Psychiatry. 2018;89:1215-9.
5. Smith MJ, Isidor B, Beetz C, et al. Mutations in LZTR1 add to the complex heterogeneity of schwannomatosis. Neurology. 2015;84:141-7.

DOI: 10.4274/MMJ.galenos.2024.82710
Medeni Med J 2024;39:239-240

Letter to the Editor Regarding Our Case Report on "Solitary Submandibular Schwannoma Mimicking a Salivary Gland Tumor in a Child"

"Bir Çocukta Tükürük Bezi Tümörünü Taklit Eden Soliter Submandibular Schwannoma" Olgu Sunumumuzla İlgili Editöre Mektup

Wong Kim Yew RICHARD[1], Nur Kamilia Mohd MOHSIN[2]

[1]Tawau Hospital, Department of Otorhinolaryngology-Head and Neck Surgery, Sabah, Malaysia
[2]Queen Elizabeth Hospital, Department of Pathology, Sabah, Malaysia

Keywords: Submandibular gland neoplasms, neurilemmoma, salivary gland neoplasms
Anahtar kelimeler: Submandibular bez neoplazmları, nörilemmoma, tükürük bezi neoplazmları

Dear Editor,

We would like to thank the readers for their interest in our article[1]. Regarding their queries on our article[2], our responses are as follows:

Figures 4 and 5 are equivalent to 20x and 100x magnification, respectively. We have added arrows and annotated the areas as mentioned. We have included the scale bars in the original image that was attached to Figure 5 (down and left in the image), but they were perhaps too small for one to easily miss. However, we acknowledge that the scale bar is missing in Figure 4. we have added them in the attached file. We also performed S-100 immunohistochemistry, and the lesional cells were diffusely positive for S-100, supporting the diagnosis. We acknowledge that this detail was not included in the article.

There was no familial history of peripheral nerve sheath tumor in this young patient. We agree that if there were any familial predisposition for peripheral nerve sheath tumors; ideally, genetic testing should be offered. However, in our very resource-limited setting, our center could not afford to perform molecular studies on this case. Unfortunately, in this part of the world, or Sabah especially; it is mainly offered in research settings or for complex, diagnostically challenging cases. The family members of the patient were also not keen and could not afford to pay for the tests themselves; therefore, we were unable to proceed with the genetic testing.

We hope that readers and the reader will find our responses and explanations satisfactory. Thank you for your consideration.

Address for Correspondence: W.K.Y. Richard, Hospital Tawau, Department of Otorhinolaryngology-Head and Neck Surgery, Sabah, Malaysia
E-mail: richardwky@gmail.com **ORCID ID:** orcid.org/0000-0002-0165-0895

Received: 12 July 2024
Accepted: 16 July 2024
Online First: 08 August 2024

Cite as: Richard WKY, Mohsin NKM. Letter to the Editor Regarding Our Case Report on "Solitary Submandibular Schwannoma Mimicking a Salivary Gland Tumor in a Child" Medeni Med J. 2024;39:239-240

Keywords: Submandibular gland neoplasms, neurilemmoma, salivary gland neoplasms

Anahtar kelimeler: Submandibular bez neoplazmları, nörilemmoma, tükürük bezi neoplazmları

Ethics

Author Contributions

Data Collection or Processing: W.K.Y.R., N.K.M.M., Analysis or Interpretation: W.K.Y.R., N.K.M.M., Writing: W.K.Y.R., N.K.M.M.

Conflict of Interest: The authors have no conflict of interest to declare.

Financial Disclosure: The authors declared that this study has received no financial support.

REFERENCES

1. Wong KYR, Hakim I, Sawali H, Lim RCA, Mohd Mohsin NK. Solitary Submandibular Schwannoma Mimicking a Salivary Gland Tumor in a Child. Medeni Med J. 2024;39:132-5.
2. Kumar R, Borthakur D. Comment on "Solitary Submandibular Schwannoma Mimicking a Salivary Gland Tumor in a Child". Medeni Med J. 2024 July 24. [Epub ahead of print].

DOI: 10.4274/MMJ.galenos.2024.47650
Medeni Med J 2024;39:241-242

Letter to the Editor

Response to the Commentary on "Clinical and Sonographic Evaluation of the Effectiveness of Extracorporeal Shock Wave Therapy in Patients with Lateral Epicondylitis"

"Lateral Epikondilitli Hastalarda Ekstrakorporeal Şok Dalga Tedavisinin Etkinliğinin Klinik ve Sonografik Değerlendirmesi" Başlıklı Yazıya Yorumun Cevabı

Sadiye MURAT[1], Bilinc DOGRUOZ KARATEKIN[2], Melisa ZENGIN[2]

[1]Istanbul Medeniyet University Faculty of Medicine, Department of Physical Medicine and Rehabilitation, Istanbul, Türkiye
[2]Goztepe Prof Dr. Suleyman Yalcin City Hospital, Clinic of Physical Medicine and Rehabilitation, Istanbul, Türkiye

Keywords: ESWT, lateral elbow tendinopathy, ultrasonography
Anahtar kelimeler: ESWT, lateral dirsek tendinopatisi, ultrasonografi

Dear Editor,

We are pleased to address the inquiries and comments regarding our paper, "Clinical and Sonographic Evaluation of the Effectiveness of Extracorporeal Shock Wave Therapy in Patients with Lateral Epicondylitis" authored by Murat et al.[1]. We appreciate the interest and constructive feedback from our peers, which we believe will contribute to the understanding and application of extracorporeal shock wave therapy (ESWT) in the treatment of lateral epicondylitis (LE)[2]. Below, we provide clarification of the points raised:

1. Pain Assessment Methodology: In our study, the visual analog scale (VAS) was used to assess pain levels. We acknowledge the importance of patient positioning during pain assessment given that LE is related to the origin of the extensor carpi radialis brevis muscle, where pain can be influenced by the positioning of the forearm extensors. To ensure consistency, all patients were assessed in a neutral position (forearm in natural droop position) during VAS measurements. We admit that this detail was not explicitly mentioned in the paper and appreciate the opportunity to clarify this point to ensure an accurate interpretation of our findings.

2. Terminology and Diagnostic Precision: The terminology used to describe LE can indeed vary widely, including terms like "tennis elbow," "epicondylalgia," "tendinitis," "tendon degeneration," and "tendinopathy". In our study, we used the term "lateral epicondylitis" due to its widespread acceptance and understanding in clinical practice. However, we agree that "lateral elbow tendinopathy" is a more precise and appropriate term that accurately reflects the pathophysiology of this condition. We will consider adopting this terminology in future studies to enhance its clarity and accuracy.

3. Consideration of Baseline Characteristics: Our study assessed baseline characteristics, such as age, sex, and pain pressure threshold, and showed no significant

Address for Correspondence: M. Zengin, Goztepe Prof Dr. Suleyman Yalcin City Hospital, Clinic of Physical Medicine and Rehabilitation, Istanbul, Türkiye
E-mail: melisazngn@gmail.com **ORCID ID:** orcid.org/0009-0005-4462-5154

Received: 31 July 2024
Accepted: 03 August 2024
Online First: 28 August 2024

Cite as: Murat S, Dogruoz Karatekin B, Zengin M. Response to the Commentary on "Clinical and Sonographic Evaluation of the Effectiveness of Extracorporeal Shock Wave Therapy in Patients with Lateral Epicondylitis". Medeni Med J. 2024;39:241-242

differences between the treatment and control groups. We acknowledge that additional baseline factors like occupational background, lifestyle habits, smoking history, and dominance of the affected side were not considered. These factors can indeed influence the outcomes and applicability of the findings. Future studies will aim to include a more comprehensive set of baseline characteristics to ensure more nuanced interpretation and to enhance the accuracy and relevance of the results.

In conclusion, we are grateful for the insightful comments and suggestions, which will undoubtedly aid future research on the effectiveness of ESWT in the treatment of LE. We hope that our responses have provided the necessary clarification and look forward to making further contributions to this important field of study.

Ethics

Author Contributions

Surgical and Medical Practices: S.M., B.D.K., M.Z., Concept: S.M., B.D.K., M.Z., Design: S.M., B.D.K., M.Z., Data Collection or Proccessing: S.M., B.D.K., M.Z., Analysis or Interpretation: S.M., B.D.K., M.Z., Literature Search: S.M., B.D.K., M.Z., Writing: S.M., B.D.K., M.Z.

Conflict of Interest: The authors have no conflict of interest to declare.

Financial Disclosure: The authors declared that this study has received no financial support.

REFERENCES

1. Murat S, Dogruoz Karatekin B, Zengin M. Clinical and Sonographic Evaluation of the Effectiveness of Extracorporeal Shock Wave Therapy in Patients with Lateral Epicondylitis. Medeni Med J. 2024;39:109-16.
2. Gong Y, Wang X. Letter to the Editor Regarding "Clinical and Sonographic Evaluation of the Effectiveness of Extracorporeal Shock Wave Therapy in Patients with Lateral Epicondylitis" Medeni Med J. 2024 August 8. [Epub ahead of print].